

# COMPARISON OF MODELS FOR LOAD DISTRIBUTIONS IN A SKEW PRECAST BOX GIRDER VIADUCT

MARCH 2015  
MASTER THESIS  
MOHSIN AL HADI

**HASKONINGDHV NEDERLAND B.V.  
INFRASTRUCTURE**

George Hintzenweg 85  
Postbus 8520  
3009 AM Rotterdam  
+31 10 443 36 66 Telefoon  
Fax  
info@rotterdam.royalhaskoning.com E-mail  
www.royalhaskoningdhv.com Internet  
Amersfoort 56515154 KvK

Document title Comparison of models for load distributions in  
a skew precast box girder viaduct

Status MASTER THESIS FINAL  
Date MARCH 2015  
Project name Master thesis

Auteur Mohsin Al Hadi

## *PREFACE*

This thesis is written to complete the master “concrete structures – structural engineering” at the technical university of Delft in the Netherlands. The research has been performed with the collaboration of Royal HaskoningDHV.

I would like to thank my graduation committee members for all their assistance: prof.dr.ir. D.A. Hordijk, dr.ir. C. van der Veen, dr.ir. M.A.N. (Max) Hendriks, Ir. C.M.P. ’t Hart and Ir. L.J.M. Houben. I would also like to express my gratitude to Ir. R.P.H. Vergoossen, from Royal HaskoningDHV, for being my external supervisor.

This research has been conducted at the office of Royal HaskoningDHV in Rotterdam. I would like to thank Royal HaskoningDHV for providing me the required facilities and guidance. I have had a good time with my colleagues of the infrastructure department and I am grateful for the warm welcome and their help during my stay.

*Mohsin Al Hadi,  
Rotterdam, March 2015*

## **ABSTRACT**

In the past many viaducts in the Netherlands have been built with precast box beam girders. Precast box beam girders have many advantages compared to other types of girders. One of these advantages is the property of being torsion stiff. Because of boundary conditions some viaducts are skew and not straight. A few examples of these boundary conditions are the limitation due to surroundings or the layout of the (road) intersections. The load path in these types of structures is different compared to a straight viaduct. Increase of torsional moments is expected.

Currently there is not a lot of knowledge available about the distribution of forces, mainly concerning shear and torsion, in these types of viaducts. More research is needed to understand the real behavior of these structures and how these can be modelled in a finite element program. The current method of analyzing this type of structures is to use an orthotropic plate model. The shear force and torsional moments cause an increase of the shear stresses in the webs of the girder. This phenomenon cannot be analyzed using an orthotropic plate model because of the difference in cross-sections. In the Eurocode and literature a method approach is provided to be able to translate these forces in a plate model in to shear stresses in the box girder.

In this thesis two models are analyzed in DIANA: an orthotropic plate model and a more complex 2,5D shell model. The results of both analyses are compared with each other and the differences are investigated. The analysis is based on a typical box beam viaduct and only the linear elastic stage is considered. The focus is on the comparison of models for the load distributions rather than determining the required reinforcement and capacity calculations.

The self-weight and prestressing do not cause torsion in a girder because these loads are applied for the statically determined beam in the factory. The internal forces due to these loads are calculated separately and therefore not inserted in the models.

For the Eurocode loading it was found that the maximum value for the longitudinal moment was overestimated by 3,5 percent with the orthotropic plate model when the moment due to the self-weight and the prestressing was taken in to account. The maximum value for the shear stresses was overestimated by the orthotropic plate model 18% when the shear stresses due to the self-weight and prestressing are taken in to account. This led to 23% more shear reinforcement.

It is expected that the 2,5D shell model will take two weeks longer to analyze. This means that this will cost 7200 euro for engineering. It is therefore not worth to use the 2,5D shell model to save up money for shear reinforcement (2500 euro) only.

It is advised to use the orthotropic plate model for the analysis of new skew box beam viaducts with a skew angle of 60 degrees and the same dimensions as the case study viaduct. This model approach is cost efficient if the design is based on maximum values for the shear stress and the same stirrups are applied over the length of the girder.

In case of a reassessment of an existing viaduct where the combination of shear force and torsional moment are governing, the difference of 18% for the shear stress could be decisive in whether the viaduct fulfills the current codes and requirements or not (with the present shear reinforcement). The use of the 2,5D shell model should then be reconsidered.

## ***GRADUATION COMMITTEE***

### Chairman

Prof.dr.ir. D.A. Hordijk  
Department of Structural Engineering, Concrete Structures  
Faculty of Civil Engineering and Geosciences  
Delft University of Technology

### Committee members

Dr.ir. C. van der Veen  
Department of Structural Engineering, Concrete Structures  
Faculty of Civil Engineering and Geosciences  
Delft University of Technology

Dr.ir. M.A.N. (Max) Hendriks  
Department of Structural Engineering, Structural Mechanics  
Faculty of Civil Engineering and Geosciences  
Delft University of Technology

Ir. C.M.P. 't Hart  
FEA expert, Concrete, Steel, Nonlinear mechanics  
Royal HaskoningDHV Nederland B.V.  
Rotterdam

Ir. L.J.M. Houben  
Department of Structural Engineering, Road and Railway Engineering  
Faculty of Civil Engineering and Geosciences  
Delft University of Technology

### Second supervisor Royal HaskoningDHV

Ir. R.P.H. Vergoossen  
Expert concrete structures  
Royal HaskoningDHV Nederland B.V.  
Rotterdam

### Author

M. Al Hadi BSc.  
Student ID: 1503944  
Mohsin90@live.nl

## TABLE OF CONTENTS

	Blz.
1 INTRODUCTION	6
1.1 Reading guide	6
1.2 Background	6
1.3 Previous studies	8
1.4 Important aspects and conclusions from literature	9
2 RESEARCH SCOPE	11
2.1 Problem definition	11
2.2 Objective	12
2.3 Research approach	13
2.4 Research questions	15
3 DESCRIPTION OF THE CASE STUDY VIADUCT	16
3.1 Type of girder, examples and manufacturer	16
3.2 Example cases	17
3.3 Schematization and dimensions	18
4 MODELING	22
4.1 Model choice	22
4.2 Material properties	24
4.3 Structural checks	24
4.4 Loads	25
4.5 Load cases, load masks and governing configurations	28
4.6 Statically determined beam model	32
5 ORTHOTROPIC PLATE MODEL	33
5.1 Introduction	33
5.2 Geometry and parameters	33
5.3 Finite element modeling	37
5.4 Introduction and influence of various aspects	39
5.5 Results Eurocode loading	57
5.6 Summary	69
6 2,5D SHELL MODEL	71
6.1 Introduction	71
6.2 Finite element modelling	71
6.3 Verification	76
6.4 Results due to uniformly distributed load	79
6.5 Results Eurocode loading	90
6.6 Summary	99
7 COMPARISON	100
7.1 Uniformly distributed load	100
7.2 Eurocode loading	106
7.3 Summary	114

8	CONCLUSION	116
9	RECOMMENDATIONS	118
10	LITERATURE	119
11	APPENDIX A: DETERMINING CROSS-SECTION PARAMETERS	120
11.1	Introduction	120
11.2	Surface	120
11.3	Axial stiffness	121
11.4	Flexural stiffness	121
11.5	Torsional stiffness	127
11.6	Shear stiffness	128
11.7	Summary of the parameters	131
12	APPENDIX B: GEOMETRY ORTHOTROPY AND MATERIAL ORTHOTROPY	132
12.1	Defining the material orthotropy	132
12.2	Hand calculation	135
12.3	Comparing FEM elements	135
12.4	Results distributed load	137
12.5	Conclusion	139
13	APPENDIX C: STIFFNESS OF THE BEARINGS	140
13.1	Introduction	140
13.2	Stiffness	140
13.3	Finite element modelling	140
13.4	Results	142
13.5	Conclusions	143
14	APPENDIX D: THE MOST CRITICAL CONFIGURATION	144
14.1	Introduction	144
14.2	Finite element modelling; load masks	144
14.3	Load cases	146
14.4	Longitudinal moments	147
14.5	Transverse moments	153
14.6	Shear force	157
14.7	Torsional moments	159
15	EXCEL SHEETS	164
15.1	Load mask	164
15.2	Orthotropic plate model – calculation of shear stresses	164
16	DIANA FILES	165
16.1	Introduction	165
16.2	DATA files	165
16.3	OUTPUT files	167

## **1 INTRODUCTION**

### **1.1 Reading guide**

Chapter 1 gives an introduction to this topic. Some background information is also given. The research scope (problem definition, objective, approach and questions) is presented in chapter 2. The case study viaduct is a box beam viaduct with a skew angle of 60 degrees. Other details, about the cross section for example, are found in chapter 3.

In chapter 4 several aspects of modeling are presented. The assumptions, material properties and loads are included in this chapter.

In chapter 5 and 6 the details and results of the both models, the orthotropic plate model and the 2,5D shell model, are summarized. These results are compared in chapter 7.

Chapter 8 includes the conclusions of this Master Thesis and in chapter 9 recommendations are given for students or companies who want to continue researching this topic.

### **1.2 Background**

In the past many viaducts in the Netherlands have been built with precast box beam girders. Precast box beam girders have many advantages compared to other types of girders. One of these advantages is the property of being torsion stiff. Because of boundary conditions some viaducts are skew and not straight. A few examples of these boundary conditions are the limitation due to surroundings or the layout of the (road) intersections. The load path in these types of structures is different compared to a straight viaduct. Increase of torsional moments is expected. At the same time a decrease of the longitudinal moment will take place.

#### **1.2.1 Developments of precast viaducts**

In some countries precast bridges and viaducts are mainly used for the infrastructure while in other countries the mainly used building method is cast-in-situ.

The Netherlands belongs to the first category. Precast viaducts have a lot of advantages compared to cast-in-situ solutions.

The real break-through took place in the fifties and sixties. The growth of road traffic demanded a new, economic and fast solution for underpasses and overpasses.

Another contribution to this development was the introduction of long-line prestressing.



### 1.2.2 Box beam girders

This system consists of longitudinal prestressed box-shaped beams. The viaduct deck is composed of a series of box beams placed side by side or at a small distance. The beams are also prestressed in transversal direction.

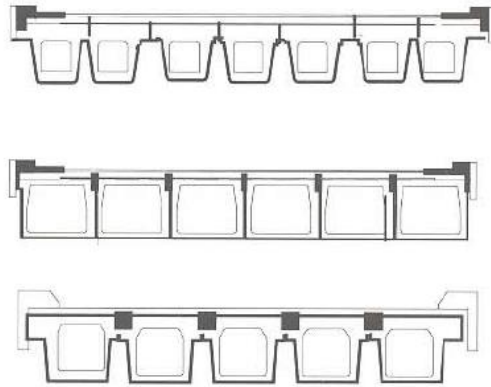


Figure 1, cross-section box beam girders

### 1.2.3 Execution

After erection, the site work is limited to the filling of the longitudinal joints and the transversal post-tensioning of the girders.

### 1.2.4 Skew viaducts

For moderate angles, between 70 and 100 degrees, the viaducts concept for the beams and the deck is nearly the same as straight viaducts. The design becomes more complex for lower angles. The path of the load from application to the supports differs for skew viaducts compared to straight viaducts.

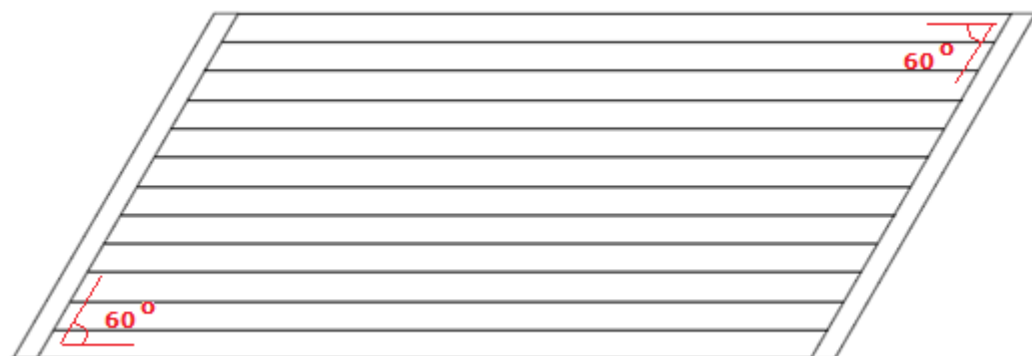


Figure 2, top view skew viaduct

### 1.2.5 Supports for skewed viaducts

Bearings allow built-in movement of the viaduct deck to accommodate thermal expansion and shear stress strains. They are also used to transfer forces from the superstructure to the substructure. There are several different types of bearing to suit different loading and movement requirements.

Elastomeric bearing can be used for skew viaducts. This is one of the simplest supports that are available. The elastomeric bearing works as a soft part between sub- and superstructure and allow movements in all directions by elastic displacements or rotations. The bearing can be reinforced by steel plates and that can prevent the block from bulging. Every displacement and rotations leads to restraining forces and moments which have to be taken into account on the whole structure.

For skew viaducts often oval rubber bearings are being used. Regular dimensions are:

Length: 300 – 500 mm

Width: 200 – 400 mm

Height: 20 – 50 mm

The stiffness of these supports can be modelled by giving the elements a value corresponding to 0,5 mm of deflection as a consequence of the dead load. The dimensions of the bearing from the case study are taken in to account.

## 1.3 Previous studies

John J. Panak [9] did a study in 1977 about moments in skewed bridges. A field test was conducted on five prestressed concrete box-beam highway bridges. One of these bridges was constructed under a 45 degree angle. The load on the bridges was a close simulation of the AASHO (American Association of State Highway Officials) design vehicle. The transversal load transmission between the beams was accomplished by using a reinforced concrete deck slab and cast in situ diaphragms. The main goal was to evaluate the effect of a 45° skew on the lateral distribution of live load in one of the bridges tested.

Canadian Highway Bridge Design Code, CHBDC specifies empirical equations for the moment and shear distribution factors for selected bridge configurations but not for adjacent precast concrete box-girder bridge type. In this report of Khan (2010) [17], a parametric study was conducted, using the 3D finite-element modeling, and a set of simplified equations for the moment, shear and deflection distribution factors for the studied bridge configuration was developed.

Three finite element models have been developed to analyze the cross-sectional forces in the joints of multi-beam box girder concrete bridges. A major theme of this paper, by C. M. Frissen, M. A. N. Hendriks, N. Kaptijn, A. de Boer and H. Nosewicz in 2012 [8], is to indicate the limits of current design methods based on linear analysis.

In 2010 Minalu [4] did his master thesis about finite element modelling of Skew slab-girder bridges. In this study, a search for an appropriate finite element modelling technique was conducted, which was capable of predicting the three-dimensional behavior of high skew bridges consisting of a cast in-place concrete deck on precast prestressed inverted T-girders. The influence of diaphragm beams was also investigated.

In 2012 van Vliet [16] continued with the study of Minalu and researched the torsion behavior of the ZIP girders and cast-in-situ deck. The focus of this research was on a skew bridge with a skew angle of 45 degrees. The main question of this research is when the cracks, as a consequence of torsion, will occur and when the reinforcement will become active. Two different load configurations governing for torsional moments and shear force are used: a configuration which is used at Spanbeton and a configuration developed by Minalu.

#### 1.4 Important aspects and conclusions from literature

Already more than 30 years ago first researches were done about the influence of the skew angle on the live moments for example. It was found that if the angle was taken in to consideration the design live moments could be reduced as much as 40 or 50 percent. This is only applicable to box beam girders. With other beams, with less torsional rigidity, the effect is not as much as with box beam girders. The decrease in longitudinal bending moments means also an increase in transversal and torsional moments.

The research completed under this project demonstrated the reduction in required design moment that can be achieved by consideration of the skew angle. This was concluded for several cases. The magnitude of the reduction is not the same for every angle but can be linked to the skew angle. Less skew viaducts have a higher design moment and have to be prestressed at a higher level.

Deflections measured in skew viaducts were generally smaller than those in the right viaduct.

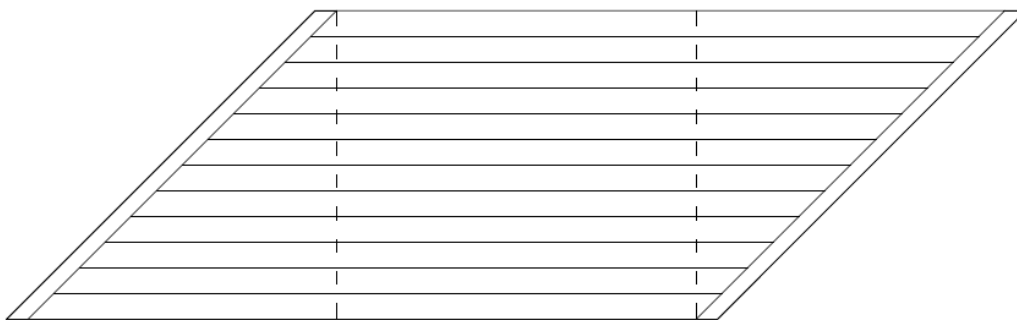


Figure 3, skewed viaducts (60 degrees)

It is found that the viaduct span length and width (amount of girders and number of design lanes) play a significant role on the values of the load distribution factor. It is also found that the deflection is less dependent on the skew angle than the moment and shear distribution. The deflection distribution factors are generally smaller than the distribution factors of the moments for typical viaduct configuration.

Several models have been used to model the shape of box beam viaducts. A few examples are the orthotropic plate model and a model that uses shell elements (membrane-bending elements). A 3D model is also possible but the complexity of this model is very high. The output is difficult to interpret.

Before starting with the model it is important to consider what exactly is needed for the research. Thinking about available input, required output and expected available time can reduce the modeling time and can the modeling accuracy.

Linear and non-linear models can be used. Once again a good consideration between these two has to be made. Nonlinear models are very complex and require a lot of time. An advantage is that, if done right, nonlinear analysis can provide information about the nonlinear behavior of the structure. It can prove extra capacity and it can determine the utmost capacity.

In conclusion: two important aspects about modelling are time and accuracy. Based on these aspects a choice can be made between the models.

It is pointed out that a 3D model is only refined when quadratic elements are used. This is important to model the shear stresses. The stresses due to the prestressing and the dead load can be computed with a hand calculation because spreading of these loads will not occur.

When shear stresses are modelled it is important to use enough elements over the thickness of the web.

The results due to the self-weight and prestressing are calculated separately because these forces are applied for a statically determined beam. In the final results and comparison the results of these loads should be added up with the results of the Eurocode loading.

The stiffness of the supports can be modelled by giving the elements a stiffness corresponding to 0,5 mm of deflection as a consequence of the dead load. The corners of the viaduct are also important areas. Concentration of forces and uplifting can occur.

## **2 RESEARCH SCOPE**

### **2.1 Problem definition**

Currently there is not a lot of knowledge available about the distribution of forces, mainly concerning shear and torsion, in box girder viaducts. More research is needed to understand the real behavior of these concrete structures. It is known that the load path is different in a skew viaduct compared to a straight viaduct. Torsional moments arise for box beam viaducts and the critical areas for the internal forces will be at a different location.

In the current engineering practice it is often the case that a viaduct of box girder beams is analyzed with an orthotropic plate model. The obtained internal forces will then be translated in to stresses for the webs and flanges of the girder as described in the Eurocode. Another method is to neglect the torsional stiffness and obtain the maximum shear stresses through shear force only.

The question is if these models and methods will provide sufficient accuracy compared to a more accurate model where the real geometry is inserted and where the stresses are calculated in the webs.

A more accurate model would be a 2,5D shell model, where the webs and the flanges are inserted as shell elements. The model will then determine the orthotropic parameters and calculate the stresses in the various part of the cross-section. With this model the current engineering practice models could be verified.

## 2.2 Objective

The main objective of this research is to investigate skew precast box girder viaducts and gain insight in the behavior and model approach for the internal forces, mainly concerning shear and torsion.

The following sub-objectives can be formed:

- 1) Provide information about modelling skew box girder viaducts in finite element programs.

The influences of several aspects of modeling on the results are investigated. It is important to determine the required parameters and the time needed to build the model.

- 2) Determine the critical areas for each internal force for skew box beam viaduct.

The load path is different for a skew viaduct compared to straight viaduct. The critical areas for the internal forces will therefore also be at different locations.

- 3) Conclude if the orthotropic plate model will give a significant accuracy compared to 2,5D shell model for the internal forces.

The current engineering practice uses an orthotropic plate model and this does not provide sufficient accuracy for all the internal forces because the cross-section of the plate is not the same as the cross-section of the box girder. If this objective is reached, then a lot of time can be saved, because the time required for modeling an orthotropic plate is far less compared to a complex 2,5D shell model. If this cannot be proven then a different or modified method approach should be used in the engineering practice.

The forces found in the orthotropic plate model can be translated in to stresses with the Eurocode. This is compared with the output of stresses in the 2,5D shell model.

- 4) Formulate the lessons learned from this research.

It is important to know how the design for this type of viaduct can be optimized. Recommendations are given about the aspects mentioned above.

The results of this research can be used to design new skew precast box beam girders and it can be used for the assessment of existing skew viaducts built with precast box beam girders.

## 2.3 Research approach

This research is based on a typical box beam viaduct as described in chapter 3. First, the geometry and the cross-sectional parameters are determined. An important parameter is the transverse stiffness. This is calculated with FEM (Finite Element Model).

Two models are used to determine the load distribution for this viaduct. The first model is an orthotropic plate model. With this model the critical areas for the internal forces are searched for. Different load configurations are used to obtain the maximum force. The output is forces and moments and not stresses. With the Eurocode the shear force and the torsional moment are expressed in to shear stresses. The second model is the more complex 2,5D shell model where the flanges and webs are modelled with shell elements. The output for this model is the exact stresses in the webs.

The calculation is more accurate based on the used model; orthotropic plate model (1) or a shell model (2). This is because the 2,5D shell model represents the real geometry better.

The results for both model approaches are compared with each other using the Eurocode and the output from DIANA.

The self-weight and prestressing do not cause torsion in a girder because these loads are applied for the statically determined beam in the factory. The internal forces due to these loads are calculated separately and therefore not inserted in the models.

For this analysis only the linear elastic stage is considered. The focus is on the comparison of models for the load distributions rather than determining the required reinforcement and capacity calculations.

### **GENERAL ASSUMPTIONS**

- Only the super structure is modelled and examined
- The edge is inserted as load and not as additional stiffness
- The asphalt layer is taken in to account as load and the influence on the spreading of the load is neglected
- Horizontal, temperature and wind loading are not taken in to account
- The length of the massive part at the end of each girder is taken equally for each girder.

Linear elastic analysis assumes linear material behavior. This means that the stress of a member is proportional to its strain by means of the Youngs Modules. According to the Eurocode 2 (5.4) the following may be assumed for this analysis:

- Linear stress-strain relationships
- Mean values of elastic modulus
- Geometrically linear
- Reinforcement is not modeled because it does not have an influence on the stiffness in the linear phase and for uncracked cross sections:

When the bending stiffness of the cross-section is considered, the cracked concrete cross-section is taken in to account. For the strength this is not the case. The difference is that for the strength the weakest cross-section is considered. This is the cracked cross-section. The bending stiffness is a contribution of all cross-sections.

It's a summation of cracked and uncracked cross-sections. This means that the stiffness will decrease after cracks. For this analysis only the linear phase is considered. For that phase the effect on the stiffness distribution is very low.

Until the concrete cracks, the reinforcement will not have a big influence. After the concrete cracks the influence of the reinforcement starts but for prestressed girders this cracked phase will not be big and so uncracked cross-sections are assumed. This assumption can be checked in the more advanced model.

**(TNO) DIANA**

For this research iDIANA is used as pre- and postprocessor. DIANA is special software package for (3D) modeling that can be used by structural engineers. It's possible to analyze linear and non-linear analysis of concrete, steel, soil and soil-structure interaction.

This program can provide detailed results and it's possible to model a plate with eccentric ribs, shell elements and 3D solid elements.

**ASSUMPTIONS FOR THE AXIS AND FORCES IN DIANA**

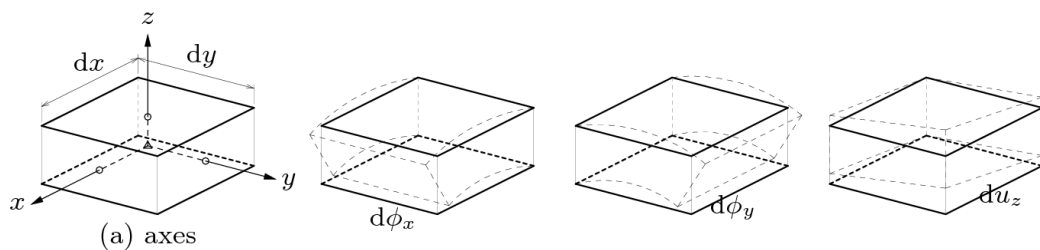


Figure 4, positive conventions

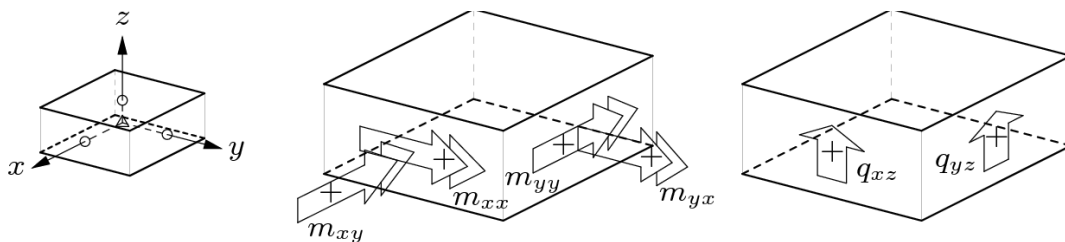


Figure 5, positive conventions



## 2.4 Research questions

### Main question:

What is the behavior, mainly concerning shear and torsion, of skew box girder viaducts and how can these be modelled in FEM?

### Sub questions:

1. What modeling aspects are important for skew box beam viaducts?
2. What are the critical areas for skew viaducts built with box beam girders?
3. How can the stresses of the 2,5D shell model be related to the forces of the orthotropic plate model and this is a valid relation?
4. What is the benefit on the internal forces when using a 2,5D shell model instead of an orthotropic plate model for the case study viaduct? How much is this benefit on the costs?
5. What model approach is the most accurate, efficient and gives the best results for this type of viaducts and what model approach is advised for the engineering practice?

### 3 DESCRIPTION OF THE CASE STUDY VIADUCT

Since the thesis is focused on existing box girder viaducts, the case study is also based on existing examples of these viaducts. This is important regarding the dimensions, materials and technique used.

#### 3.1 Type of girder, examples and manufacturer

For this thesis the box beams of the manufacturer Spanbeton is used. Spanbeton uses SKK box beams. A 3D model of this beam is found in figure 6.

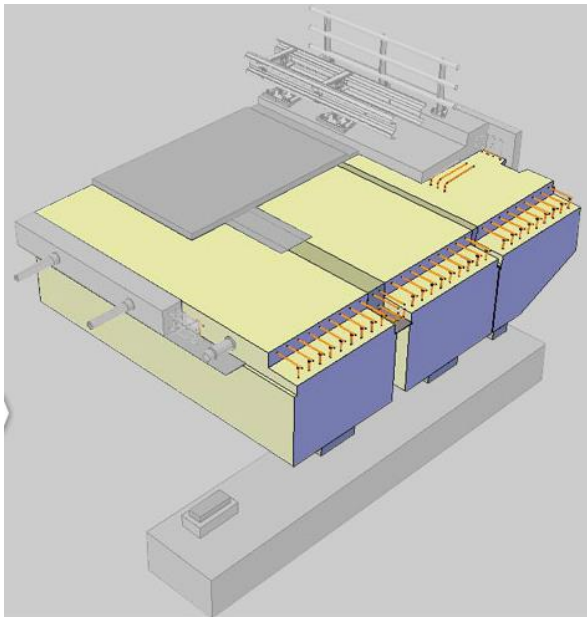


Figure 6, SKK beams from [Spanbeton.nl](http://Spanbeton.nl)

A cast in-situ deck is not necessary anymore for these types of girders. The top flange of the box beam acts as a compressive layer. The beams are prestressed in longitudinal direction in the factory and in transversal direction at site. Connections make use of protruding reinforcement in the beams.

The possible span varies between 15 and 60 meters. The slenderness  $\lambda$  of these girders is 30.

### 3.2 Example cases

The case study viaduct is based on existing skew viaducts in the Netherlands. These viaducts have a skew angle of approximately 67, 60 and 55 degrees. An average viaduct with a skew angle of 60 degrees is defined.

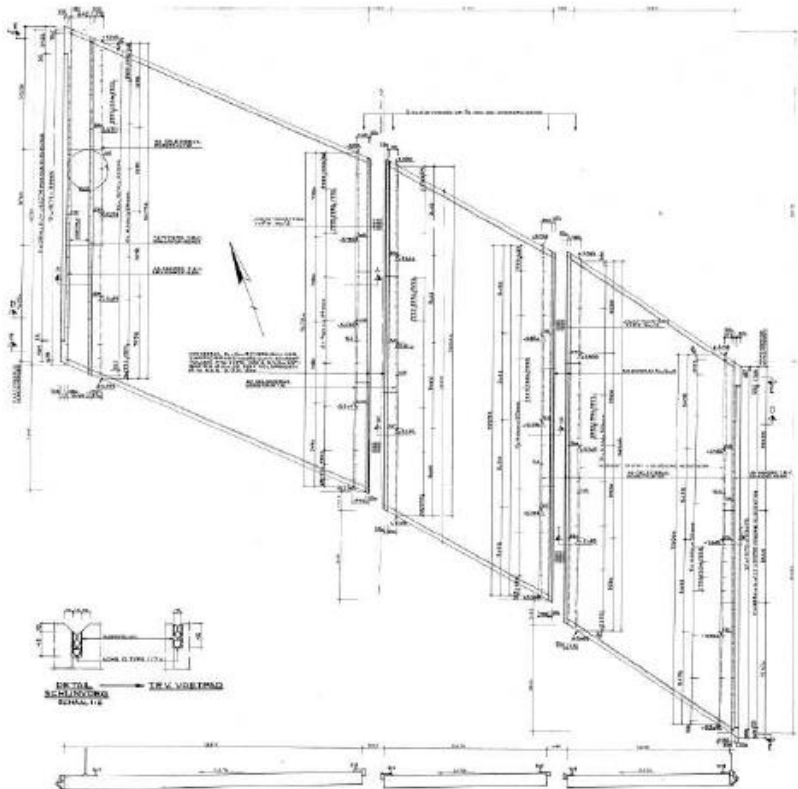


Figure 7, example viaducts

Table 1, parameters of the example viaducts and the case study

Viaduct (fig 7)	Width (m)	# of girders	Span (m)	Angle	Prestressing Longitudinal
<b>Left</b>	26,4	22	30,09	67	# 36 Ø12
<b>Middle</b>	14,4	12	31,46	60	# 40 Ø12
<b>Right</b>	14,4	12	33,45	55	# 47 Ø12

For a starting point a viaduct with the same dimensions as the “Middle” viaduct is chosen. This viaduct has ratio of approximately 2 between the width and the span.

### 3.3 Schematization and dimensions

Taking in to account the width of the viaduct, the skew angle (60 degree) and the center to center distance of the transverse prestressing (1200 mm) the following dimensions for the skew viaduct are found:

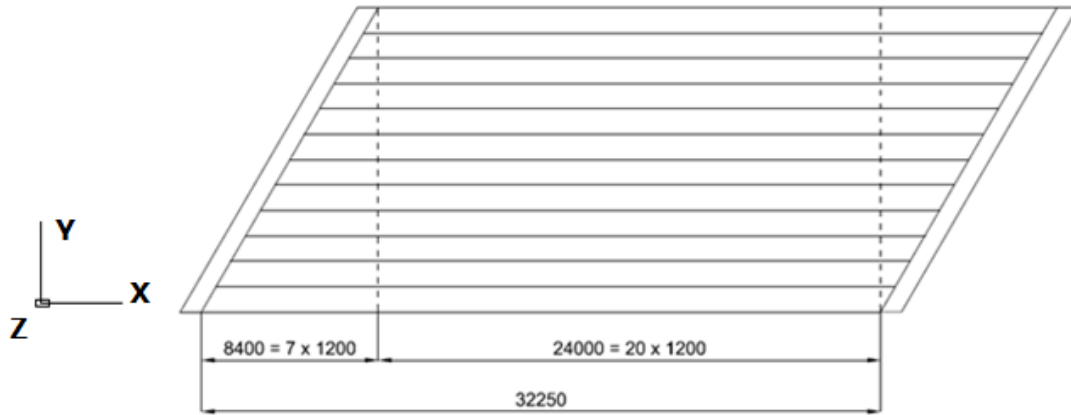


Figure 8, top view case study viaduct [mm]

In the following paragraph information about the cross-section, inner moulds, reinforcement and the prestressing is given.

#### CROSS-SECTION

The cross-section of the box girder can be schematized as shown in figure 9. This cross-section concerns the SKK 1100 girder from Spanbeton.

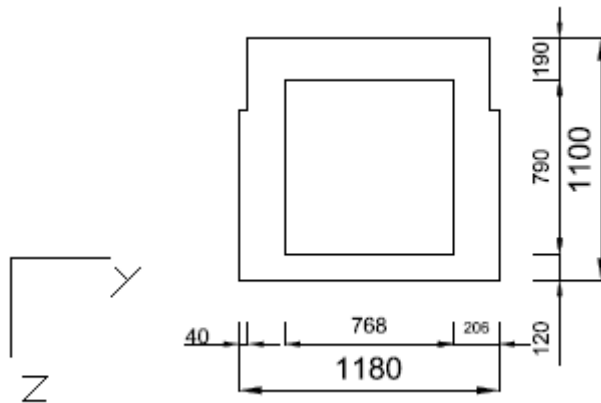


Figure 9, cross-section box girder – dimensions in [mm]

$$Z_{nc} = \frac{1180 * 190 * 80 + 2 * 790 * 206 * 585 + 1180 * 120 * 1040}{1180 * 1100 - 790 * 768} = 514 \text{ mm}$$

In figure 10 the total cross-section and the division of the viaduct is shown. At both ends an area of 1000 mm is available for the safety barrier. At the left the hard strip is present and at the right the hard shoulder. The area where traffic could drive is:

$$1500 + 7400 + 3500 = 12\,400 \text{ mm}$$

This area is important for the division of the theoretical lanes as described in the Eurocode 2.



Figure 10, cross-section viaduct – dimensions in [mm] (12 box girders)

#### **INNER MOULDS FOR THE BEAMS**

The box beam girders have a hollow part at the inside, but at the end the girder is massive. This is to ensure the introduction of the prestressing and to have enough capacity for the shear force.

Out of the available information the maximum and the minimum distances for the inner moulds are determined.

An end distance of 1020 mm (minimum) and 1480 mm (maximum) is determined. Figure 11 below is a schematization of the inner moulds. At the right side distances for the inner moulds are the same.

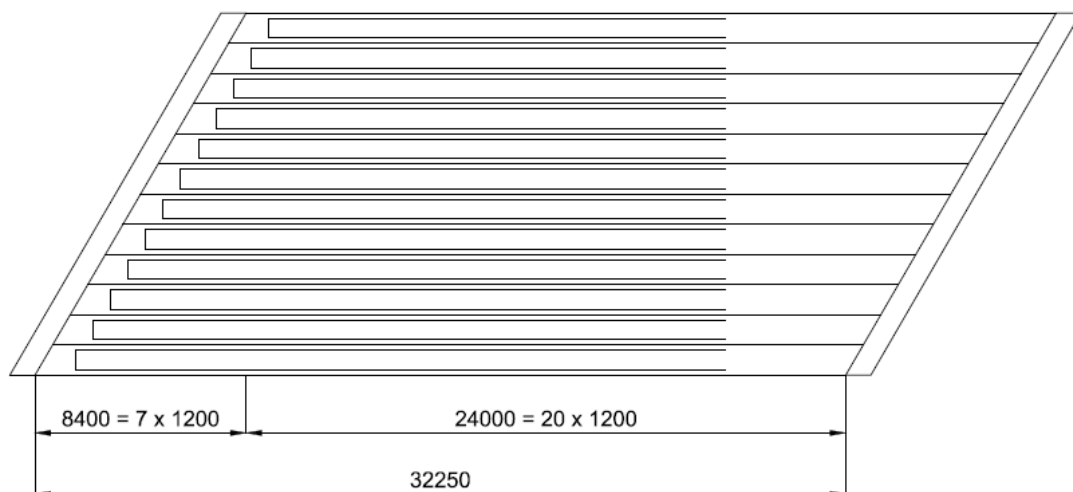


Figure 11, schematization for the inner moulds [mm]

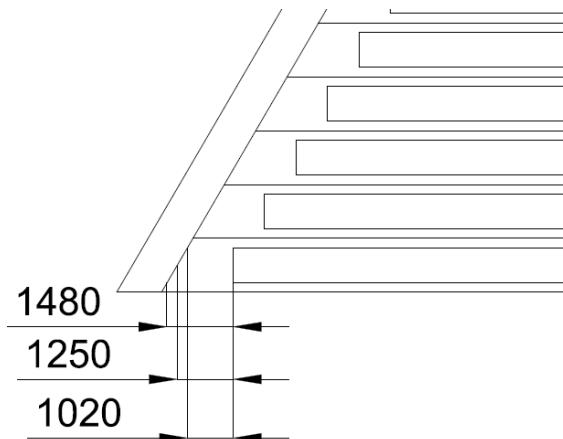


Figure 12, distances for the inner moulds [mm]

**LONGITUDINAL PRESTRESSING**

As presented before, the case viaduct has 40 strands for each girder. The strands have a diameter of 12,5 mm and a total surface of 93 mm<sup>2</sup>. 18 out of 40 strands are kinked, 9 at each web.

The initial level of prestressing  $\sigma_{pi} = 1344.8$  MPa  
The working level of prestressing  $\sigma_{pw} = 1155.8$  MPa

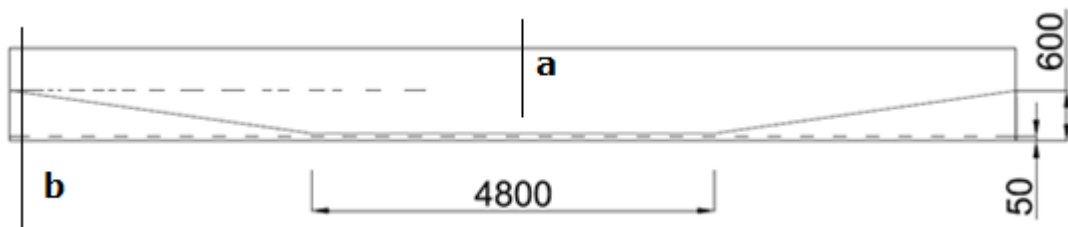


Figure 13, longitudinal prestressing [mm]

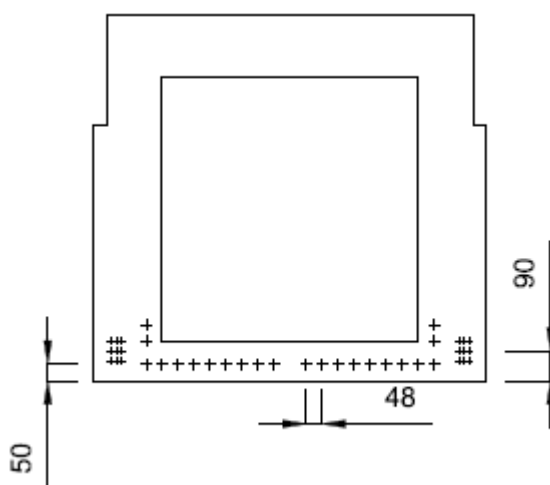


Figure 14, Prestressing at mid cross-section A - dimensions in [mm]

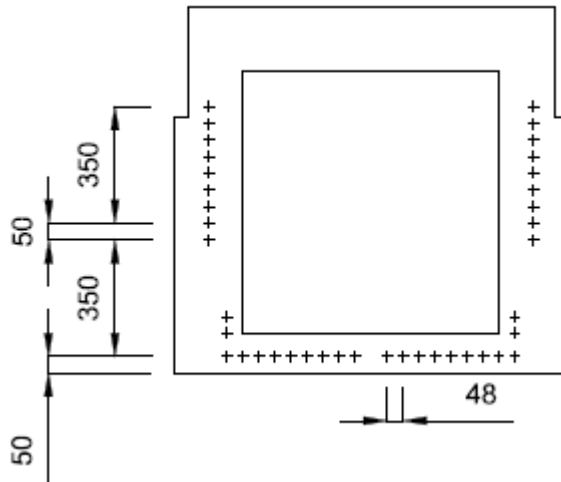


Figure 15, Prestressing at end cross-section B - dimensions in [mm]

**TRANSVERSAL PRESTRESSING**

Center to center distance of the transversal prestressing is 1200 mm.

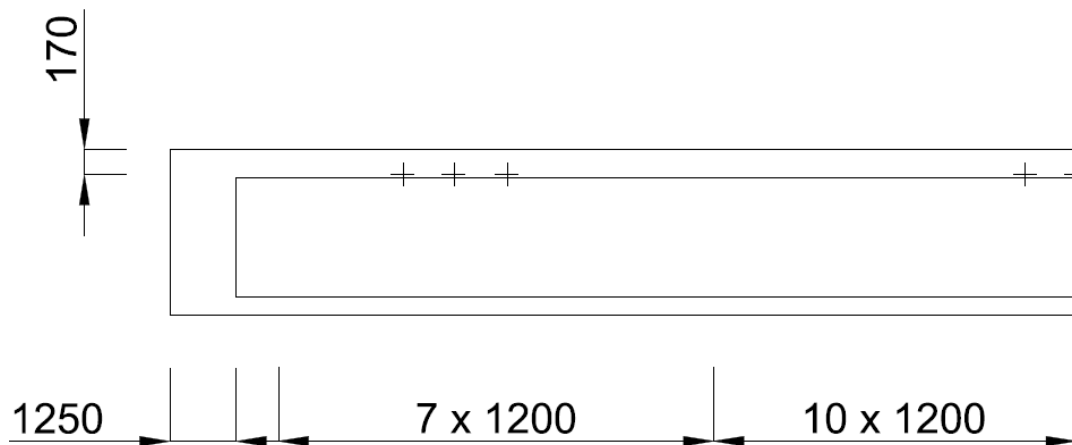


Figure 16, transverse prestressing - dimensions in [mm]

This distance is also important for the position of the box beams in horizontal view. The transversal cable should go through every beam if possible. At the end this is not possible due to the skew angle.

Each strand has a force of 131 kN. This is the average force used for the 3 example cases.

## 4 MODELING

In this chapter various aspects concerning the modeling are discussed. General information is given and the possibilities are presented.

### 4.1 Model choice

When assessing concrete structures various models could be used. Each model has its advantages (accuracy, output etc.) and disadvantages (calculation time, complexity etc.).

It is important to consider what exactly is needed for the research before choosing the model. Thinking about available input, required output and expected available time can reduce the modeling time and can the modeling accuracy.

*Conclusion from previous studies showed:* that the isotropic plate model with centric beam element has the least accuracy. The 3D volume has the best. Concerning the aspect time (modelling and computational) the results were vice versa. In case of a ZIP beam girder and a cast in situ deck, it was found that the model consisting of shell elements for the deck and eccentric beam elements for the girders is the best for engineering practice. For this choice the simplicity of interpreting the result is also taken into account.

For this viaduct linear and non-linear models can be used. Once again a good consideration between these two has to be made. Nonlinear models are very complex and require a lot of time for pre- and post-processing. An advantage is that, if done right, nonlinear analysis can provide information about the nonlinear behavior of the structure. It can prove extra capacity and it can determine the utmost capacity.

To achieve the objectives, two models are used in the linear elastic phase: the orthotropic plate model and the 2,5D shell model.

#### 4.1.1 Orthotropic plate model

In the RBK [12] it is mentioned that the box beams can be modelled as an orthotropic plate model with centric or eccentric ribs. These models are more accurate, by 10% approximately, than a beam model using Guyon Massonet.

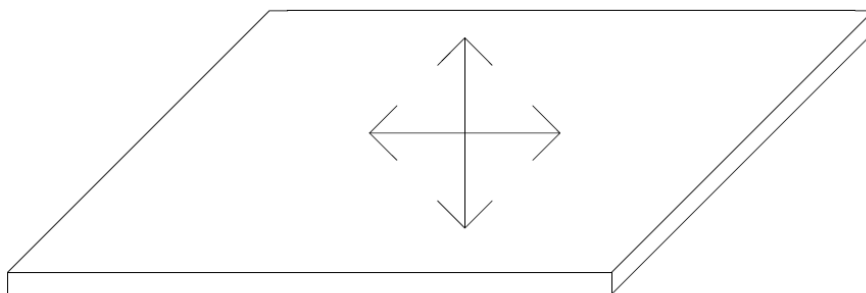


Figure 17, orthotropic plate

As an introduction to the program (DIANA), the first model is the **orthotropic plate model**. This model replaces the beams with an orthotropic plate.



Box beam girders have a high torsional stiffness, even compared to the bending stiffness. This will arise torsional moments. It is expected that these moments cannot be calculated properly with this model, compared to a more accurate 2,5D model because of the presence of the webs.

The reason that this model is still used for this thesis is because of mainly three aspects:

- 1) This is a relatively easy model to begin with. The important part is determining the orthotropic parameters of the girders.
- 2) The accuracy for the deflection and the bending moment can be determined when it is compared to a more complex shell model. The expectation is that this is relatively accurate.
- 3) To conclude about the use of this model for box beam viaduct. It is important to know if it's useful and if so, for what forces is this model accurate enough?

This model is discussed in chapter 5.

**Advantages:** easy to model in geometry, practice shows results are reasonably accurate for moments and deflection for certain types of viaducts and skew angles.

**Disadvantages:** cannot be used for modelling of the shear stresses and torsional moments because the presence of the webs.

In conclusion, this model will help understand the behavior of skew viaducts and the distribution of forces in these types of structures.

#### 4.1.2 Curved shell model

**(Curved) shell elements** are basically a combination of plane stress elements and plate bending elements. This model is more accurate than the orthotropic plate model because the distribution of the stresses in the webs can be presented.

The exact geometry can be modelled which is expected to give more accurate results (about 10-20%). The internal forces can also be determined with this model and stresses can be presented for each part of the cross-section.

An disadvantage is that the results are more difficult to interpret.

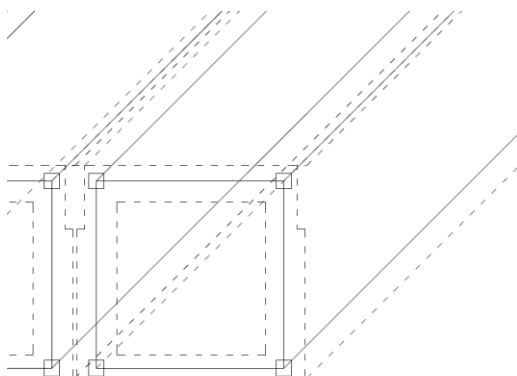


**Figure 18, 2,5D shell elements**

### 4.1.3 Verification

To verify the results hand calculations are made parallel to the modelling. The results of a straight plate are also used as verification because for a distributed load a straight plate can often be modelled as a beam.

It is possible to check the deflection and the moments. In case of a uniformly distributed load the results should be (almost) the same.

Together with this step, the boundary conditions are checked. To check force equilibrium, the total of the applied force is compared to the sum of the support reactions.

No experiments were found that could verify the results of the model.

## 4.2 Material properties

The following material properties are used:

Table 2, material properties

Prefab beams			
Material	E - modules	Poisson ratio	Self-weight
Concrete B52.5	35 000 [N/mm <sup>2</sup> ]	0.20 [-]	2,5 * 10 <sup>-6</sup> [N/mm <sup>3</sup> ]
Joints			
Material	E - modules	Poisson ratio	Self-weight
Concrete B37.5	30 000 [N/mm <sup>2</sup> ]	0.20 [-]	2,5 * 10 <sup>-6</sup> [N/mm <sup>3</sup> ]

Table 3, prestressing steel properties

Prestressing steel	f <sub>pre</sub>	f <sub>pu</sub>	F <sub>pre</sub>	f <sub>p</sub>	E <sub>p</sub>
FeP 1860	1860	1690	1600	1450	200 000

All values are in N/mm<sup>2</sup>.

The prestressing steel is applied with strands with a diameter of 12,5 mm. Each strand has a surface of 93 mm<sup>2</sup>.

## 4.3 Structural checks

The starting point for a reassessment or check is making use of the Eurocode 2 (NEN-EN 1992-1-1) in combination with the NEN 8700 and additions from the RBK.

The main goal is to determine the structural safety. The assessment is carried out from a coarse model to fine and more accurate one. The calculation is linear.

Only the super structure is examined. Besides the checks on strength, stability is checked for box beam girders. This means that no tensile forces are present at the supports. If this is the case, two options are available:

- 1) Remove the supports which have tensile forces and check the stability again until there are no supports under tensile anymore.
- 2) Reduce the load by applying a lower level of safety.

If the structure does not fulfill the requirements according to future use, the safety level can be reduced to actual use or even disapproval.

## 4.4 Loads

The loads are determined according to the Eurocode. Only vertical loads are taken into account. Horizontal loads (wind, braking forces etc.) and temperature loads are not modelled because they are not governing.

Due to the building order of the girders, the self-weight and the longitudinal prestressing are applied at a statically determined beam before the coupling (due to the transverse prestressing). The contribution of these loads to the internal forces should be calculated separately, because if they are inserted in the plate model they would arise torsional moments and this does not hold in practice.

### 4.4.1 Permanent load

#### **SELF-WEIGHT (ACCORDING TO NEN 6702)**

- Reinforced/prestressing concrete: 25 kN/m<sup>3</sup>

$$G = S \left[ \frac{\text{N}}{\text{mm}^3} \right] * \frac{A [\text{mm}^2]}{W [\text{mm}]} = 25 * 10^{-6} * \frac{664880}{1200} = 0.014 \text{ N/mm}^2$$

- Asphalt:
  - o 23 kN/m<sup>3</sup>
  - o 121 mm (assumed according to ROBK 14.2.1). This is the minimal thickness for future use.

$$P_{\text{asphalt}} = S * t = 23 * 10^{-6} \left[ \frac{\text{N}}{\text{mm}^3} \right] * 121 [\text{mm}] = 0.0028 \text{ N/mm}^2$$

**Note:** The contribution of the asphalt thickness to the spreading of the load is neglected.

**EDGE LOAD:**

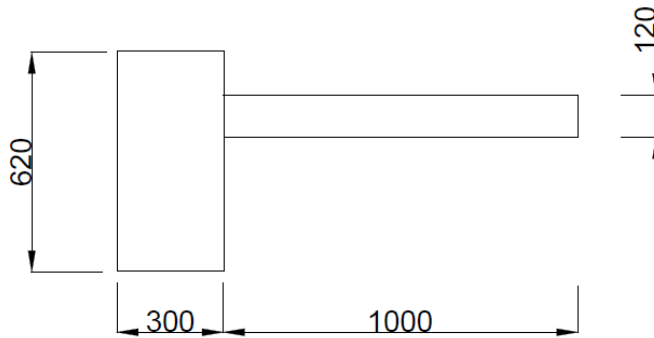


Figure 19, dimensions for the edge of the viaduct [mm]

- Line load at edge: the load of the main curb edge
  - o 4,83 kN/m (dimensions 650 mm x 300 mm).
    - This is inserted as line loading at the edge: 4,83 N/mm
- Surface load (0-1 m from edge): rest of curb edge, guard rail and hand rail
  - o Guard and handrail: 1,4 kN/m
  - o Rest of curb edge: 3,15 kN/m
  - o Total: 4,55 kN/m

$$P_{edge} = \frac{S}{w} = \frac{4,55}{1000} = 0,0045 \text{ N/mm}^2$$

4.4.2 Prestressing

**LONGITUDINAL**

The load from prestressing is taken in to account by computing the corresponding normal force and the contribution to the shear force (resistance)  $F_{pw} \cdot \sin(\alpha)$ .



Figure 20, longitudinal prestressing

$$\tan \alpha = \frac{550}{32250 \cdot \frac{1}{2} - 4800 \cdot \frac{1}{2}} = 0,04$$

$$\alpha = 2,3 \text{ degrees} > \text{small angle} > \cos(\alpha) = 1, \sin(\alpha) = 0$$

The horizontal force at the end span:

**At the center of the cross-section:  $18 \cdot 1156 \cdot 93 = 1935 \ 144 \text{ N}$**

Vertical component:  $\sin(2,3) \cdot 1935 \ 144 = 77 \ 323 \ (4\%)$

Horizontal component:  $\cos(2,3) \cdot 1935 \ 144 = 1933 \ 586 \ (96\%)$

**Vertical component (Fv1) at x=13727:  $\sin(2,3) \cdot 1935 \ 144 = 77 \ 323 \ (4\%)$**

**At the bottom of the cross-section:  $22 * 1156 * 93 = 2365\ 176\ N$**

When applying this at the natural axis of the beam, a moment is introduced:

The moment (M1) is equal to:  $2365\ 176\ N * 310\ mm = 733 * 10^6\ Nmm$ .

The total horizontal force (Fh1) is:  $4300\ 320\ N$

**TRANSVERSE PRESTRESSING:**

Only a few of the transverse prestressing cables are shown in figure 21. Each cable has a force of 131 kN and the distance in between is 1200 mm.

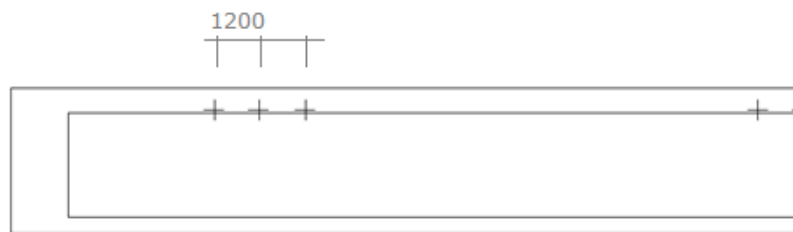


Figure 21, a few of the transverse prestressing cables [mm]

The transverse prestressing is not present at the massive ends of the girders.

4.4.3 Variable traffic load

The traffic load according to the Eurocode 1 is applied. Only traffic load model 1 is used. To apply this model, the area where traffic is possible is divided in notional lanes. The length of the notional lane is 3 m. The total width of the viaduct is 14,4 m. The area that must be divided in notional lanes is the area between the safety girders.

This distance is:

$$14,4 - 2 * 1,0 = 12,4\ meter$$

This means that 4 notional lanes are present with a rest area of 400 mm.

Table 4, loads according to Eurocode 1 (load model 1)

Notional Lane	Qi;k (axial load) αQi (=1) Tandem (2 axis), per ax: [kN]	qi;k (UDL) αqi=1 (1.15) αqi>1 (1.40) [kN/m <sup>2</sup> ]
1 (3.0 m)	300	9.0 * 1.15 = 10.35
2 (3.0 m)	200	2.5 * 1.40 = 3.50
3 (3.0 m)	100	2.5 * 1.40 = 3.50
4 (3.0 m)	0	2.5 * 1.40 = 3.50
5 (0.4 m)	0	2.5 * 1.00 = 2.50

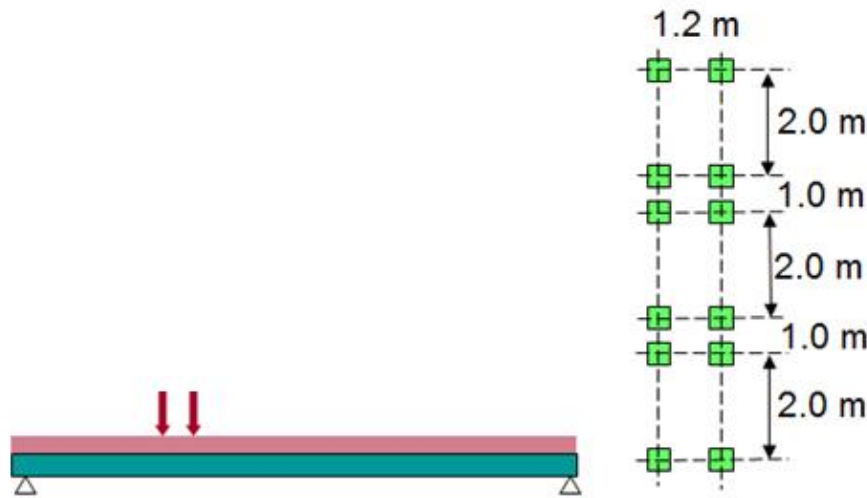


Figure 22, loads on notional loads

The distributed load due to traffic is modelled as an overall load of  $2,5 \text{ kN/m}^2$  ( $0.0025 \text{ N/mm}^2$ ). At the position of the first notional lane this is increased with  $6,5 \text{ kN/m}^2$  ( $0.0065 \text{ N/mm}^2$ ).

#### **WHEEL LOADS**

The size of one wheel is  $400 \times 400 \text{ mm}$ . The point load is converted to a distributed load. The load mask makes only that area effective. This is explained in appendix D.

Table 5, information about the wheel loads

Tandem axle	Force per wheel [N]	Area per wheel [ $\text{mm}^2$ ]	Distributed load [ $\text{N/mm}^2$ ]
1	150 000	$400 \times 400$	0.9375
2	100 000	$400 \times 400$	0.6250
3	050 000	$400 \times 400$	0.3125

By applying a load mask in DIANA, specific areas are excluded or appended to a uniformly distributed load. With this option the distributed load are applied over the full viaduct and only specific areas are made effective.

#### **4.5 Load cases, load masks and governing configurations**

In this paragraph an overview is given of the load cases. Different configurations for the 'load model 1' are used to find the maximal membrane forces, bending- and torsional moments.

In this chapter the load cases and configuration are presented for the distributed loads as determined in 4.4 (also in appendix D) and for the tandem axles as determined in appendix D. Every load applied is appended to a load case. In the post-processing the governing combination is used.

These configurations have been determined with the orthotropic plate model.

**DISTRIBUTED LOADS**

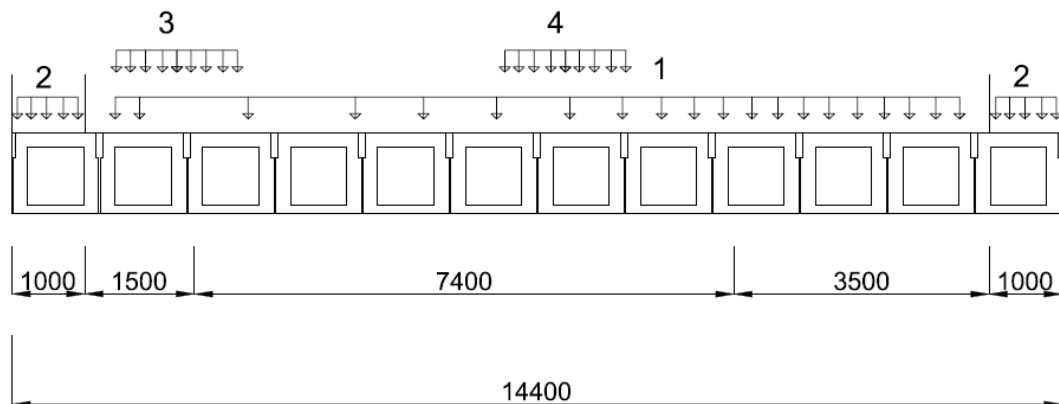


Figure 23, load masks for distributed loads [mm]

Table 6, distributed loads

Load case				Load mask*
1	Self-weight	00.014	N/mm <sup>2</sup>	[-]
2	Asphalt	0.0028	N/mm <sup>2</sup>	1
3	Edge line	4.8300	N/mm	Line
4	Edge surface	0.0045	N/mm <sup>2</sup>	2
5	Distributed traffic load	0.0025	N/mm <sup>2</sup>	1
6	Lane 1 extra load (side)	0.0065	N/mm <sup>2</sup>	3
7	Lane 1 extra load (mid)	0.0065	N/mm <sup>2</sup>	4

\*This is explained in appendix D (Chapter 12.2)

**WHEEL LOADS**

As presented in appendix D, different positions for the tandem axial loads are considered. The governing positions for different internal forces are then determined. In the tables below the governing load cases are presented per internal forces.

Table 7, point loads location for maximum longitudinal moment

Load case				Load mask
12	Q <sub>1;k</sub>	300 000	N	5 – 8
13	Q <sub>2;k</sub>	200 000	N	9 – 12
14	Q <sub>3;k</sub>	100 000	N	13 – 16

*(Load case 8-11 were reserved for the potential use of the prestressing)*

The load cases 12-14 are appointed to the wheel loads. The load masks are redefined for each analysis (for a different configuration) because it is not possible to append more than one load mask to a load case. This means that if all load masks are inserted in the same analysis, 12 load cases and 48 load masks will have to be inserted. To keep a good overview on the load cases, the load masks 5-16 are redefined instead of this. This is done by means of BATCH files.

Longitudinal moments (load combination 1)

Distributed permanent and traffic load: Load case 1-6  
Wheel load (traffic): 12-14 (configuration 1)

It is expected that the governing girder will be close to the edge. The difference with the girder in the middle of the transverse direction is the presence of permanent loading from rails at the edge for example. Furthermore the width over which the load can spread is less. This means the moment per millimeter is higher.

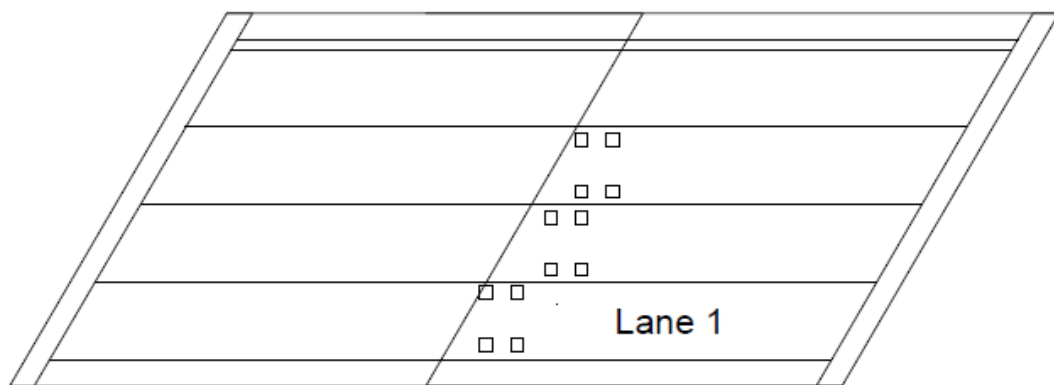


Figure 24, configuration 1 - governing configuration for moments in longitudinal direction

Moment in the transverse direction (load combination 2)

Distributed permanent and traffic load: Load case 1-5, 7  
Wheel load (traffic): 12-14 (configuration 2)

The heavy traffic lane is positioned in the middle of the width to find the maximum transversal moment.

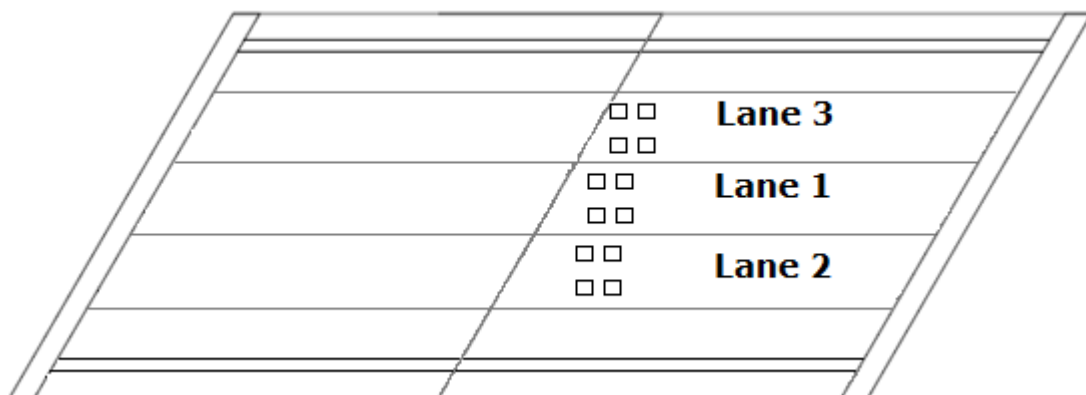


Figure 25, configuration 2 - governing configuration for moments in transverse direction with unloaded areas at the sides



Shear force (load combination 3):

The configuration for the governing shear force is shown in figure 26. To have a high shear force the loads must be close to the supports. Exactly near the support the shear capacity is remarkably increased because of the massive cross-section and the force in that area is transferred to the supports directly. It is advised to position the first wheel load 1d-2d from the support.

Distributed permanent and traffic load: Load case 1-6

Wheel load (traffic): 12-14 (configuration 3)

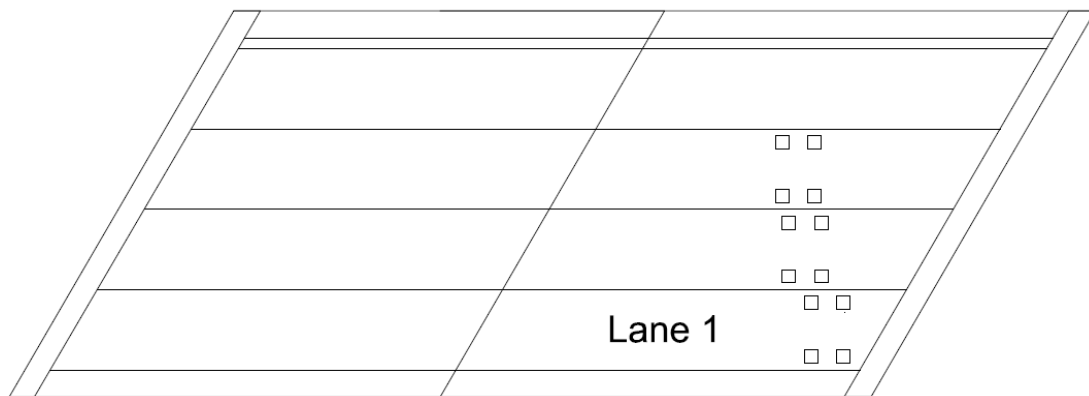


Figure 26, configuration 3 - governing configuration for the shear force

Torsional moments (load combination 4):

The configuration for the governing torsional moments is difficult to determine. Minalu [4] did a short study about this internal force and determined two configurations besides the ones that were available from practice.

Distributed permanent and traffic load: Load case 1-6

Wheel load (traffic): 12-13 (configuration 4)

For the most positive torsional moment, only lane 1 and lane 2 should be loaded with traffic UDL and the rest must be unloaded.

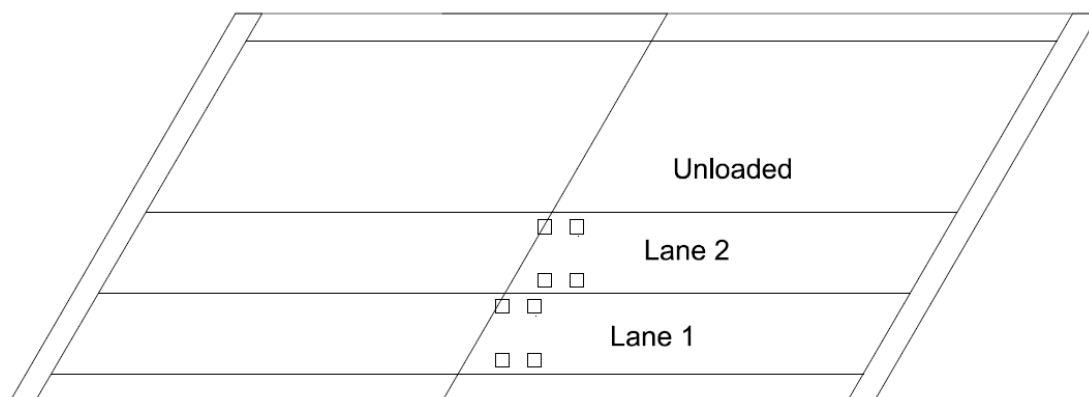


Figure 27, configuration 4 - governing configuration for the torsional moment

#### 4.6 Statically determined beam model

The prestressed girders are produced in the factory. As mentioned before, the self-weight and the prestressing are thus applied before the viaduct is assembled. The contributions of these loads to the internal forces are determined from a beam model and not from the plate model because the self-weight and the prestressing do not contribute to torsion. If the loads were to be inserted in the plate model they would induce torsional moments.

The beam model with self-weight and prestressing is schematized as follow:

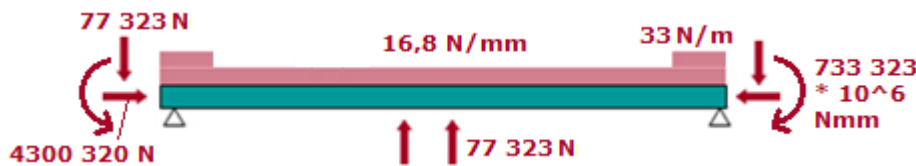


Figure 28, model for statically determined beam with self-weight and longitudinal prestressing

Because these loads are applied at individual beams and are symmetric, no torsional moments occur.

#### LONGITUDINAL MOMENT DIAGRAM

```
Model: ANALYSIS2
LC7: Load case 7
Element EL.MX..L MZ
Max = .733E9
Min = -.398E9
Factor = .259E-5
```

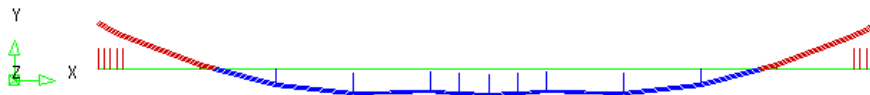


Figure 29, longitudinal moment in beam due to self-weight and prestressing [Nmm/mm]

#### SHEAR FORCE DIAGRAM

```
Model: ANALYSIS2
LC7: Load case 7
Element EL.NX..L QY
Max = .21E6
Min = -.21E6
Factor = .1E-1
```

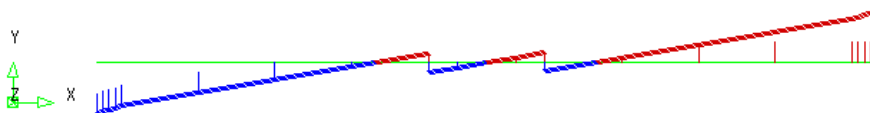


Figure 30, shear force in beam due to self-weight and prestressing [N/mm]

The shear stresses due to this shear force are:

$$\tau_{xz} = \frac{V}{2(\text{per web}) * t * z} = \frac{0,21 * 10^6}{2 * 200 * 1100} = 0,52 \frac{N}{mm^2}$$

## 5 ORTHOTROPIC PLATE MODEL

### 5.1 Introduction

As an introduction to the program (iDAINA) and to these types of viaducts (skew precast box beam) an orthotropic plate model is used for the analysis. The findings for this model are used for comparison with the 2,5 D shell model.

From theory it seems that the orthotropic 2D plate model is very applicable for modeling the deflections and the longitudinal moments. The goal of this part of the thesis is to use this model to find the critical areas in the plate for the internal forces. It is important to get a first estimation for the order of magnitude of these forces.

Several parameters are determined to model this viaduct as an orthotropic plate in DIANA. This is explained extensively in appendix A & B. The most important aspects are summarized in this chapter.

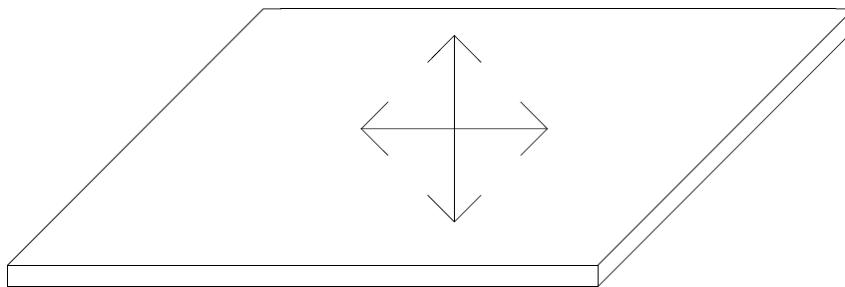


Figure 31, orthotropic plate

### 5.2 Geometry and parameters

#### 5.2.1 Span and width

The span of the plate is 32250 mm and the width is 14400 mm. The skew angle is 60 degrees.

#### 5.2.2 Cross-section

The cross-section of the box girder is schematized as shown in figure 32. This cross-section is based on the SKK 1100 girder from Spanbeton.

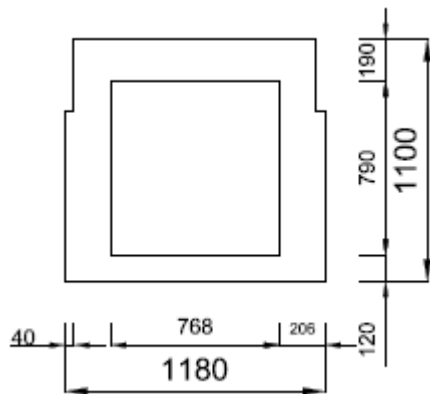


Figure 32, cross-section box girder – dimensions in [mm]

### PARAMETERS

The cross-sectional parameters are determined in appendix A. In table 9 the summary of the parameters is found.

### TRANSVERSAL STIFFNESS

Special attention is paid to the transversal stiffness. For this kind of girders this stiffness can be modelled in several ways. A short study has been done in DIANA.

In theory books it is advised to determine this stiffness with the following model (method 1):

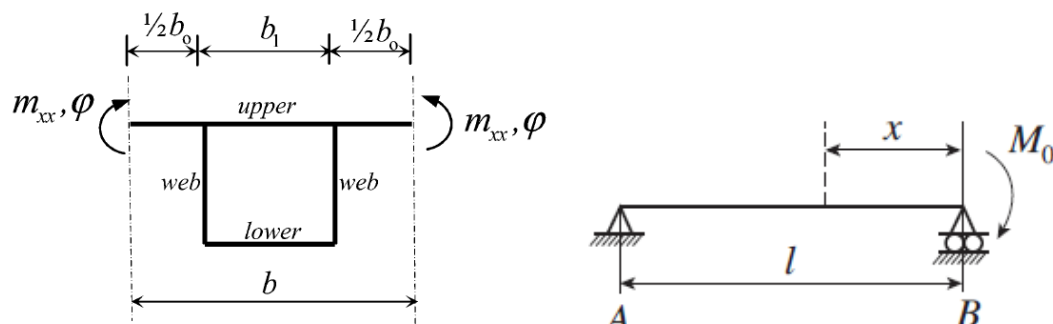


Figure 33, model for determining the stiffness - fig 21.8 [14] & Figure 34, vergeet-me-nietje for the relation between a moment and the rotation and deflection

This model has been derived from the following “vergeet-me-nietje” where the moment is present at both ends. The question arises: is it possible to determine this stiffness with only a moment at one side?

Formula for the relation between the rotation and the moment if present at one side:

$$EI_{yy} = \frac{m_{yy} * W_{beam}}{3 \varphi}$$

Formula for the relation between the rotation and the moment if present at two sides:

$$EI_{yy} = \frac{m_{yy} * W_{beam}}{2 \varphi}$$

This aspect is investigated and it is found that the boundary condition plays a big role. If only one girder is modelled then this aspect is very sensitive and the girder is modelled too stiff. It is found that if two moments are applied (one at each end) the boundary conditions are not governing anymore.

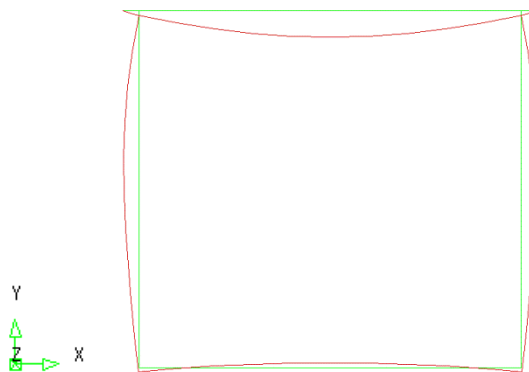


Figure 35, rotation of the cross-section due to moments at both ends (DIANA result)

Another configuration (method 2) has also been investigated. This configuration is based on the following “vergeet-me-nietje”:

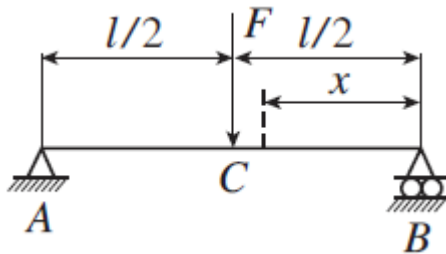


Figure 36, vergeet-me-nietje for the relation between the deflection and a force

$$EI_{yy} = \frac{F * W^3_{beam}}{48 * w}$$

It was already found that if one girder is modelled, the boundary conditions would be very sensitive. For this reason three girders were modelled in DIANA:

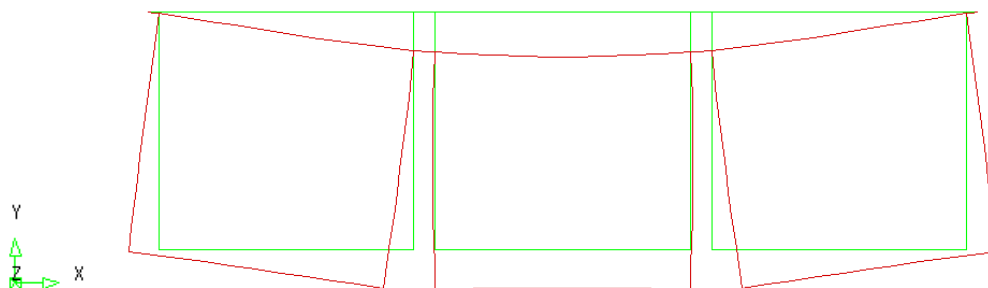


Figure 37, geometry and deflection due to point load (schematized as distributed load) (DIANA result)

Both methods prove to give almost the same results.

Table 8, results from the analysis for determining the transverse stiffness

Method	Stiffness ( $D_{yy}$ ) Nmm <sup>2</sup>
1 (moment – rotation)	46 * 10 <sup>9</sup>
2 (force – deflection)	48 * 10 <sup>9</sup>

### Conclusions

It is best to apply two moments at each ends for one box beam girder. Because the moments are in equilibrium, the boundary conditions do not affect the result. If this is not done (only one moment for example), the exact stiffness should be determined of the joints between the girders.

A hand calculation, as presented in appendix A, is a safe assumption but the exact stiffness is much higher and should be determined by a FEM.

It is also possible to apply a few girders next to each other and to apply the following relation:

$$EI_{yy} = \frac{F * w_{beam^e}}{48 * w}$$

Where “w” is the deflection. This solution has less accuracy because of the boundary conditions. These are modelled with fixed support while in the real situation a translation spring would be a better model.

All the material and cross-section parameters are found in the table below:

Table 9, cross-section parameters

Parameter	Symbol	Value	Unit
Young's Modules	E	3,50 * 10 <sup>4</sup>	N/mm <sup>2</sup>
Poisson's Ratio	v	2,00 * 10 <sup>-1</sup>	[-]
Shear Modules	G	1,50 * 10 <sup>4</sup>	N/mm <sup>2</sup>
Flexural Stiffness (x)	i <sub>x</sub>	8,00 * 10 <sup>7</sup>	mm <sup>4</sup>
Flexural Stiffness (y)	i <sub>y</sub>	0,13 * 10 <sup>7</sup>	mm <sup>4</sup>
Diagonal Term	i <sub>v</sub>	0,90 * 10 <sup>4</sup>	mm <sup>4</sup>
Surface	A <sub>x</sub>	564	mm <sup>2</sup>
Surface	A <sub>y</sub>	310	mm <sup>2</sup>
Torsional Stiffness (xy)	i <sub>xy</sub>	1,6 * 10 <sup>8</sup>	mm <sup>4</sup>
Torsional Stiffness (yx)	i <sub>yx</sub>	1,1 * 10 <sup>6</sup>	mm <sup>4</sup>
Shear Area (x)	A <sub>sx</sub>	4,5 * 10 <sup>2</sup>	mm <sup>2</sup>
Shear Area (y)	A <sub>sy</sub>	1,9 * 10 <sup>2</sup>	mm <sup>2</sup>

These stiffness parameters are calculated for 1 mm strip of the plate. Further details can be found in appendix A.

### 5.3 Finite element modeling

For the orthotropic plate model several types of elements can be used to cope with the orthotropy. The orthotropy can be coped with using a plate bending element (CQ24P) for example. With this type of element orthotropic parameters can be inserted as geometry orthotropy. The disadvantage of these types of elements is that it can only be loaded within its plane.

Because the influence of the prestressing is also investigated, it is better to use (flat or curved) shell elements (CQ40S). These are a combination of plate bending element and a plane stress element.

In appendix B it is shown that the results using curved shell elements are also very accurate with less numerical imperfections.

#### 5.3.1 Meshing and element size

The maximum element size is determined according to the "Guidelines for Nonlinear Finite Element Analysis of Concrete Structures". These are still applicable, even though the calculation is linear, because it is expected that for a linear calculation the fineness of a mesh is less critical. The maximum is:

$$\max \frac{l}{50}, \frac{b}{50}, \frac{h}{5}$$

$$\frac{32550}{50} = 645 \text{ mm}$$

$$\frac{14400}{50} = 288 \text{ mm}$$

$$\frac{500}{5} = 100 \text{ mm}$$

The limitation of the division for one line is 100. Because of this the span is modelled in two lines and a division of 60 per line is used. This gives 30 elements per half span. With a total of 60 for the span the size of the element:

$$\frac{32250}{60} = 537,5 \text{ mm}$$

For the width a division of 60 is used over one line. This gives an element size of:

$$\frac{14400}{30} = 480 \text{ mm}$$

A total of 1800 elements are applied and this is just above the minimum amount. The calculation time of the analysis is influenced if this amount is increased. The orthotropic plate model is used as an introduction to the program. This means a lot of analysis could be carried out if needed. This is the reason to choose a minimum amount of elements for this specific model.

**VIADUCT SURFACES AND MESH**

*Element: CQ40S (8-node quadrilateral shell element) or CQ24P (8-node plate bending elements)*

*Amount of elements: 1800*

*Elements size: 560 x 480 mm*

To model the massive parts, surfaces are appointed. These surfaces can have different physical and material properties. The plate cannot be modelled with one surface because of the limit of division to one line.

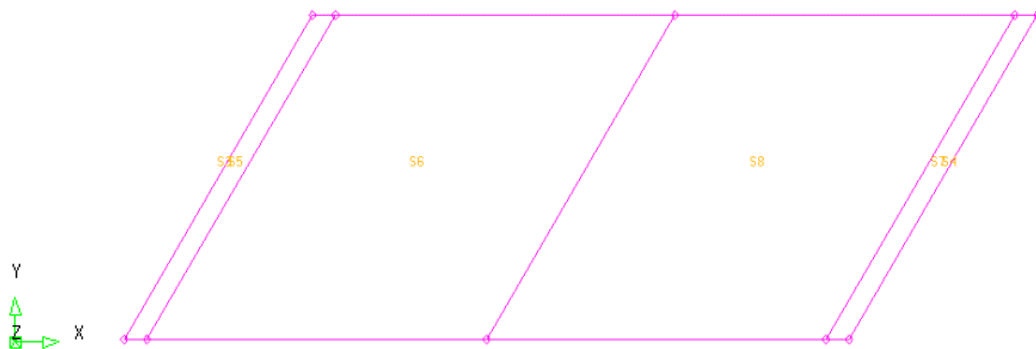


**Figure 38, division in to surfaces of the plate**

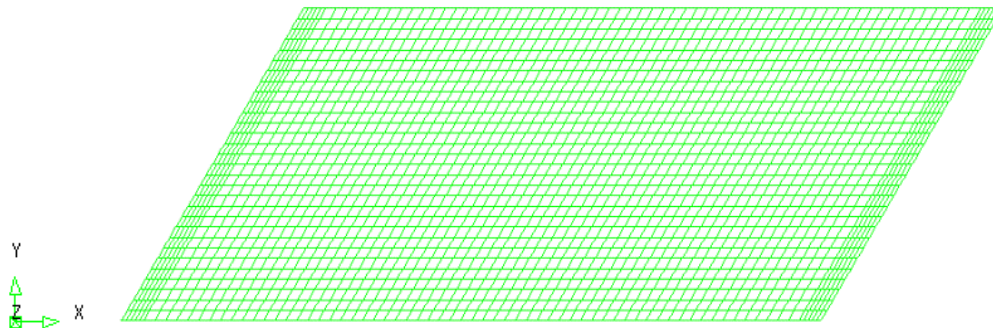


**Figure 39, mesh of the orthotropic plate (including the end beams)**



### 5.3.2 Loads

The modelling of the loads has been explained in paragraph 4.4. **The modelling of the permanent load** is relatively accurate. These loads are inserted as a surface load and the division is made using surfaces. This means the input of the loads is (almost) exactly equal to the output.

**The traffic loads have been modelled using load masks.** The advantage of this option is that the viaduct does not have to be divided into surfaces. The disadvantage is that the output has to be checked and compared to the input. The accuracy is also very sensitive to the chosen mesh. The division of the elements is not exactly between the boundaries of the load masks. The following load cases need a correction factor for the post-processing:

Table 10, correction factor for the loads

Load case		Correction factor
2	Asphalt	1,06
4	Edge surface	0,90
6	Heavy traffic lane (edge)	1,04
7	Heavy traffic lane (mid)	1,04
x	Tandem axle 1	0,80
x	Tandem axle 2	0,81
x	Tandem axle 3	0,84

## 5.4 Introduction and influence of various aspects

This paragraph is an introduction to the results gained in DIANA and the influence of various aspects on the modelling of the viaducts and on these results.

### 5.4.1 Straight and skew orthotropic plate

The plate is loaded with a uniformly distributed load (0.001 N/mm<sup>2</sup>) so that the results can be checked with a hand calculation. The supports are simply supported. The plate stiffness and material properties are as described in paragraph 4.2.

#### **DEFLECTION**

Previous studies showed that the deflection should decrease for a skew plate when compared to a straight plate. From a simple analysis this is confirmed. The reduction is approximately 15%.

The hand calculation of a beam should be approximately the same as the straight plate model loaded with a uniformly distributed load.

$$w_{max} = \frac{5}{384} * \frac{ql^4}{E * I_x}$$

When the values are filled in:

$$w_{max} = \frac{5}{384} * \frac{0.001 * 14400 * 32250^4}{35000 * 8,0 * 10^7 * 14400} = 5 \text{ mm}$$

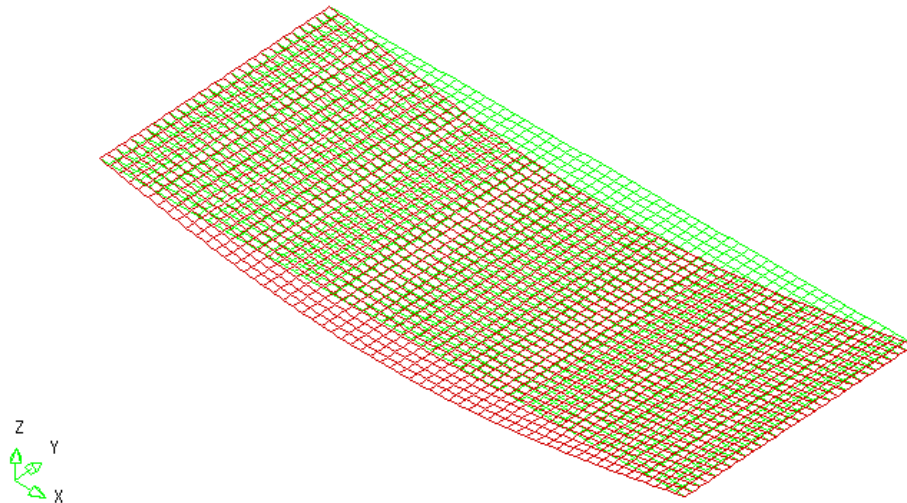


Figure 40, deflection of the skew plate

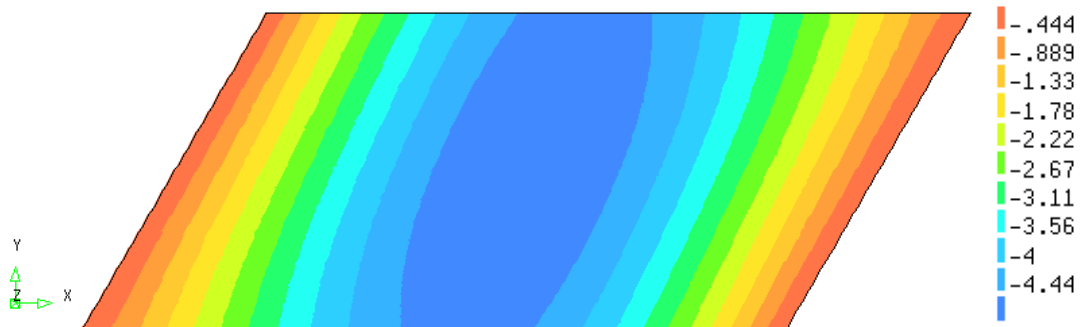


Figure 41, contour plot of the deflection [mm]

Table 11, deflection straight and skew plate

Plate	Deflection
Straight	4,85 mm
Skew ( $60^\circ$ )	4,44 mm

### **LONGITUDINAL, TRANSVERSAL AND TORSIONAL MOMENTS**

The orthotropic plate that can schematize this viaduct cannot spread the load as much as an isotropic stiff plate because of the lower transverse stiffness. The path of the loads wants to be perpendicular to the supports. The box beam viaduct has a high torsional stiffness. This means that it gives resistance to the torque and loads can be transferred. The transverse stiffness is very low compared to the longitudinal bending stiffness and the torsional stiffness. The load is transferred to the supports mainly by longitudinal and torsional moments. The results are shown in the figures on the page.

For a beam or a straight viaduct the maximum moment is found at the half of the span for every strip. This is not valid for a skew plate anymore. At the edge the maximum moment is just over the mid of the plate closer to the obtuse corner.

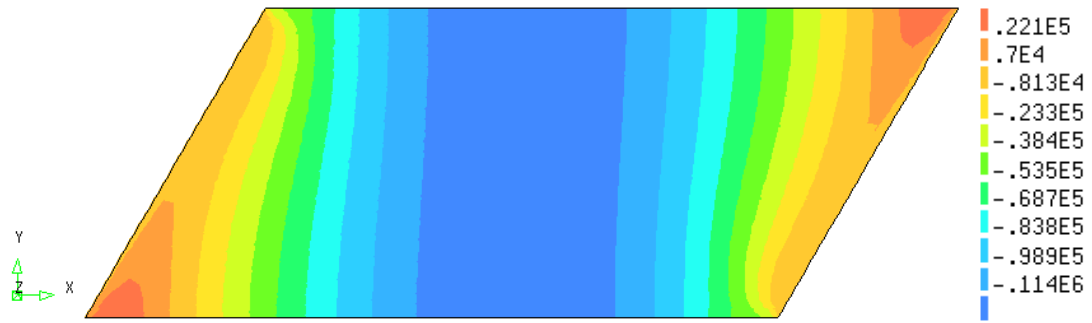


Figure 42,  $m_{xx}$  - skew plate – uniformly distributed load [Nmm/mm]

From a hand calculation a first estimation for the longitudinal moment is obtained. The plate is then schematized as a beam on simple supports:

$$M_{max} = \frac{1}{8} * q * l^2 = \frac{1}{8} * 0.001 * 14400 * 32250^2 = 1,75 * 10^9 \text{ Nmm for total girder}$$

$$\frac{1,75 * 10^9}{14400} = 0,13 * 10^6 \text{ Nmm/mm}$$

The increase in torsional moments is found in figure 43. For an isotropic plate the maximum values are found at the obtuse corners (figure 44) but the values at the middle of the plate is almost the same as for the orthotropic plate. The absence of the peaks at the corner with the orthotropic plate is due to the lower transversal stiffness. This is shown in figure 45. In accordance to the Mindlin/Reissner theory the  $m_{xy}$  is zero at the edges.

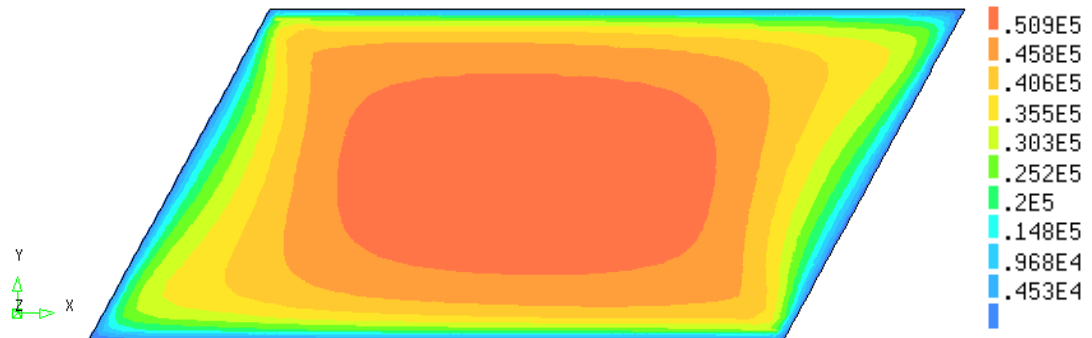


Figure 43,  $m_{xy}$  - skew plate - uniformly distributed load – orthotropic [Nmm/mm]

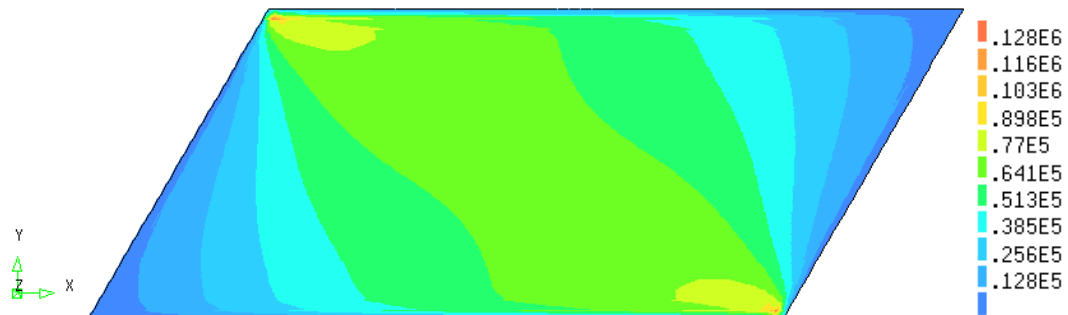


Figure 44,  $m_{xy}$  – skew plate - uniformly distributed load – isotropic [Nmm/mm]

The isotropic plate has high transversal moments at the obtuse corners, the orthotropic plate has its maximum also at the obtuse corners but the values are negligible compared to the isotropic plate. This is observed in a contour plot when the limits are manually chosen. Green means that the values are between 0.5E4 Nmm/m and -0.2E5 Nmm/m. The blue areas are the extreme values above -0.2E5 Nmm/m. It is concluded that for the isotropic plate the transversal moments at the obtuse corners are much higher (10 x) than orthotropic plate and this explains the extreme values for  $m_{xy}$  at the obtuse corners as well. For the isotropic plate, longitudinal and transversal moments are present which leads to torsion.

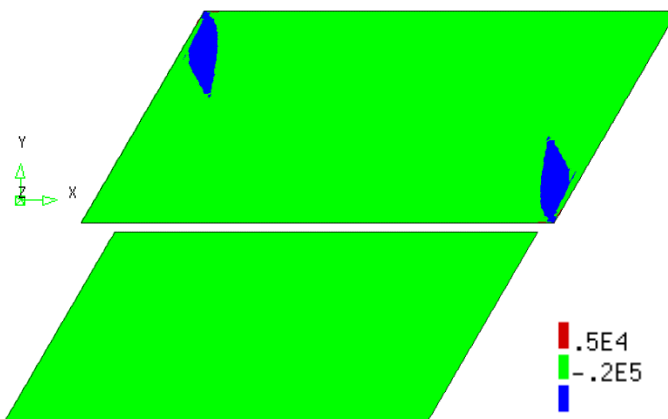


Figure 45, differences between transverse moments in iso- and orthotropic plates [Nmm/mm]

#### 5.4.2 Boundary conditions

As an introduction, the supports are assumed as simple supported. In CUR Rapport 53 [18] it is advised to model the stiffness of the supports and not schematize them as rigid supports. Each beam has one bearing at each side.

In practice the supports are often modelled as springs with a stiffness that causes a 0,5 mm deflection as a result of self-weight of the girders.

For this viaduct a stiffness of  $536 \cdot 10^3$  N per millimeter is inserted:

$$A_{girder} = 664880 \text{ mm}^2$$

$$Selfweight = 25 \frac{kN}{m^3} = 25 \cdot 10^{-6} \frac{N}{mm^3}$$

$$Force \text{ per bearing} = 25 \cdot 10^{-6} \cdot \frac{32250 \cdot 664880}{2} = 268 \text{ kN}$$

$$For \ 1 \text{ mm the stiffness is: } 268 \cdot 2 = 536 \cdot 10^3 \text{ N per mm.}$$

In DIANA an interface element is used. The thickness of the bearing is 38 mm, the width of the bearing is 500 mm approximately.

In appendix C the process of inserting this stiffness and validation is shown. The interface element is present along the width of the viaduct.

**INTERFACE ELEMENTS**

At the boundary of the plate an interface element is inserted: CL24I - line, 3+3 nodes.

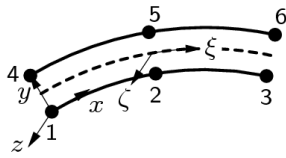


Figure 46, CL24I element

The bottom line is supported with hinges. The interface element has one element over the height and the division in the transverse direction is the same as for the plate.

In the property manager the thickness (line) is inserted as 500 mm. The stiffness is inserted in the material properties (interface) with a stiffness of:

$$k = \frac{K}{d * 1200} = 536 * \frac{10^3}{500 * 1200} = 0.9 \text{ N/mm}^3$$

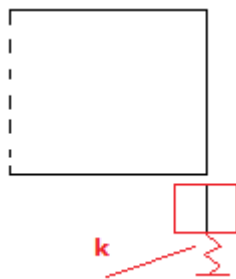


Figure 47, modelling of the bearing

**DEFLECTION**

The deflection of the plate has been determined for both a uniformly distributed load of 0.001 N/mm<sup>2</sup> and a uniformly distributed load of 0.014 N/mm<sup>2</sup> which is equal to the self-weight. The results from the self-weight are used to verify the stiffness as it was assumed that the self-weight gives a deflection of 0,5 mm at the supports.

Table 12, deflection due to a uniformly distributed load of 0.001 N/mm<sup>2</sup>

Plate	Maximum deflection at mid span
<b>Straight</b>	4,85 mm
<b>Skew (60<sup>0</sup>) – simply supported</b>	4,44 mm
<b>Skew (60<sup>0</sup>) – use of interface elements</b>	4,11 mm

For the skew plate it is seen that the distribution of the support reactions are different than for the straight plate. The support reactions at the obtuse corner have a greater magnitude and small forces are present at the acute angle or they are even uplifting as shown in this case.

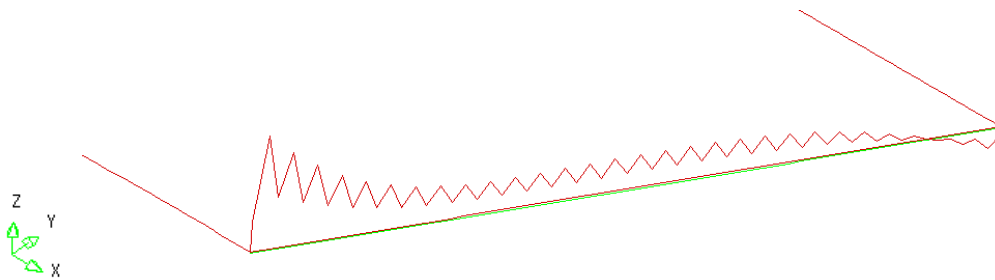


**Figure 48, distribution of the support reactions at the bearing (left is obtuse corner)**

This has only a small effect on the moment distribution. The moments decrease with approximately 5% because of the changing distribution of forces at the supports.

### 5.4.3 Massive end parts

The end of each of the girders is a massive part. This is important for the introduction of the prestressing and the capacity for the shear force.

The height is 1100 mm, the width is 1200 mm and the material property is as stated in paragraph 4.2. The transverse prestressing is not present at the massive parts. These end beams are modelled as isotropic beams.

The influence of these massive end parts on the distribution of the forces are presented shortly.

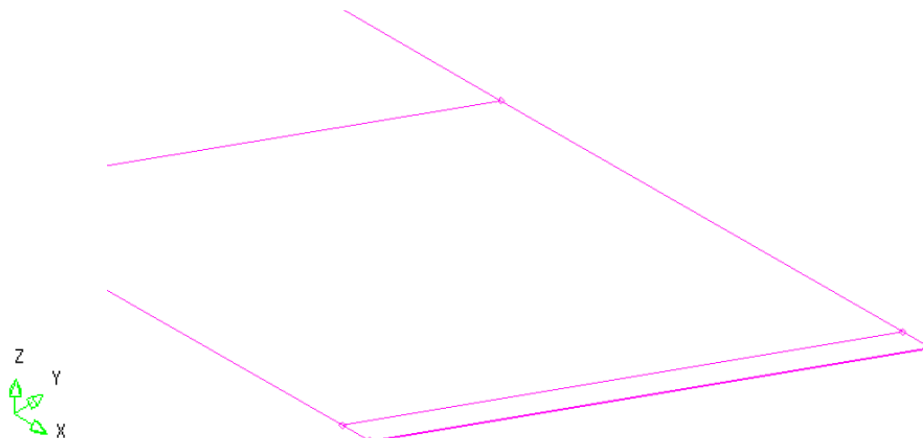


**Figure 49, massive end parts**

### **DEFLECTION**

The deflection is mainly depended on the longitudinal bending stiffness ( $EI$ ) of the plate (beams). The massive part at the inside of the beams does not have a big contribution to this stiffness and therefore the deflection is not influenced (a lot). The new deflection is 3,85 mm instead of 4,11 mm without the end massive beams.

**LONGITUDINAL MOMENTS**

The same aspect is observed for the longitudinal moment. This internal force is also very dependent on the longitudinal bending stiffness ( $EI$ ). A small reduction for the maximum value is observed.

**TRANSVERSAL MOMENTS**

The effect of the massive end beams is clearly seen when the transversal moments are observed. There is a big difference between the transversal stiffness of the box girder beams and the massive end beams.



Figure 50, transversal moments with the presence of end beams [Nmm/mm]

**TORSIONAL MOMENTS**

The presence of the end beams cause high transversal moments in the beams. This causes a change in the torsional moments as well. The plate without the end beams had the maximum torsional moments at mid span because at the obtuse corners the plate carries the load in one direction and torsion is not present. With the presence of the end beams this changes and torsional moments near the obtuse corner in the end beams are present.

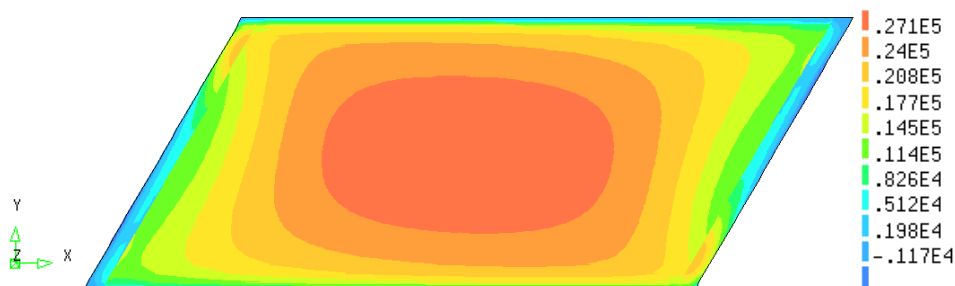


Figure 51, torsional moments with the presence of end beams [Nmm/mm]

#### 5.4.4 Transverse prestressing

Due to the transverse prestressing a compression force is present in the joints and the load spreads over the girders. With the presence of the transversal prestressing uncracked cross-section may be assumed over the transverse direction. This should be checked later.

The prestressing also causes an external moment because the applied force is not at the neutral axis. The moment due to transverse prestressing is not modelled in the practice. This moment is often not modelled because it compensates for the influence of the edge load at the edge beam (which is left out of the calculation as well).

If (curved) shell elements are used then the transverse prestressing could be modelled for a short study. The exact influence could be determined, if the transversal prestressing is modelled correctly. In practice the transverse prestressing is fully in equilibrium with itself. This is obvious for the middle part of the skew plate but this also must apply for the skew part of the plate.

A simple solution is to model the prestressing force as a distributed load (force and moment) over the edge of the viaduct and to ignore the rule of equilibrium. The exact modelling of the prestressing requires a lot of time and therefore in this paragraph only the simple solution and its influence on the results is examined.

The distributed force is:  $131\ 000 / 1200 = 110\ \text{N per mm}$ .

In the plate model the transverse prestressing cannot be inserted at the applied height. Because it's a plate with only the neutral axis modelled, the prestressing is applied at the neutral axis. This means that an external moment is modelled with a magnitude of:

$110\ \text{N} \times 430\ \text{mm} = 47300\ \text{Nmm per mm}$ .

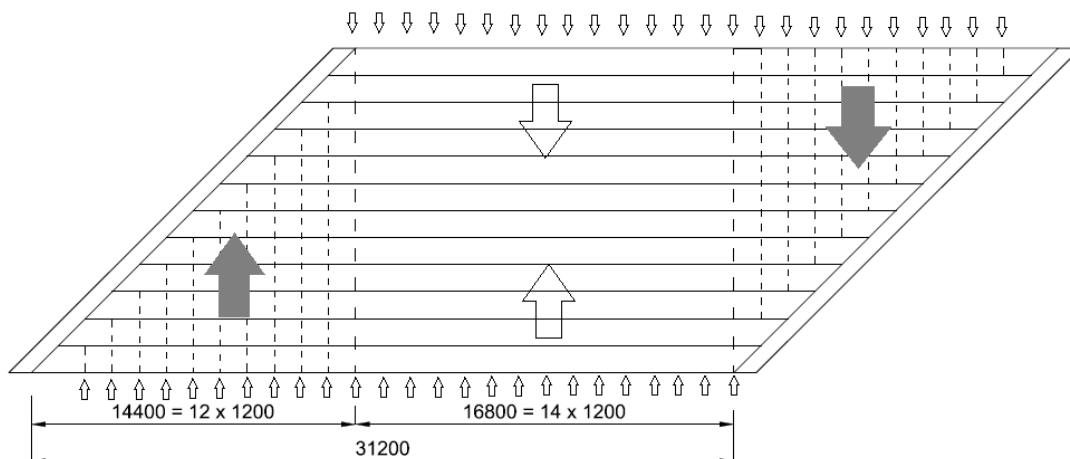


**Figure 52, transverse prestressing - distributed load and moments [mm]**

The forces showed in figure 52 were inserted in the model and the results are checked.

In figure 53 the shear force is presented along the edge (longitudinal direction) for both cases: with and without transversal prestressing.



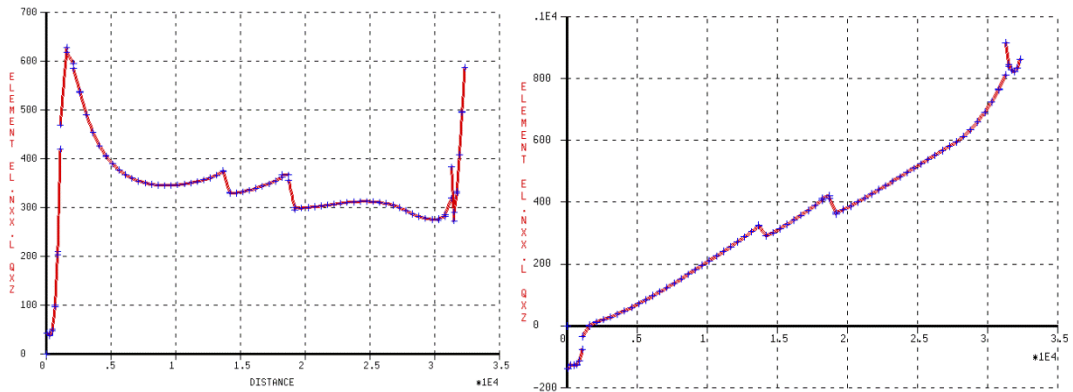


Figure 53, shear force - cross section 1<sup>st</sup> girder along the edge (with and without prestressing) – EC 1 traffic load [N/mm]

The two white arrows (figure 52) are in equilibrium at the middle of the plate. At the skew part the gray arrows should make equilibrium with the individual anchored prestressing. This is not taken in to account for the simple model.

If only the forces of figure 52 would be modelled then an extra moment would be introduced which gives rise to extra forces in the corners to take it up. This is shown by plotting the shear force in the first beam near the edge.

The moment due to transversal prestressing causes the load to spread better but effect is negligible for this case.

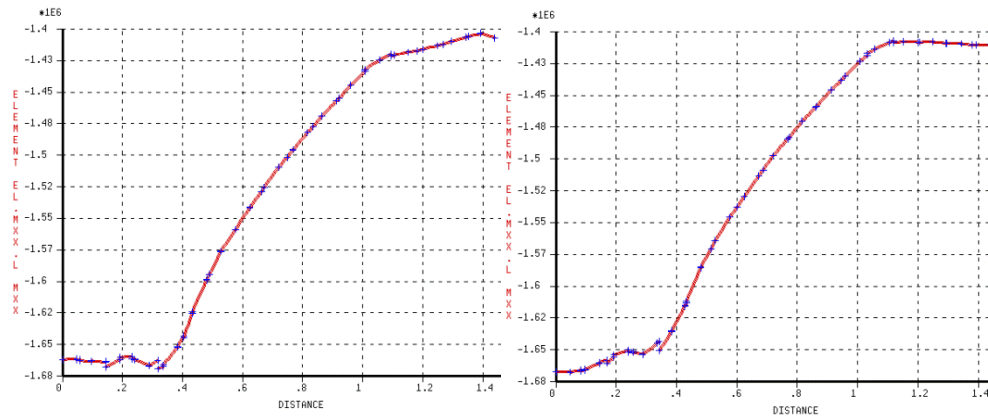


Figure 54, longitudinal moment over the width - left is with transverse prestressing; right is without – EC 1 traffic load [Nmm/mm]

The influence of the transverse prestressing on the transversal moment is better visible. In figure 55 the transversal moment along the width (of the mid span) is presented. It is seen that the influence is only within the first few meters. Part of this is due to the prestressing moment and part of it is due to the extra introduced moment.

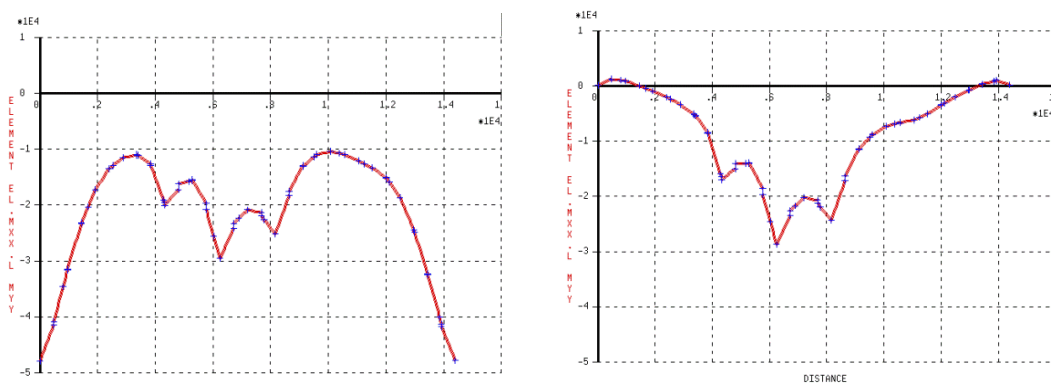


Figure 55, transverse moment over along the width (with and without) the transverse prestressing [Nmm/mm]

**CONCLUSION**

From these results it is concluded that simple modelling of the prestressing is not a good representation of the real situation. In practice the transversal prestressing makes equilibrium with itself and this is not the case with this simple model.

A separate research should be done to investigate the exact influence of the transverse prestressing. It is advised to model the anchors as a force that would be in equilibrium with the uniformly distributed load at the skew part of the viaduct.

For the results of the following chapters, the transverse prestressing is not taken into account. It is expected that the prestressing cancels the edge load out. For that reason the edge load is also not modelled.

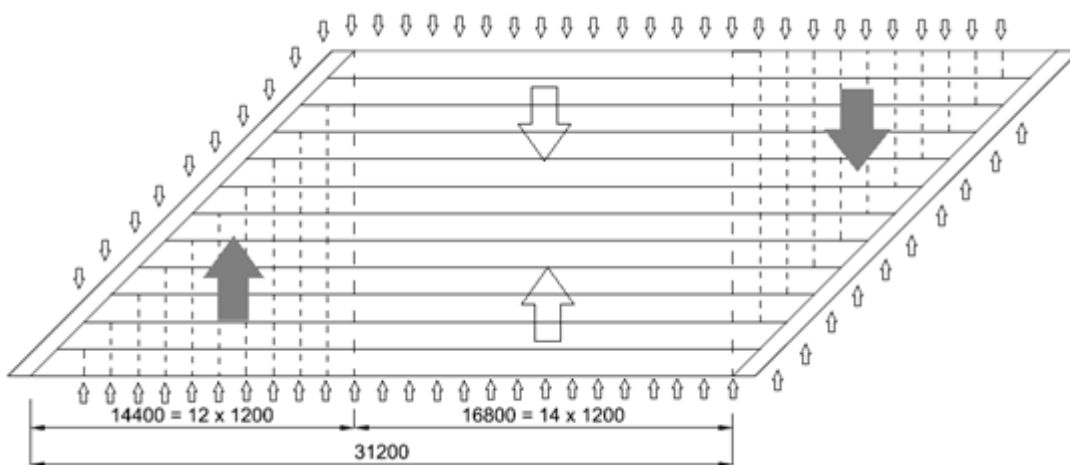


Figure 56, individual anchor forces for equilibrium [mm]

### 5.4.5 Calculation of shear stresses in a plate

The shear stresses are an important aspect for the comparison of the two models. In the plate the results are forces and these could be checked separately. This is not possible for the 2,5D shell model because the output is stresses.

This stress component ( $S_{xz}$ ) arises from shear forces and from torsional moments in a girder. The cross-section of the plate is not representative for the cross section of the girders. Therefore the meaning of the  $S_{zx}$  in the plate cannot be related to the girders in a simple way. There are a few methods in practice for the calculation of the shear stress in the webs of the girder due to forces in the plate.

One of these methods is to mediate the shear force over the width of the girder after which the shear stresses in the webs can be calculated. The same procedure is done for the torsional moments in the plate.

The shear force is then divided over the two webs equally and the torsional moment causes forces in the webs too (directed to the other side in one of the webs). This is schematized in the following figures. It is concluded that the left web is the governing web. In this web the shear stresses due to the shear force and the torsional moment amplify each other. The contributions of the shear force and the torsional moments are calculated separately.

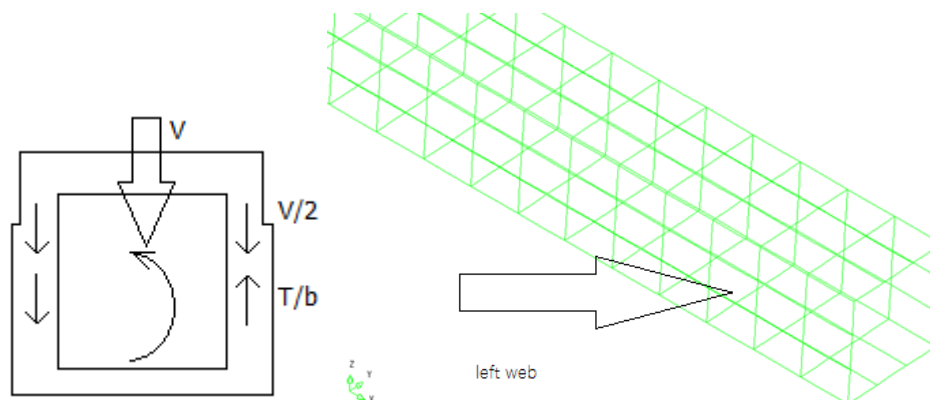


Figure 57, shear force and torsional moment working on the girder

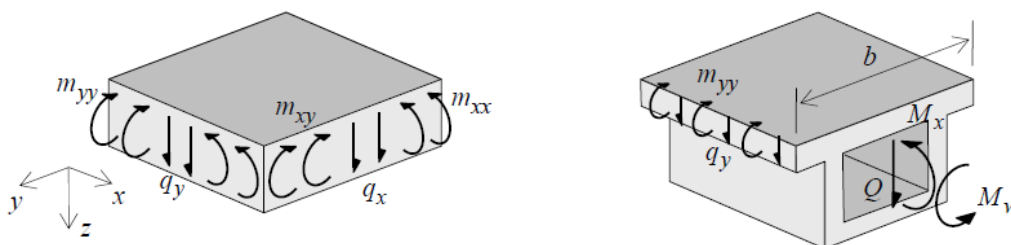


Figure 58, forces in a plate and in a box girder beam [19, p24]

It is important to notice that a plate can take up torsional moment in two directions while in an orthotropic girder only one is available. Because of equilibrium the two torsional moments in a plate are equal. This is not the case for the girder. The calculation of the shear stresses due to the torsional moment is done according to the Eurocode 2 paragraph 6.3.2.

$$\tau_{t,i} * t_{ef,i} = \frac{T_{ed}}{2 * A_k}$$

$$V_{ED,i} = \tau_{t,i} * t_{ef,i} * z_i$$

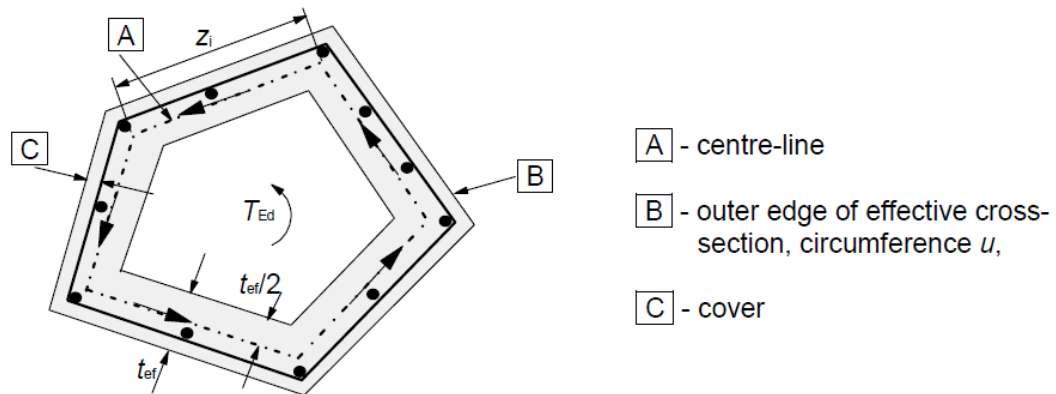


Figure 59, Notations and definitions used in Section 6.3 (Eurocode 2)

$A_k$  = area enclosed by the centre-lines of the connecting walls, including inner hollow areas.

$\tau_{t,i}$  = torsional shear stress in wall  $i$

The average torsional moment is determined according to **J. Blaauwendraad (2010)**, Plates and FEM: Surprises and Pitfalls (chapter 21.2.2):

$$m_{xy} = \frac{2i_{xy}}{i_{xy} + i_{yx}} m_{av}, \quad m_{yx} = \frac{2i_{yx}}{i_{xy} + i_{yx}} m_{av}$$

This is demonstrated in the next pages. For the following calculations the plate is loaded with a uniformly distributed load (0.001 N/mm<sup>2</sup>).

Two cross-sections are examined: one just after the massive part (maximum shear force) and one at the middle of the plate (where the torsional moments has a maximum value in the plate model). In the results "left" and "right" webs are mentioned. Because this might be unclear, in figure 57 the left web is appointed for that perspective.

**FIRST CROSS-SECTION**

Shear force

At the acute corner (the last few meters) an uplifting force is present. The maximum value is found at the edge close to the obtuse corner.

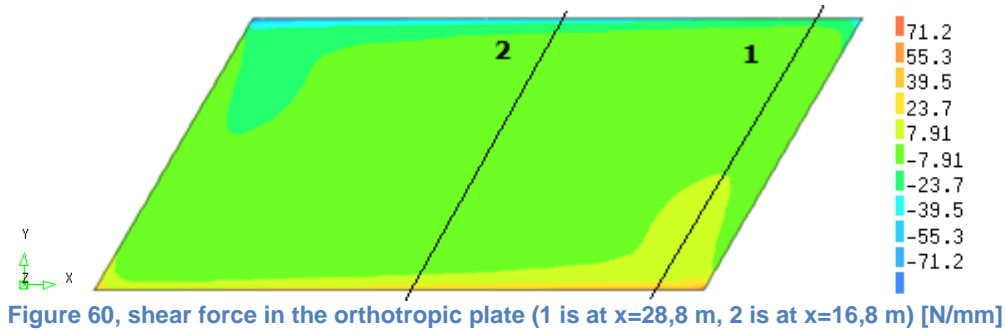


Figure 60, shear force in the orthotropic plate (1 is at x=28,8 m, 2 is at x=16,8 m) [N/mm]

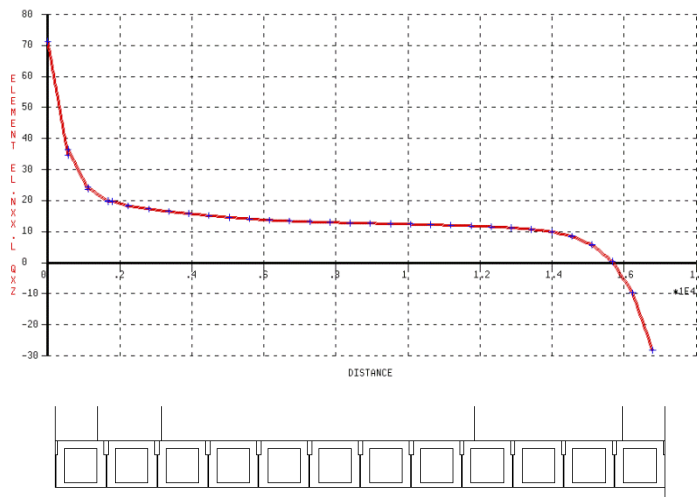


Figure 61, shear force over the width [N/mm]

The shear force over the first girder is:

$$V_{average,1\ girder} = V_{avg} * width - beam = \frac{72 + 22}{2} * 1200 = 56,4 * 10^3\ N$$

Table 13, shear force per girder (average shear force from graph x 1200 mm)

# Girder	Shear force [kN]	# Girder	Shear force [kN]
1	56,4	7	18,0
2	24,0	8	16,8
3	22,8	9	16,8
4	20,4	10	14,0
5	19,2	11	11,0
6	18,0	12	-12,0

If this force is equally divided for the two webs, the shear force per web is:  $28,2 * 10^3\ N$ .

The shear stress due to this force in the web is:

$$\tau_{xz} = \frac{V}{t * z} = \frac{28,2 * 10^3}{200 * 1100} = 0,12 \frac{N}{mm^2}$$

The second girder has the following shear stress per web:

$$\tau_{xz} = \frac{12 * 10^3}{200 * 1100} = 0,06 \frac{N}{mm^2}$$

Torsional moment

The torsional moment over the width is presented in figure 63.

The shear stress in the web should be calculated according to the following formula:

$$\tau_{t,i} * t_{ef,i} = \frac{T_{ed}}{2 * A_k}$$

A<sub>k</sub> is the area enclosed by the webs and the flanges = 768 \* 790 = 606 720 mm<sup>2</sup>

T<sub>d</sub> is the torsional moment per girder: 2 \* m<sub>xy</sub> \* b (explained in the introduction)

z = 1100 mm

t = 200 mm

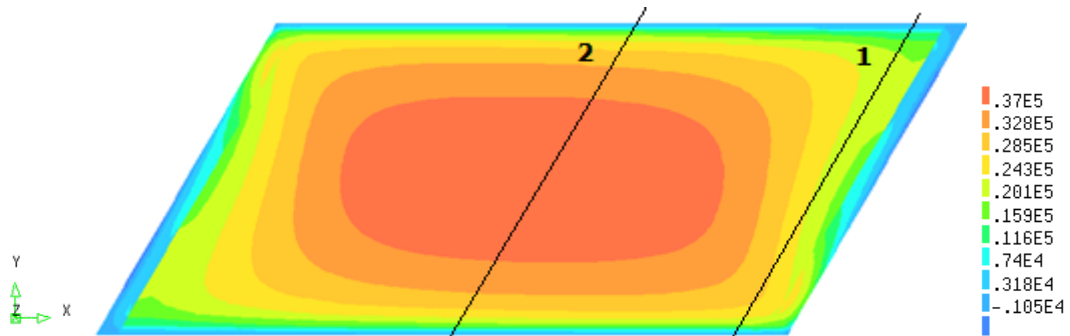


Figure 62, contour plot of the torsional moment in the skew plate model [Nmm/mm]

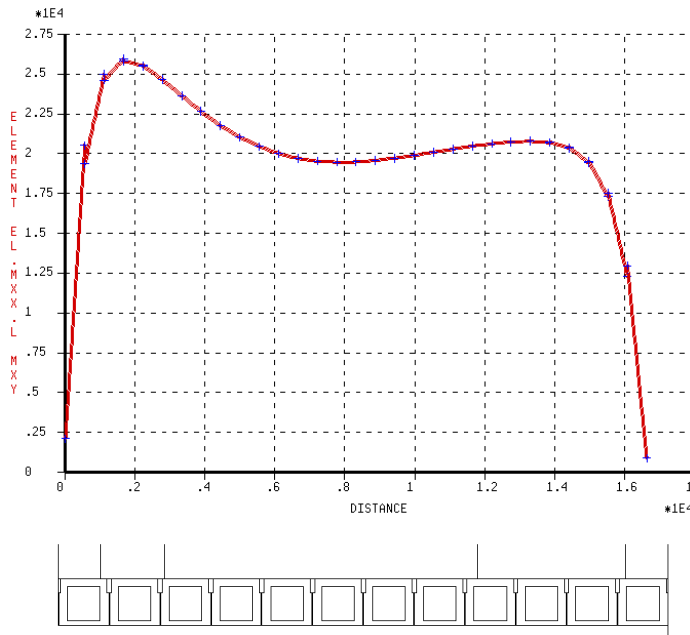


Figure 63, torsional moment over the width (at transition between massive and hollow) [Nmm/m]

Table 14, torsional moment over the width (average from graph \* 1200)

# Girder	Torsional moment * 10 <sup>6</sup> Nmm	# Girder	Torsional moment * 10 <sup>6</sup> Nmm
1	15,0	7	30,0
2	27,0	8	25,8
3	24,0	9	22,8
4	22,8	10	24,0
5	25,2	11	25,2
6	24,0	12	9,0

The average torsional moment is:  $1,25 * 10^4$  Nmm/mm

The torsional moment  $m_{xy}$  for the first girder is:  $1,25 * 10^4 * 1200 = 15 * 10^6$  Nmm

The shear stress due to the torsional moment ( $2 * m_{xy}$ ) is:

$$\tau_{t,i} = \frac{T_{ed}}{2 * A_k * t_{ef,i}} = 30 * \frac{10^6}{2 * 606720 * 200} = 0,11 \frac{N}{mm^2}$$

If the stresses are added, then in the left web of the first girder the total shear force is:  $0,120 + 0,115 = 0,24$  N/mm<sup>2</sup>.

The shear force in the right web of the first girder is:  $0,120 - 0,115 = 0,004$  N/mm

In the table below the shear stresses due to the shear force and the torsional moment for all the girders are added up as has been done for the first girder:

Table 15, summation of the shear stress due to shear force and torsional moment

Girder	Average shear stress per web N/mm <sup>2</sup>	Shear force (stress) due to torsional moment per web N (N/mm <sup>2</sup> )	Shear stress left web	Shear stress right web
1	0,120	0,115	0,24	0,00
2	0,060	0,226	0,29	-0,17
3	0,052	0,210	0,26	-0,16
4	0,050	0,201	0,25	-0,15
5	0,044	0,193	0,24	-0,15
6	0,041	0,177	0,22	-0,14
7	0,041	0,177	0,22	-0,14
8	0,038	0,185	0,22	-0,15
9	0,038	0,197	0,24	-0,16
10	0,032	0,197	0,23	-0,17
11	0,025	0,189	0,21	-0,16
12	-0,027	0,065	0,04	-0,09

When the values of the shear stresses due to the shear force and the torsional moments are compared it is seen that for 2 – 12 the shear stresses due to the torsional moments are much bigger. This causes negative shear stresses in the right web but of smaller magnitude.



**SECOND CROSS-SECTION**

The same procedure is done for the cross-section at mid span where the torsional moments have a maximum value and the shear force contribution is mainly at the edge.

Shear force

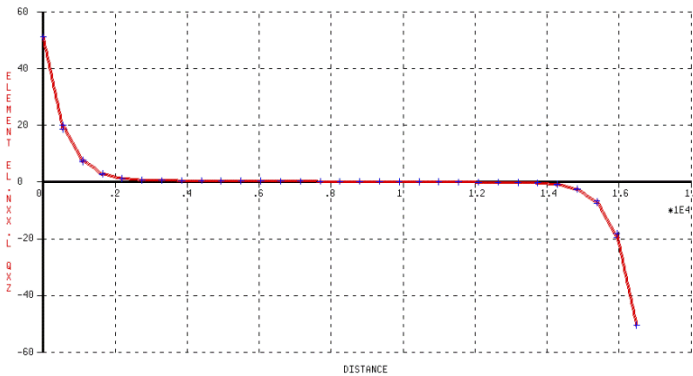


Figure 64, shear force over the width at mid span [N/mm]

Table 16, shear force per girder (average shear force from graph x 1200 mm)

# Girder	Shear force	# Girder	Shear force
1	30,0 kN	2	6 kN
3	0 kN	4	0 kN
5	0 kN	6	0 kN
7	0 kN	8	0 kN
9	0 kN	10	0 kN
11	-6 kN	12	-30 kN

The same procedure has been followed as for the first cross-section. First, the average shear force has been calculated:

$$V_{average,1\ girder}$$

This is often zero because it is mid span and the load is a uniformly distributed load. After the force is calculated, the shear stress is found:

$$\tau_{xz} = \frac{V}{t * z}$$

Torsional moment

The torsional moment is calculated as has been done for the previous case.

$$\tau_{t,i} = \frac{T_{ed}}{2 * A_k * t_{ef,i}}$$

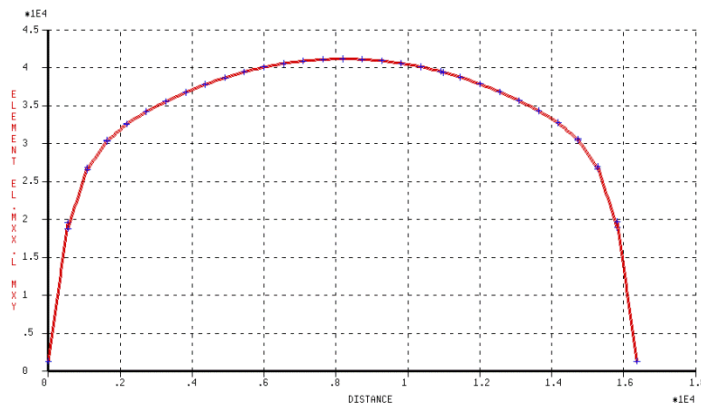


Figure 65, torsional moment over the width at mid span [Nmm/mm]

Table 17, torsional moment over the width (average from graph \* 1200)

# Girder	Torsional moment * 10 <sup>6</sup> Nmm	# Girder	Torsional moment * 10 <sup>6</sup> Nmm
1	15,0	7	49,2
2	37,2	8	48,0
3	43,2	9	45,0
4	45,0	10	43,2
5	48,0	11	37,2
6	49,2	12	15,0

Table 18, summation of the shear stress due to shear force and torsional moment – maximum torsional moment configuration

Girder	Average shear stress per web N/mm <sup>2</sup>	Shear force (stress) due to torsional moment (2 * mxy) per web N (N/mm <sup>2</sup> )	Shear stress left web	Shear stress right web
1	0,068	0,124	0,19	-0,05
2	0,014	0,307	0,32	-0,29
3	0	0,356	0,36	-0,35
4	0	0,371	0,37	-0,37
5	0	0,396	0,39	-0,39
6	0	0,405	0,40	-0,40
7	0	0,405	0,40	-0,40
8	0	0,396	0,39	-0,39
9	0	0,371	0,37	-0,37
10	0	0,356	0,35	-0,35
11	-0,014	0,307	0,29	-0,32
12	-0,068	0,124	0,05	-0,19

The shear force has no contribution for this cross-section. The shear stresses are therefore symmetrical but of different sign.

## 5.5 Results Eurocode loading

In this paragraph the results are presented for the case study viaduct for the loads as described in paragraph 4.4.

For these results it is important to determine the governing cross-section and where the internal force should be checked. This has been done for each internal force. The governing load combinations are presented in paragraph 4.5.

### 5.5.1 Longitudinal moments

First the contour plot for longitudinal moments is plotted. For this internal force load combination 1 is applied.

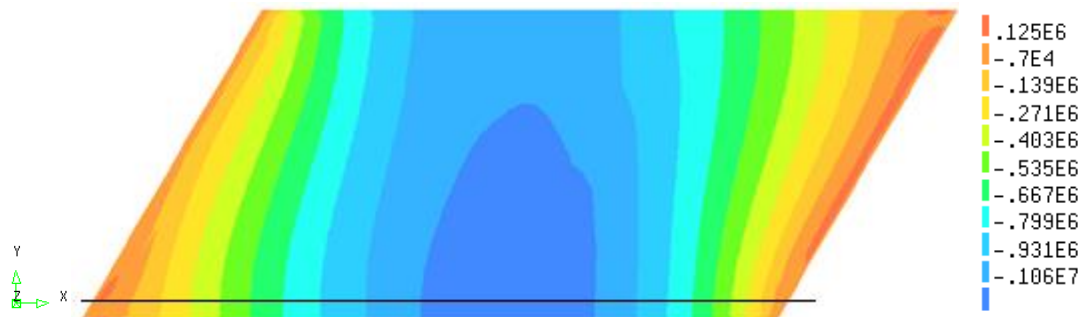


Figure 66, contour plot of the longitudinal moments (line at y=1,5 m) [Nmm/mm]

The governing cross-section for the second girder is just right from mid span. This is confirmed when the graph is presented of the longitudinal moment over the second girder. At both corners a positive moment is present. This is due to the boundary conditions and the end massive beam. An interface element with a width of 500 mm is modelled. Over that area a moment is transferred.

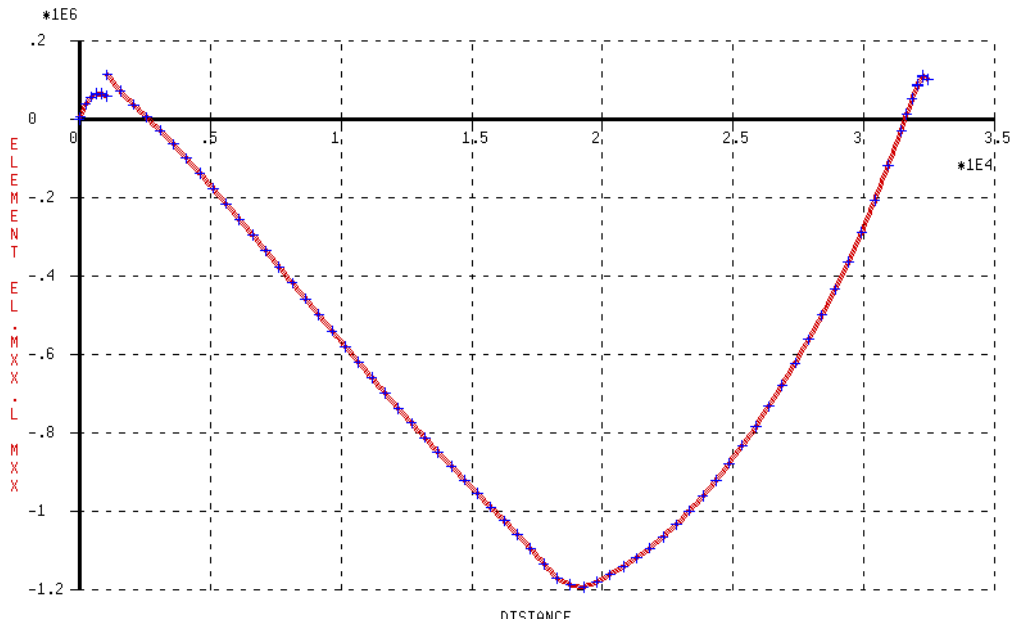


Figure 67, longitudinal moment 1st girder [Nmm/mm]

When the moment is presented over the width at that location it is seen that it's almost constant over the first few meters (first national lane, heavy traffic load). So the first two girders are considered as the governing girders. The second one has a slightly higher value because of the presence of the wheel loads.

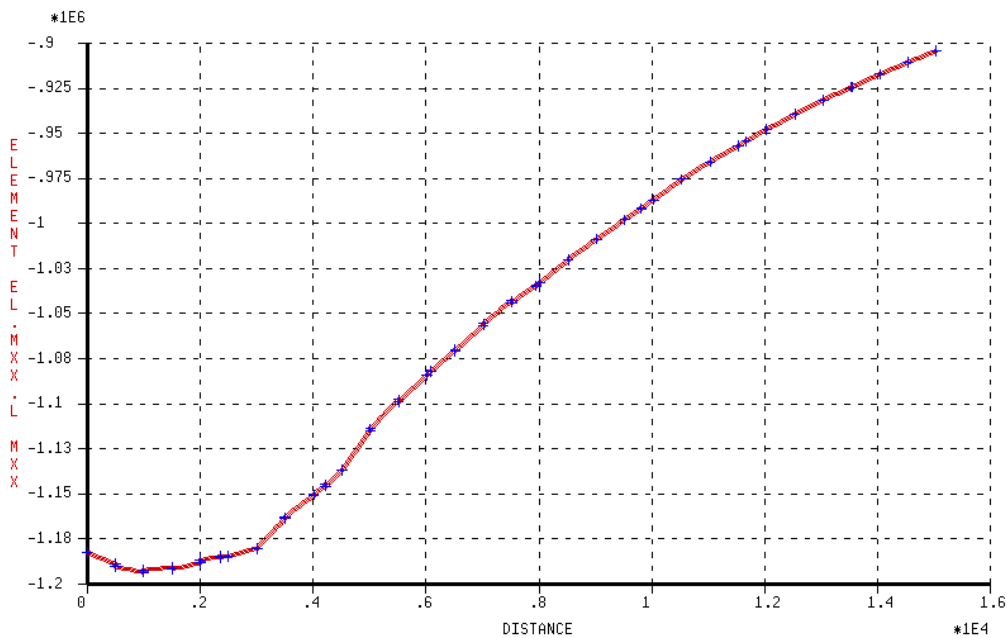


Figure 68, longitudinal moment over the width - x = 19,5 meter [Nmm/mm]

The average value found for the maximum longitudinal moment is  $0,119 \cdot 10^7$  Nmm/mm.

5.5.2 Transversal moment

For this internal force combination 2 is used. The heavy traffic lane is placed at middle of the viaduct together with the 300 kN tandem axles. The contour plots for the transversal moment in shown in figure 69. For this plot the massive ends of the beams are present but not plotted. As shown in appendix D the contour plot would not show relevant results if they are plotted because of the big difference in transverse stiffness.

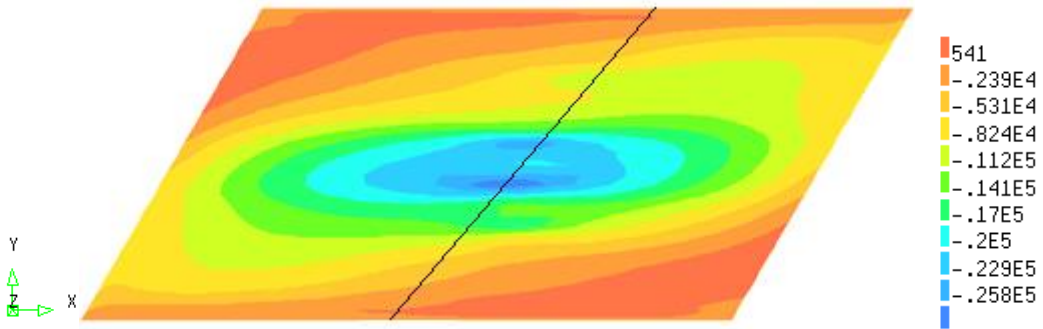


Figure 69, contour plot of the transversal moment (massive ends of beams not plotted) [Nmm/mm]

When the transverse moment over the governing cross section is presented an average should be taken at mid span over 4 'd' and at the edge an average is taken over one notional lane (because of the present of the peak). After the average is taken the value does not differ a lot.

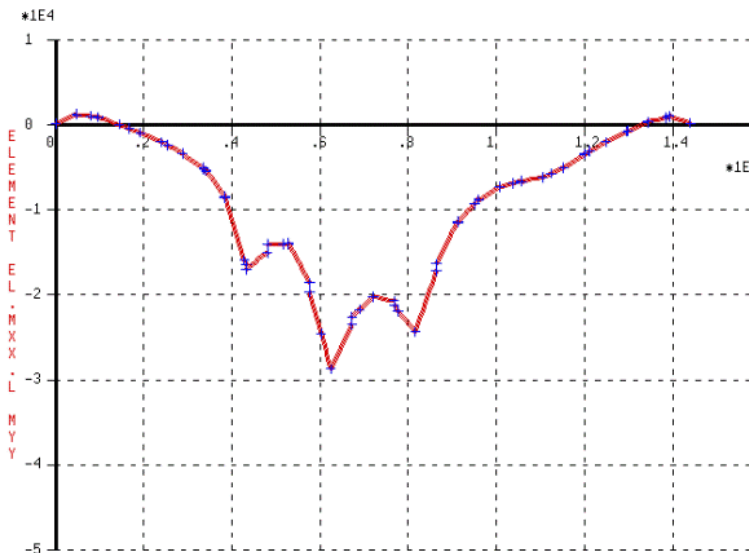


Figure 70, transverse moment over mid span [Nmm/mm]

5.5.3 Shear force

The shear force is an important internal force for skew viaducts. The skew angle of the viaduct influences the distribution of the shear force over the supports. In previous studies (and also according to CUR rapport 53) it is mentioned that the shear force has a maximum in the obtuse corner. This effect is more visible as the skew angle decreases (viaduct becomes more skew).

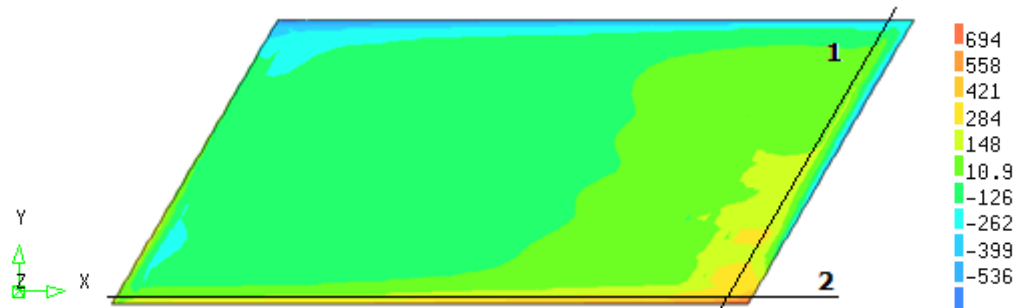


Figure 71, contour plot of the shear force [N/mm]

In the obtuse corner a maximum value of the shear force is present. Exactly along the edge maximum values are also present. In the next figures the shear force is plotted along the edge in the longitudinal direction and transverse direction (line 1 in figure 71).

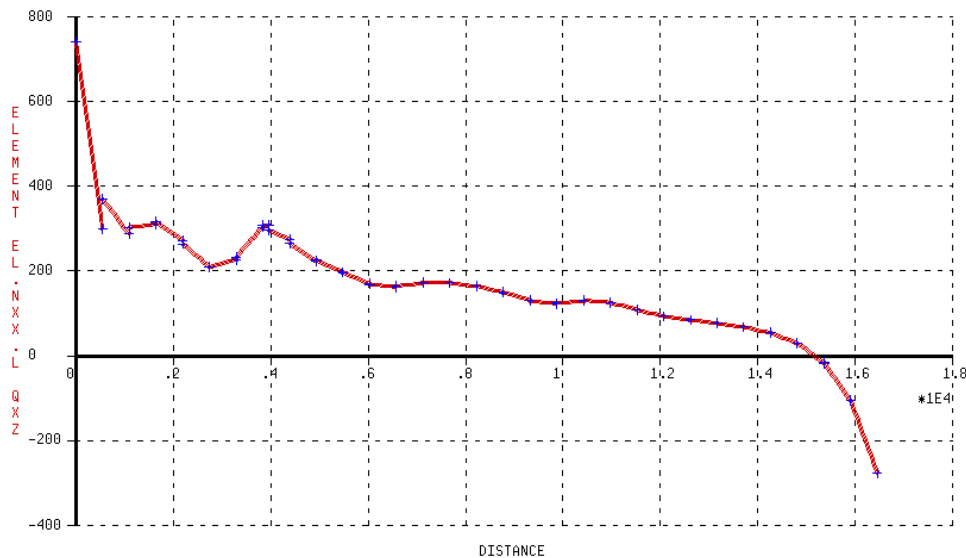


Figure 72, shear force - cross section 1 [N/mm]

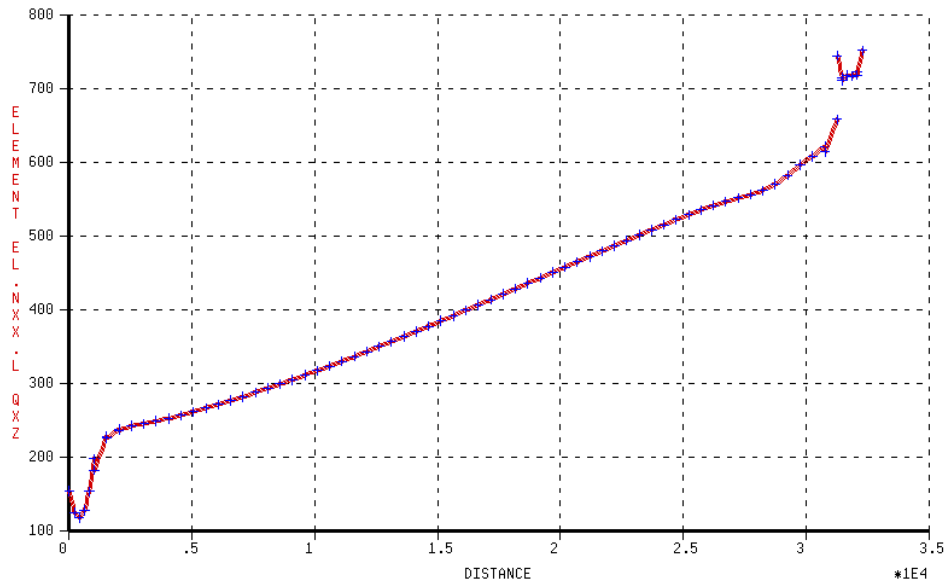


Figure 73, shear force diagram of cross-section 2 [N/mm]

For the comparison of the shear stresses with the 2,5D shell model in a later chapter the torsional moment distribution accompanying with this configuration and for the same cross-section is needed.

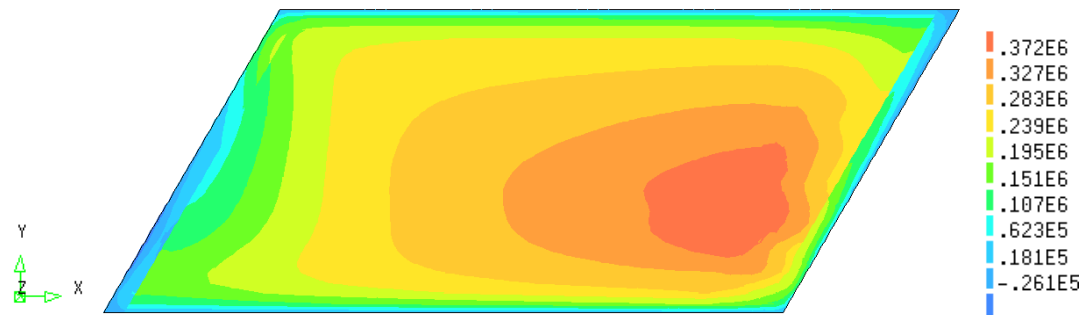


Figure 74, torsional moment in the plate for the maximum shear force configuration [Nmm/mm]

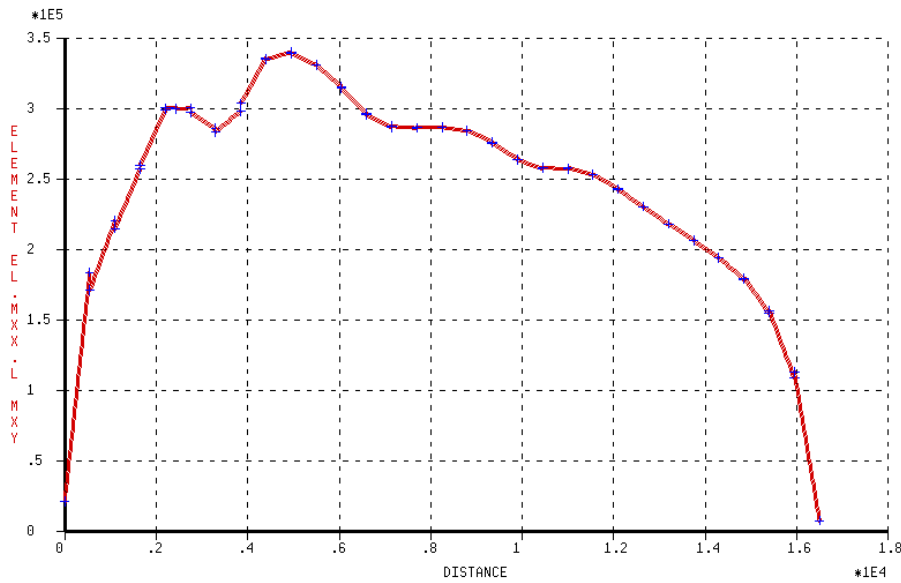


Figure 75, torsional moment over cross-section 1 due to maximum shear force configuration [Nmm/mm]

5.5.4 Torsional moments

The torsion calculated is in accordance with the theory of Mindler Reissner. The deformation by shear force is taken in to account and the torsional moments are zero at the edge of the pate.

The torsional moment due to the distributed load is presented in appendix D. As a consequence of the boundary conditions and the presence of the massive ends of the girders the maximum torsional moment was in the middle of the plate. When all the loads are included the torsional moment goes towards the supports.

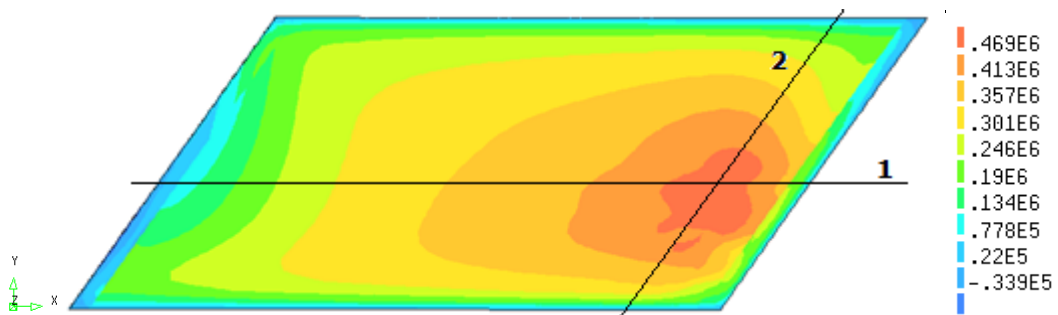


Figure 76, contour plot torsional moment in the plate [Nmm/mm]

The maximum torsional moment is found at  $x = 23$  m approximately. In the width direction it's at  $y=6$  m. This means that the fifth and sixth girder take up the torsional moments.

In figure 77 and 78 the torsional moments over the span and width are presented. In the figures below the shear force for cross-section 2 is also given. This is because the shear force for the same cross-section is needed to calculate the shear stresses for the comparison with the 2,5D model.



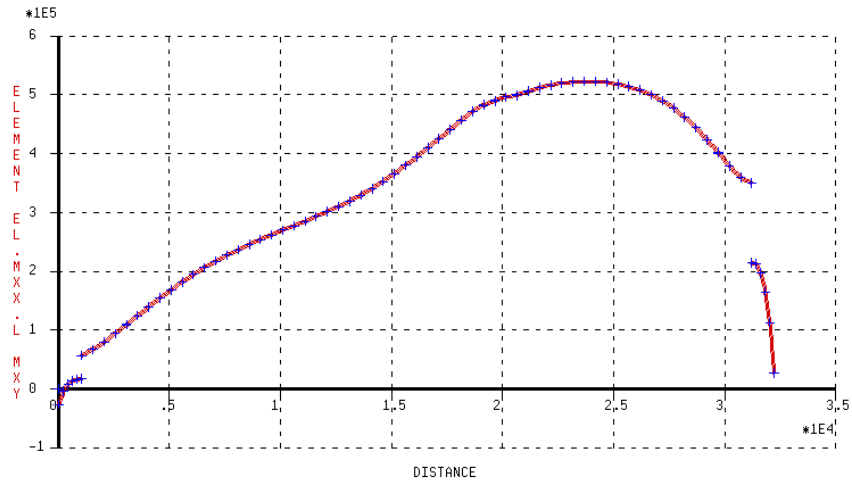


Figure 77, Torsional moments over the span direction at y=6 m (cross-section 1) [Nmm/mm]

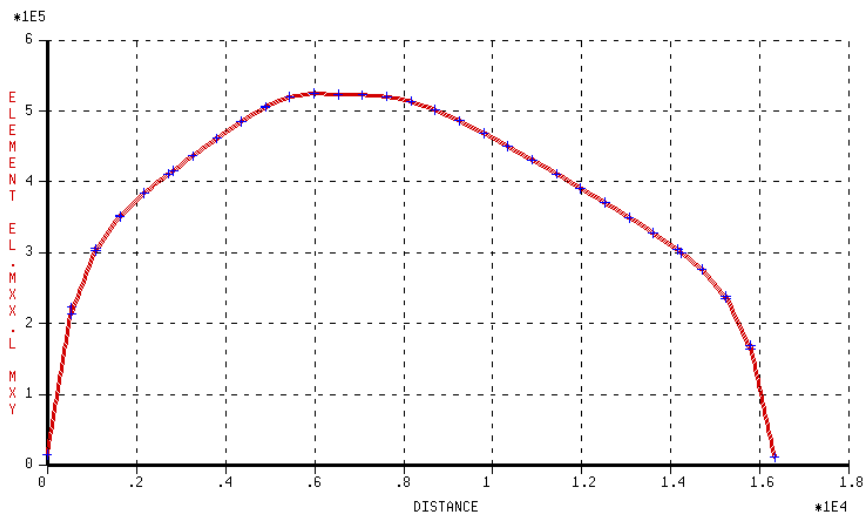


Figure 78, Torsional moments over the transversal direction at x=23 m (cross-section 2) Nmm/mm]

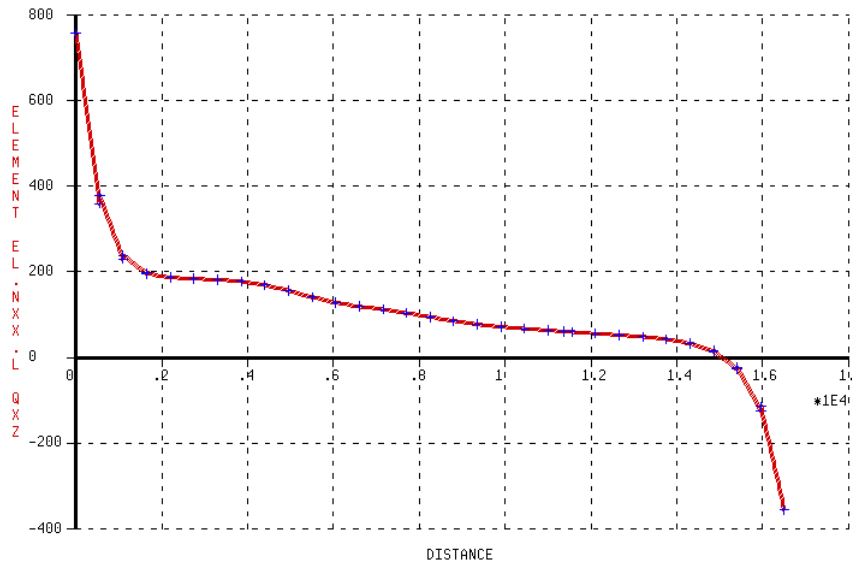


Figure 79, shear force - cross-section 2 [N/mm]

### 5.5.5 Shear stresses

The calculation of the shear stresses due to the shear force and the torsional moment is explained in paragraph 5.4.5. In that paragraph only a distributed load was inserted. In this paragraph the results due to the Eurocode loading are calculated. Two configurations are examined: maximum shear force and maximum torsional moment configuration. Each configuration has a different critical cross-section. The results for the left and right web are presented.

#### **MAXIMUM SHEAR FORCE - LOAD COMBINATION 3 (PARAGRAPH 4.5)**

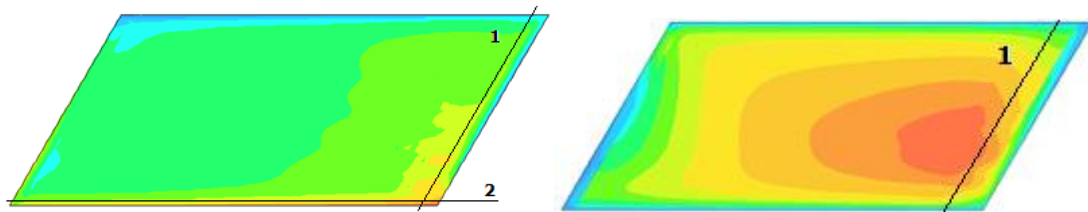


Figure 80, contour plot for the shear force (left) and the torsional moment (right)

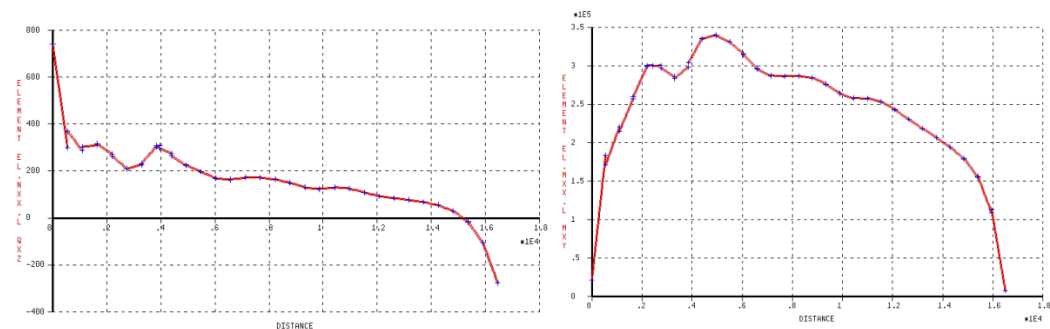


Figure 81, shear force (left) and torsional moment (right) for cross-section 1

For this configuration the shear force is governing for the shear stresses.

Maximum shear force is present for the first girder near the obtuse corner. The average value over the first girder is:  $520 \text{ N (per mm)} * 1200 = 6,3 * 10^5 \text{ N}$

The shear stresses per web due to the shear force for the first girder:

$$\tau_{xz} = \frac{V}{t * z * 2} = 6,3 * \frac{10^5}{200 * 1100 * 2} = 1,5 \frac{N}{mm^2} \text{ (per mm)}$$

The shear stress due to the average torsional moment ( $2 * mxy$ ) for the first girder:

$$\tau_{t,i} = \frac{T_{ed}}{2 * A_k * t_{ef,i}} = \frac{3,6 * 10^8}{2 * 606720 * 200} = 1,2 \frac{N}{mm^2} \text{ (per mm)}$$

**Table 19, shear stresses at cross-section 1**

Girder v / Shear stresses >	Left [N/mm <sup>2</sup> ]	Right [N/mm <sup>2</sup> ]
<b>1</b>	2,65	0,18
<b>2</b>	3,61	-1,82
<b>3</b>	3,71	-2,02
<b>4</b>	3,73	-2,59
<b>5</b>	3,58	-2,55
<b>6</b>	3,23	-2,20
<b>7</b>	3,17	-2,17
<b>8</b>	3,11	-2,13
<b>9</b>	3,03	-2,11
<b>10</b>	2,78	-1,96
<b>11</b>	2,25	-1,71
<b>12</b>	0,71	-1,26



Figure 82, shear stresses for the left web - cross-section 1

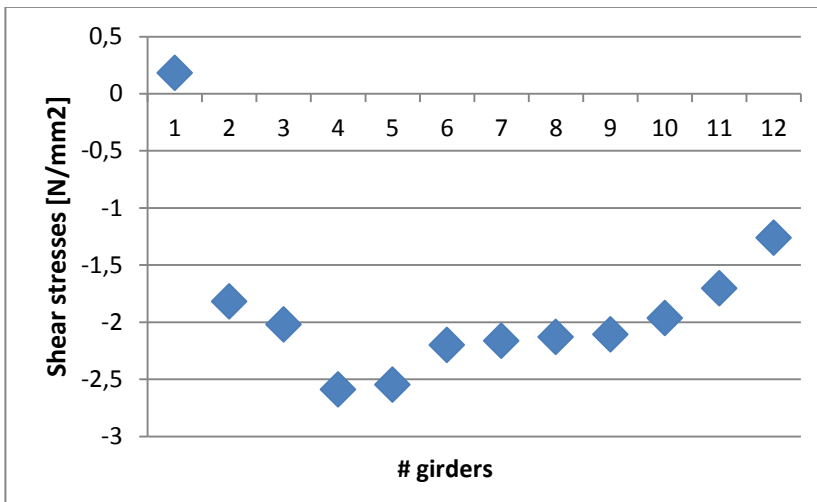


Figure 83, shear stresses for the right web - cross-section 1

**MAXIMUM TORSIONAL MOMENT - LOAD COMBINATION 4 (PARAGRAPH 4.5)**

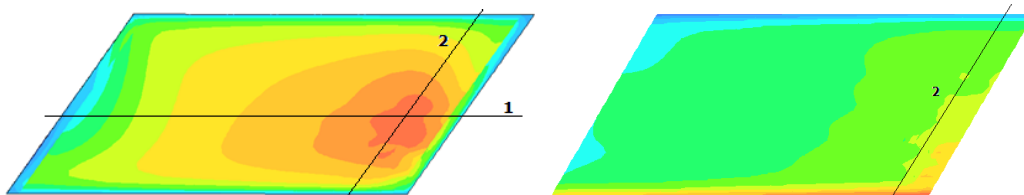


Figure 84, contour plot for the torsional moment (left) and the shear force (right)

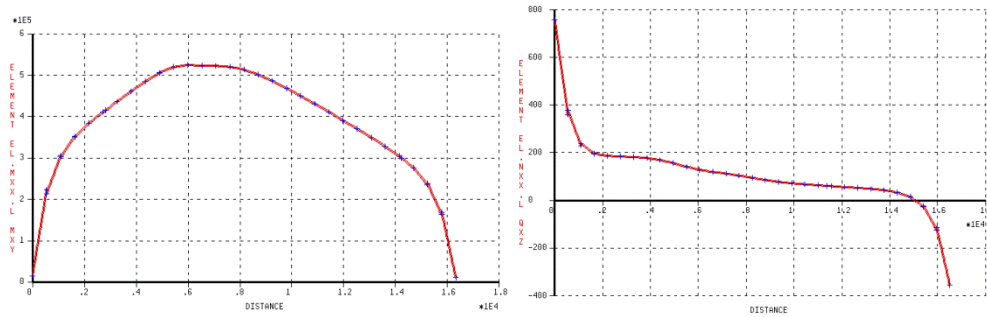


Figure 85, contour plot for the torsional moment (left) and the shear force (right) or the maximum torsional moment configuration

For this configuration the torsional moment is governing.

Maximum torsional moment is present near the fifth or sixth girder. The average value over the first girder is:  $100 \text{ N (per mm)} * 1200 = 1,2 * 10^5 \text{ N}$

The shear stress per web due to shear force:

$$\tau_{xz} = \frac{V}{t * z} = 1,2 * \frac{10^5}{200 * 1100 * 2} = 0,27 \frac{\text{N}}{\text{mm}^2} \text{ (per mm)}$$

The shear stress per web due to the average torsional moment ( $2 * m_{xy}$ ) is:

$$\tau_{t,i} = \frac{T_{ed}}{2 * A_k * t_{ef,i}} = \frac{1,2 * 10^9}{2 * 606720 * 200} = 4,94 \frac{\text{N}}{\text{mm}^2} \text{ (per mm)}$$

The maximum value found for the left web is:  $5,2 \text{ N/mm}^2$ .

For the right web the values should be subtracted and the shear stress becomes:  $-4,6 \text{ N/mm}^2$ .

In the table on the next page the shear stress values for every girder (left and right web) are presented.

Table 20, shear stresses in every girder (for left and right web)

Girder v / Shear stresses >	Left [N/mm <sup>2</sup> ]	Right [N/mm <sup>2</sup> ]
1	2,71	-0,25
2	3,51	-2,42
3	4,44	-3,46
4	4,95	-4,13
5	5,27	-4,61
6	5,21	-4,67
7	4,96	-4,52
8	4,83	-4,45
9	4,51	-4,18
10	4,09	-3,81
11	3,51	-3,40
12	1,65	-2,30

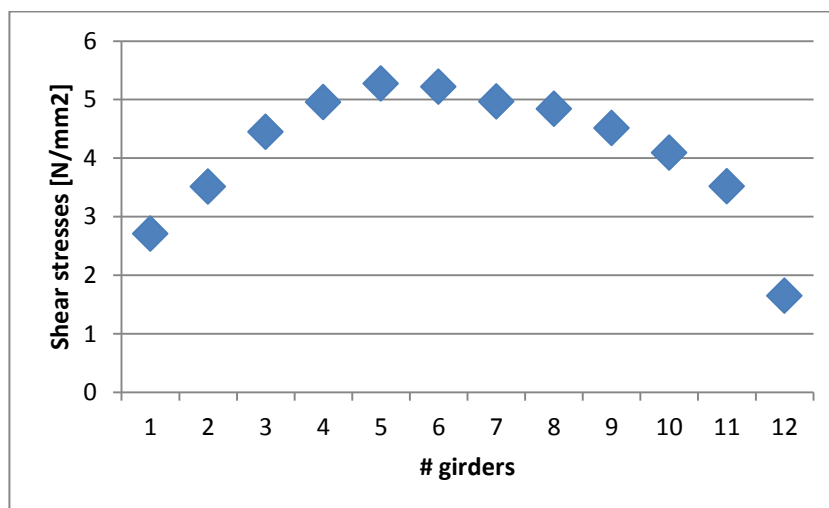


Figure 86, shear stress in every girder (left web)

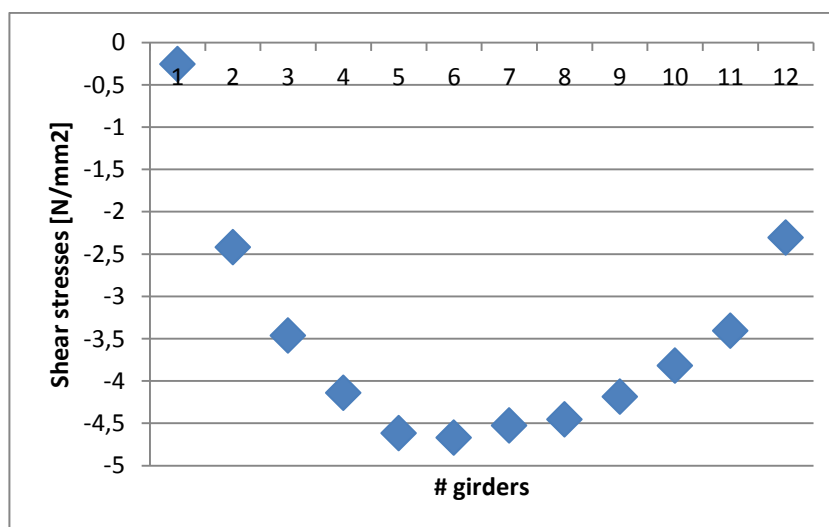


Figure 87 , shear stress in every girder (right web)

## 5.6 Summary

DIANA is a very advanced program for Finite Element Modelling. As an engineer it gives a lot of freedom to change the input and define the boundary conditions. For this case study several aspects have been modelled in DIANA. Finally, the total viaduct has been modelled as an orthotropic plate and the critical areas were found. In this paragraph the findings concerning the modeling in DIANA and the results for the orthotropic plate model are presented.

### 5.6.1 Modelling in DIANA

A model is a representation of reality. As an engineer it is challenging to model the viaduct as close as possible to reality. In DIANA a lot is possible but because it's an advanced program it needs a lot of practice and insight in FE modelling.

In the appendix of this thesis several aspects have been modelled in DIANA. In short, the conclusions are:

Appendix A: determining cross-section parameters

DIANA has been used to determine the transverse bending stiffness of the box beams and the joints. This has been done in a plane strain model. To check the results a very conservative hand calculation is made. DIANA was very capable of doing this in several ways. No real problems have been encountered.

Determining the transverse shear stiffness in DIANA did not give the expected results. Because for this analysis both bending and shear were involved (only shear does not exist) the results were very sensitive. One of the reasons is that the bending stiffness of the top flange only has to be determined first. It is not very easy to get the exact results. As a safe assumption, the conservative hand calculation is assumed.

Appendix B: determining material orthotropy

In DIANA a lot of different type of elements can be used. The prestressing is an in plane loading. This is only possible with shell elements. The advice was given to use curved shell elements instead of flat shell elements. For curved shell elements only material orthotropy is available. In appendix B the properties are determined and the result for a uniformly distributed load is presented. The results for other load configuration were also checked but these results are not included. It seems DIANA has no problems with orthotropy using both plate bending or shell elements.

Appendix C: stiffness of the bearings

In this appendix the stiffness of the bearings in DIANA has been determined. It is assumed that the bearing has a deflection of 0,5 mm due to the self-weight of the girder. To model this aspect, interface elements have been used. Some difficulties were encountered but they all could be solved. A couple of parameters should be inserted in the DATA file manually for example. In paragraph 13.5 all the conclusions and recommendations are given.

## Appendix D: determining the critical load configurations

Inserting the Eurocode traffic load was not very difficult but needed a lot of work. To get good results the axle tandem load were modelled as area loads. To use this option a distributed load over the full viaduct was inserted and only the wheel area was made effective (load mask). An area had to be defined for each wheel which means that for each wheel 4 boundaries had to be determined. This was very time consuming but not difficult per se.

### *Other modelling aspects*

The massive parts at the end of each girder were modelled with the same length. In reality these have different dimensions for each girder. The influence is not much since average values were used.

The mesh has been chosen according to “Guidelines for Nonlinear Finite Element Analysis of Concrete Structures”. Because it is a simple model and to reduce the modelling time the upper limit is chosen. If the correction factors for the wheel loads are considered, then it is concluded that the mesh was too coarse. It is not expected that for this assumptions the results would be much different.

## 5.6.2 Results

The determination of the critical areas has been done with the orthotropic plate model because it is expected that the results will not differ if the same analysis would be done for the 2,5D model and because the orthotropic plate model does not take a lot of time to insert in DIANA. The calculation time is also less.

For a good approximation of the results it is advised to leave the transversal prestressing and the edge line load out of the model.

The critical area for the longitudinal moment was found just over mid span towards the obtuse corner for the second girder. The shear force distribution differs a lot from a straight plate. The maximum value was found at the obtuse corner.

The maximum torsional moment under a uniformly distributed load was at mid span while this value was more towards the support under the Eurocode loading.

The shear stresses were calculated with the method approach explained in 5.4.5. Because of the high torsional moments the shear stresses are of opposite signs in the left and right web. From the results it is concluded that the left web is the governing web. In this web the shear stresses due to the shear force and the torsional moment amplify each other.

The configuration for the maximum torsional moment with the accompanying shear force (load combination 4) was the governing configuration for the shear stresses in the orthotropic plate model. This was the case for the uniformly distributed load and the Eurocode loading.

For the final values the shear stresses due to the self-weight and the prestressing are added up. This is done in chapter 7 for the final comparison between the two models.



## 6 2,5D SHELL MODEL

### 6.1 Introduction

As an introduction to the program (iDAINA) and to these types of viaducts (skew precast box beam) an orthotropic plate model was used in chapter 5. The findings for that model is used for the comparison. From theory it seems that the orthotropic 2D plate model is very applicable for determining the deflections and the longitudinal moments. The results are compared to the 2,5D model in this chapter.

### 6.2 Finite element modelling

In this chapter the finite element model is explained. The goal is to model the box beam viaduct as close as possible to the actual construction. For the comparison with the orthotropic plate model to be useful the same aspects used in the skew orthotropic plate model are used in the 2,5D shell model as well (e.g. same supports and end beams).

#### 6.2.1 Element type

The same shell element type is used for this model as has been used for the orthotropic plate model. The difference is that the model determines the orthotropy and no material orthotropy is used.

*Element: CQ40S (8-node quadrilateral shell element)*

The curved shell elements in DIANA are based on isoparametric degenerated-solid approach by introducing two shell hypotheses:

**Straight-normals:** assumes that normals remain straight, but not necessarily normal to the reference surface. Transverse shear deformation is included according to the Mindlin-Reissner theory.

#### 6.2.2 Cross-section

The cross-section of the box beam girder is presented before:

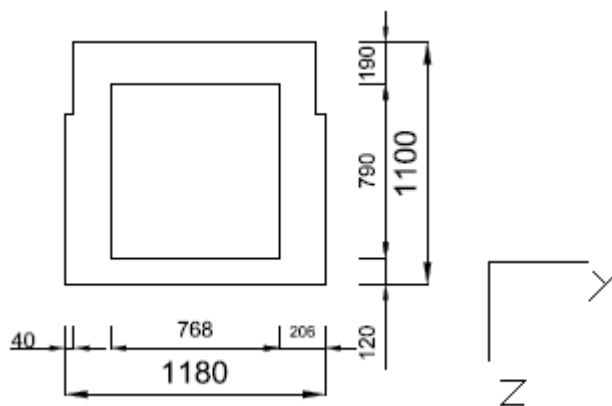


Figure 88, cross-section box girder – dimensions in [mm]

This cross-section cannot be modelled exactly with shell elements. The schematization is shown in the figure below. Specific areas are taken double in to account. Other areas are not taken in to account because of this schematization. The areas included and excluded are almost equal. It is expected that these small difference do not influence the results.

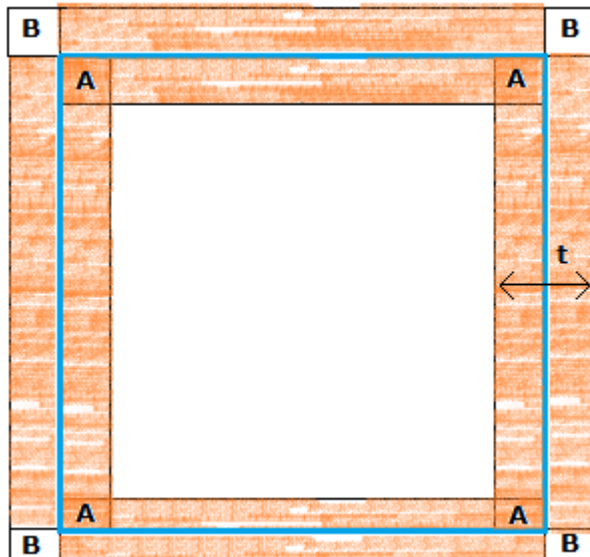


Figure 89, schematization of the cross-section

The blue lines show the cross-section with the shell elements which are given a thickness “t”. The “A” areas are the double included and the “B” areas are excluded.

Table 21, comparison moment of inertia

Cross-section	$I_{zz}$
Original / used for Skew plate model	$8,00 \times 10^7 \text{ mm}^4$
2,5D Shell model	$7,91 \times 10^7 \text{ mm}^4$

### 6.2.3 Model

This model has been build using several options in DIANA. One beam has been modelled first, after which the total viaduct had been inserted. The end beams and the joints are also present in the model. The end beams have been modelled using the same shell element but given much thicker webs and flanges.

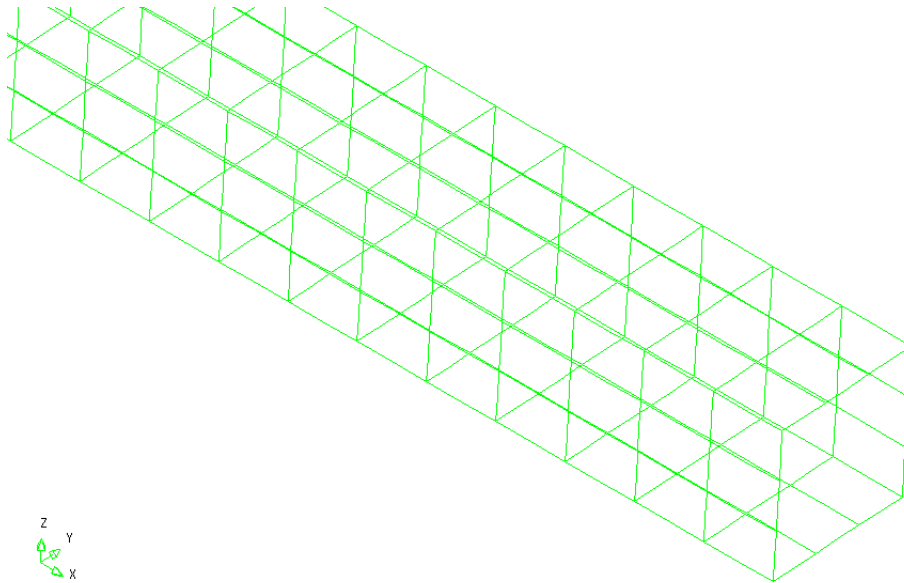


Figure 90, one box beam model in DIANA

#### 6.2.4 Mesh

For the mesh of this model the following aspects should be considered:

- Accuracy
- Calculation time
- Guidelines for Nonlinear Finite Element Analysis of Concrete Structures

This has been taken in to account and the following mesh has been determined:

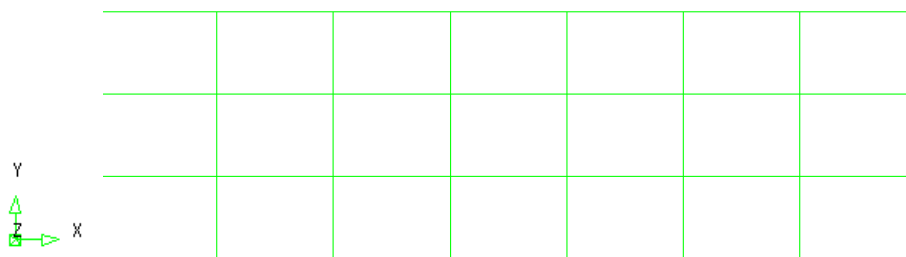


Figure 91, mesh of one box beam from side view

*Element size: 270 mm x 184 mm*

The joints have slightly smaller elements. The total mesh is seen in the figure 92.

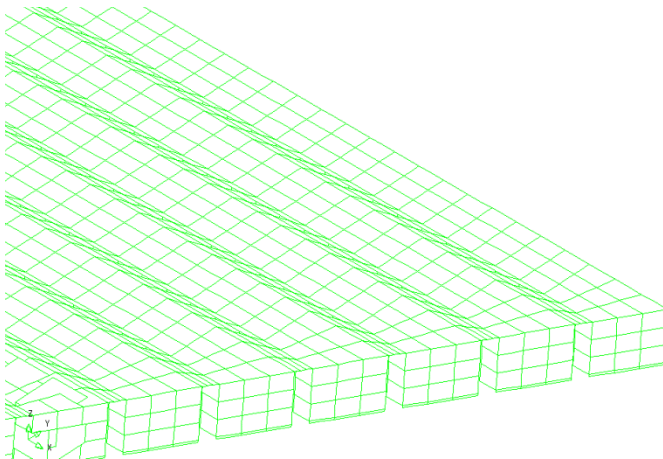


Figure 92, total mesh of the viaduct

### 6.2.5 Boundary conditions

In this model interface elements are used as has been done for the skew plate. In this case the interface element is placed under each box beam apart and not over the whole width.

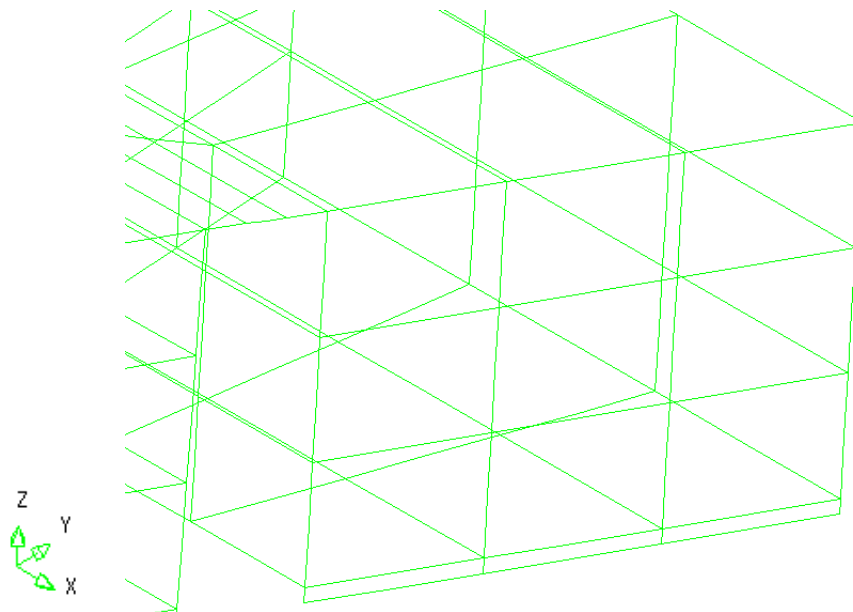


Figure 93, interface elements for modelling the bearing

The stiffness for the interface elements has been derived earlier:

$$k = \frac{K}{d * 1200} = 536 * \frac{10^3}{500 * 1200} = 0.9 \frac{N}{mm^3}$$

## 6.2.6 Loads

The loads for the skew plate model were inserted using the option “load mask”. The advantage of that model was that the viaduct could be modelled in a few surfaces in DIANA. The load masks are applied to the same surface (all loads were in the same half span). For the 2,5D shell model each girder has its own surface and this means that the load masks do not apply to the same surface (the wheel loads are applied to different surfaces). This requires a redefinition of the load masks.

Table 22, load cases and correction factors

Load case		N/mm <sup>2</sup>	Correction factor
1	Uniformly distributed load	0,0010	-
2	Asphalt	0,0028	1,02
3	Edge surface	0,0045	0,96
4	Distributed traffic load	0,0025	
5	Distributed traffic lane	0,0065	1,04
6	Heavy traffic lane (mid)	0,0065	1,04
7-10	Tandem axle 1	0,9370	0,80
11-14	Tandem axle 2	0,6250	0,83
15-18	Tandem axle 3	0,3125	0,80

Load case 1 is assigned to the uniformly distributed load (0,001 N/mm<sup>2</sup>) for the uniformly distributed load calculations (paragraph 6.3). It is not used in the Eurocode load combination.

**Note: the coordinates of the load masks applied are according to the local axis of the concerning surface**

The load configurations are the same as for the orthotropic plate model. These is found in paragraph 4.5.

### 6.3 Verification

Before the extensive results are discussed a first general comparison with the orthotropic plate model and verification by means of a hand calculation is presented. The results for the deflection and the longitudinal moment for a uniformly distributed load ( $0.001 \text{ N/mm}^2$ ) are examined. The reason to choose this load and these results is that it is possible to check it with a hand calculation.

#### 6.3.1 Deflection

In the literature it was mentioned that the orthotropic plate model should give the same results for the maximum deflection as the real structure. This statement is checked for a uniformly distributed load first. The maximum deflection calculated with the orthotropic plate model was 4,85 mm for a straight plate and 4,11 mm for the skew plate.

In figure 94 the deflection is presented for the 2,5D shell model. The maximum deflection for this model is very similar: 4,4 mm. The difference is 5 percent when the maximum values are compared.

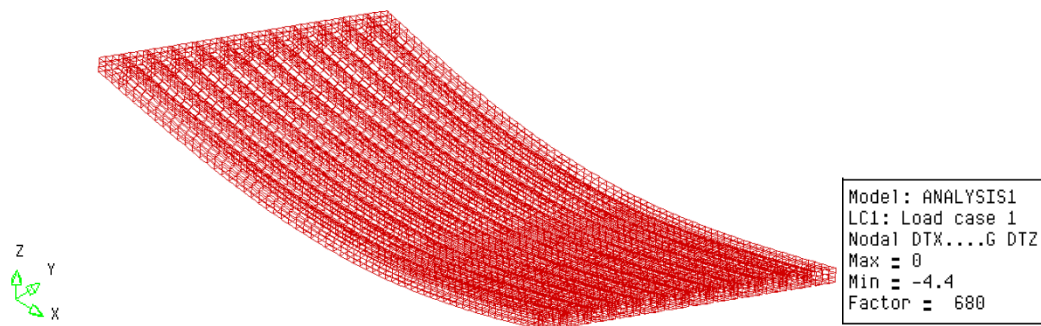


Figure 94, result for deflection [mm]

Besides the maximum deflection, the total deflection field can be compared. In figure 95 the contour plot of the deflection from the skew orthotropic plate is presented.

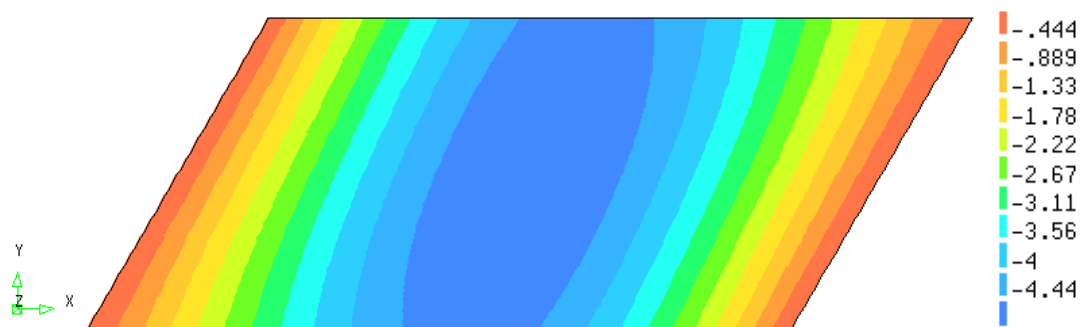


Figure 95, contour plot of the deflection in the orthotropic skew plate model (uniformly distributed load) [mm]

In figure 96, the contour plot for the 2,5D shell model is presented. It is concluded that the results are the same for the deflection under a uniformly distributed load.

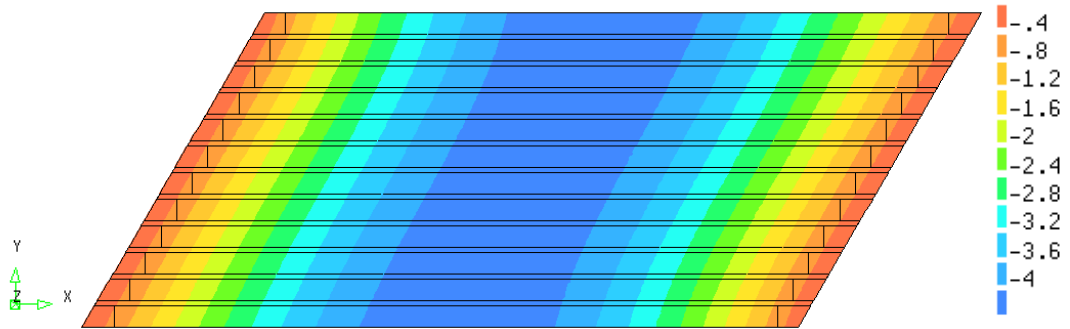


Figure 96, contour plot of the deflection in the 2,5D shell model [mm]

In the graphs below the deflection of the first girder is compared within the two models. The first graph is from the plate analysis and the second from the 2,5D shell model. It is observed that the difference is very small. The maximum value is at the same location.

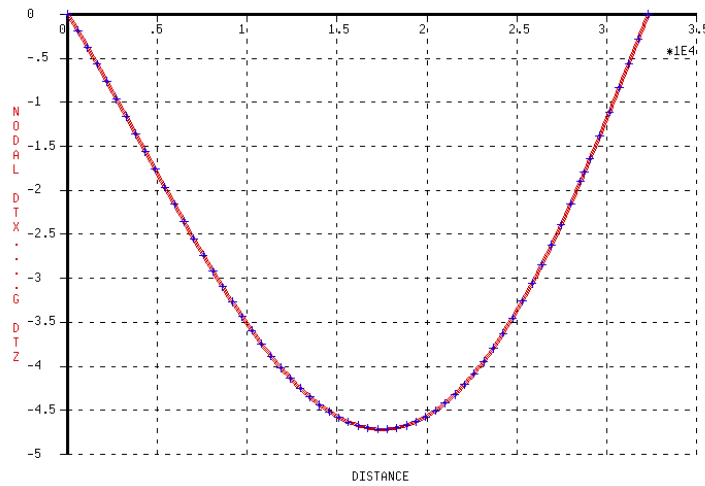


Figure 97, deflection from the orthotropic plate model for the first girder [mm]

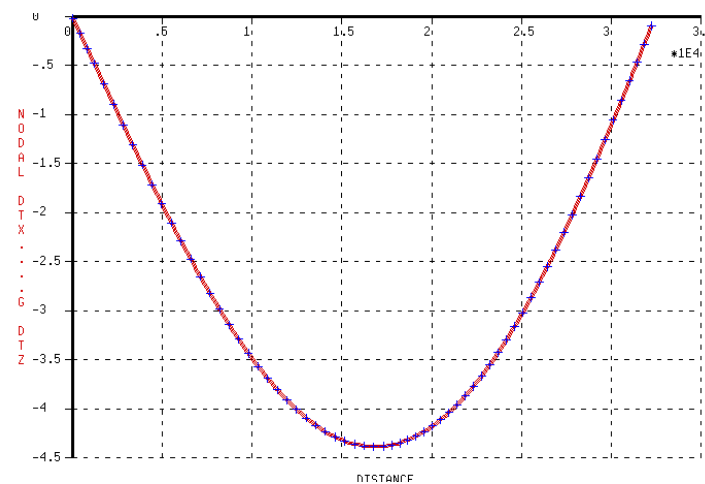


Figure 98, deflection from the 2,5D shell model for the first girder (only bottom flange) [mm]

### 6.3.2 Support reactions check

In the output file of DIANA (.OUT) the following is presented:

```
LOADSET POSITION TR X    TR Y    TR Z
      1      0.0000E+00 0.0000E+00 -0.4569E+06
```

This is approximately the same (2% difference) as the load applied:

$$0,001 * 14400 * 32250 = 0,4644 * 10^6 N$$

The support reactions from the skew plate showed that the maximum is at the obtuse corner. The support reactions for the 2,5D shell model are shown in the figure below.

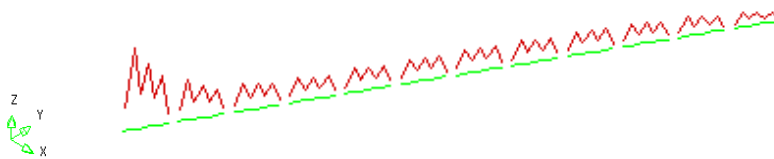


Figure 99, magnitude of the support reactions (left is obtuse corner and right is acute corner)

Approximately the same feature is observed when the support reactions are presented for the 2,5D shell model. A small difference is that in the plate model small uplifting forces are present at the acute corner while in the 2,5D model these forces are almost zero but not uplifting.

### 6.3.3 Longitudinal moment

In the skew plate model local distributed moment were presented that could be compared to the hand calculation. In the 2,5D shell model it is not simply possible to present integrated moments over the whole cross-section. To have a first estimation for the longitudinal moment in the girder “composed elements” are introduced in DIANA. These composed elements can do the integration of the stresses.

A (composed) “line element” is used and placed at the neutral axis. This composed element integrates the local  $m_{xx}$  into a global MY which is the moment over the full width.

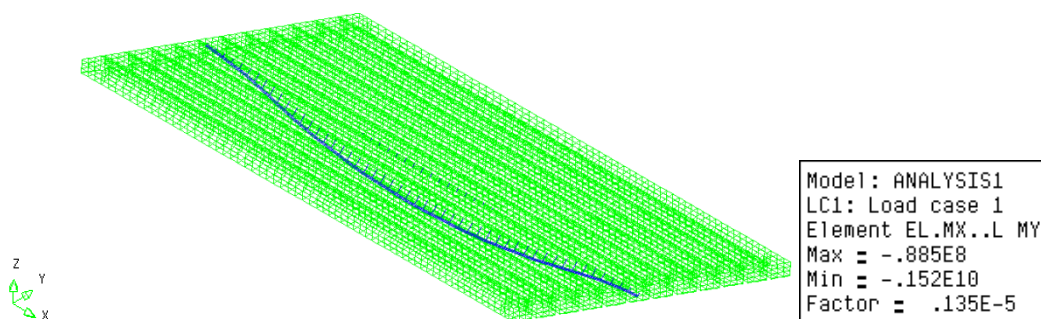


Figure 100, MY, longitudinal moment working over the full width [Nmm]



To get the moment per mm the total longitudinal moment is divided by the width:

$$\text{Longitudinal moment} = \frac{0,15 * 10^{10}}{14400} = 0,105 * 10^6 \text{ Nmm/mm}$$

The hand calculation showed a moment of  $0,13 * 10^6$  Nmm for the straight plate (beam) and the longitudinal moment calculated with DIANA for the skew plate was  $0,124 * 10^5$  Nmm/mm. The result found with the composed element is a difference of 15% with the hand calculation. This is expected because the hand calculation is for a straight simply supported beam. In the literature it is mentioned that for a viaduct with a skew angle of 45 degree the reduction of the longitudinal moment can increase to 20%.

## 6.4 Results due to uniformly distributed load

In this paragraph the stresses in the shell elements are discussed in more depth. These first results are due to uniformly distributed load ( $0.001 \text{ N/mm}^2$ ). These results are not interesting for the engineering practice but are of good use for understanding the load distribution in such a model.

### 6.4.1 Tension and compression stresses $S_{xx}$

Besides the results for the total viaduct, the results are presented for the bottom flanges, the webs and the top flanges in a separate contour plot.

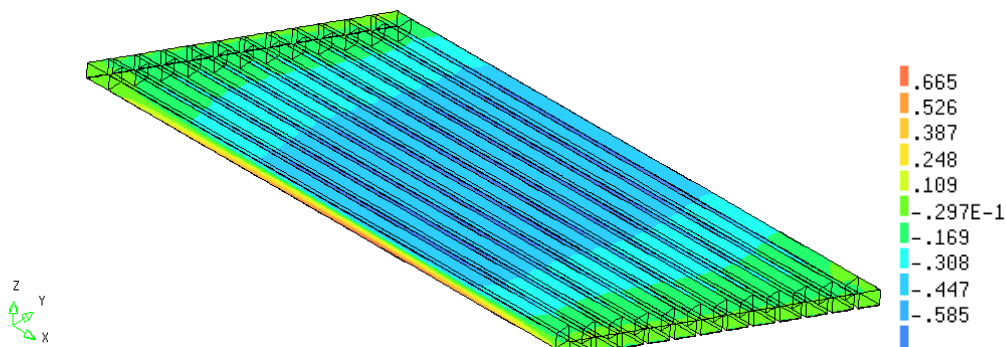


Figure 101, stress distribution ( $S_{xx}$ ) for the total viaduct [ $\text{N/mm}^2$ ]

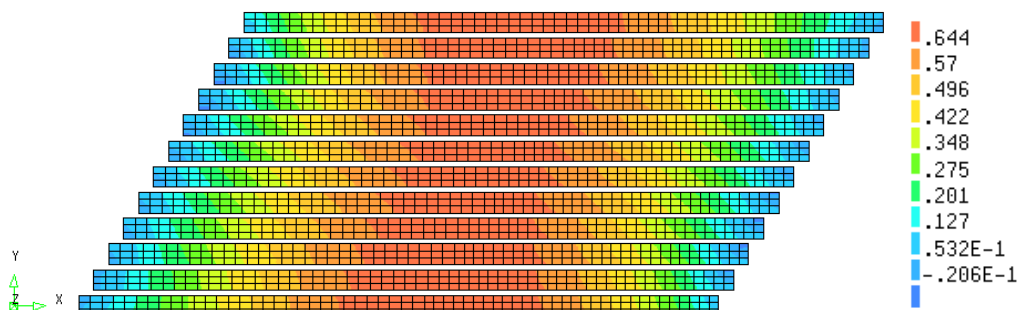


Figure 102, stress distribution ( $S_{xx}$ ) in the bottom flanges [ $\text{N/mm}^2$ ]

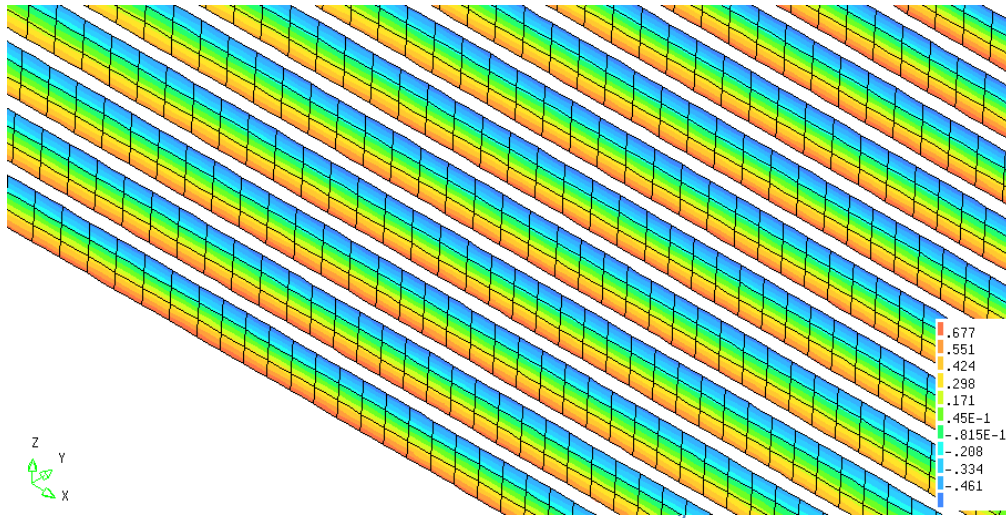


Figure 103, stress distribution ( $S_{xx}$ ) in the left webs [ $N/mm^2$ ]

The following linear analysis is done to integrate the stresses to get the moments:

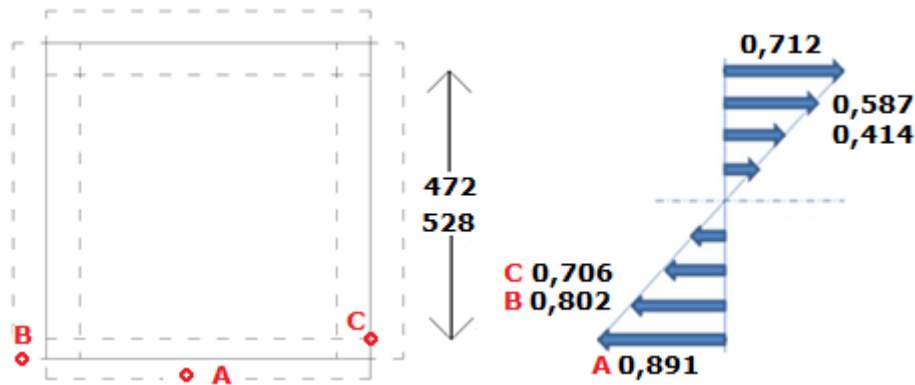


Figure 104, cross-section as shell elements and the stress distribution ( $S_{xx}$ ) [ $N/mm^2$ ]

DIANA gives results for different surfaces of each shell. Point A has been measured as the bottom surface of the bottom flange. Point B is the lowest point of the shell element of the wall. And point C is the top surface of the bottom flange. The results is as expected, point C has a lower stress than point B because it's a higher point in the cross-section even though in the model it's on the same height (thickness is not modelled). The stress distribution in the wall has been shown in the figure on the next page.

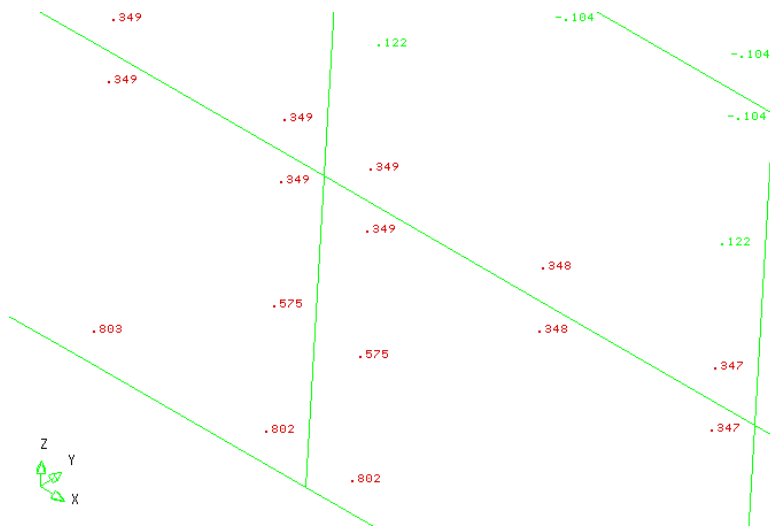


Figure 105, stress distribution in the nodes of the left wall of the first girder [N/mm<sup>2</sup>]

The cross-section has different thickness at different heights. The stresses over the whole cross-section are integrated. The total cross-section is divided in two parts: the part with the web (full cross-section width: 2 x 200 mm) and the part where only the flanges are present (width: 780 mm). The width of these parts is taken in to account to calculate the average value. For the integration of stresses in the 2,5D shell model the modelled geometry must be used. This is a little different compared to the real geometry (figure 89).

*Part one*

$$0,891 * 528 * 0,5 = 235,2 \text{ N}$$

$$0,712 * 472 * 0,5 = 172,0 \text{ N}$$

$$M = 235,2 * \left(\frac{2}{3}\right) * 528 + 172,0 * \left(\frac{2}{3}\right) * 472 = 0,137 * 10^6 \text{ Nmm}$$

*Part two*

$$\left(\frac{0,712 + 0,587}{2}\right) * 90 = 58,5 \text{ N}$$

$$\left(\frac{0,891 + 0,802}{2}\right) * 60 = 76,2 \text{ N}$$

$$M = 58,5 * (528 - 90) + 76,2 * (472 - 60) = 0,64 * 10^5 \text{ Nmm}$$

Total moment of the cross-section:

$$\frac{0,137 * 10^6 * 240 + 0,64 * 10^5 * 980}{1088} = 0,980 * 10^5 \text{ Nmm}$$

The composed element gave a result of 0,105 \* 10<sup>6</sup> Nmm. The exact value is 7 % difference. The use of composed element does give a good first estimation but because this is an average value, the exact value (detailed calculation) is more accurate.

### 6.4.2 Shear stresses $S_{xz}$

The output for this model is stresses. In the 2,5D shell model the full girder is modelled and the shear stress ( $S_{xz}$ ) in the webs is due to the shear force and the torsional moment. The following results are due to uniformly distributed load ( $0.001 \text{ N/mm}^2$ ) as mentioned before.

In the model a different SET has been created for the left and right web. In this paragraph the results of skew orthotropic plate model are compared with the stresses found in this model.

First the contour plot of both webs is shown (without the end beams):

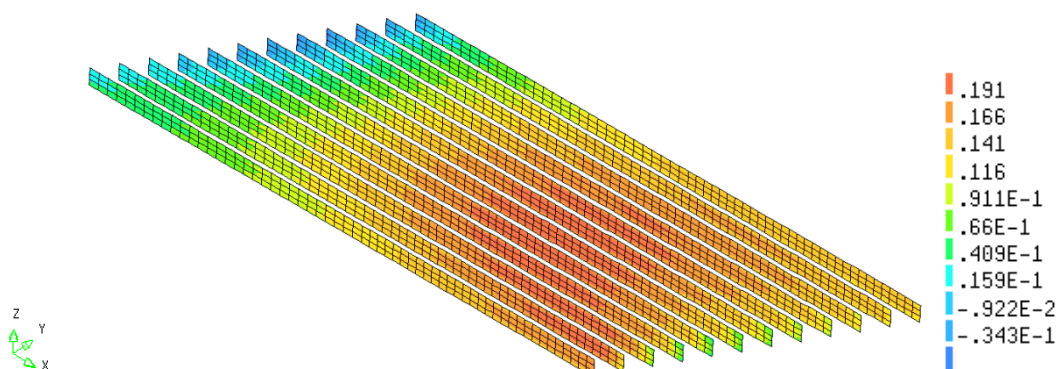


Figure 106,  $S_{xz}$  contour plot of the left web of the girders [ $\text{N/mm}^2$ ]

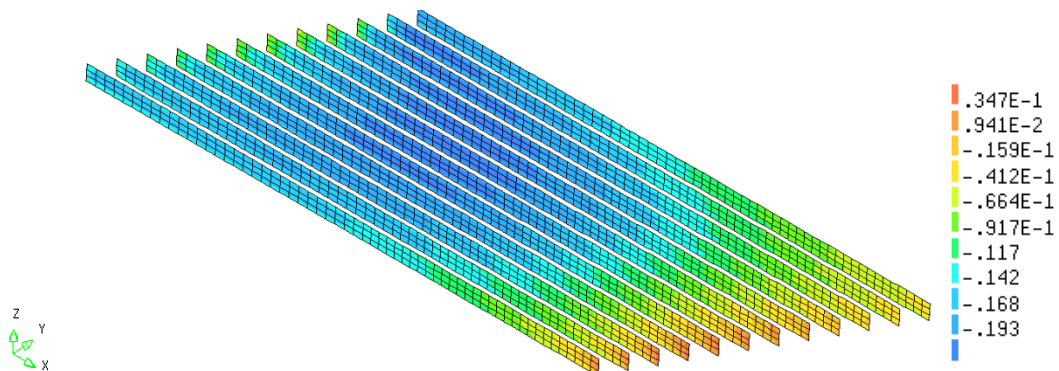


Figure 107,  $S_{xz}$  contour plot of the left web of the girders [ $\text{N/mm}^2$ ]

From the results of plate model it is known that the torsional moment has its maximum in the middle of the plate. Almost the same pattern is seen in the figures above except that the maximum value is not exactly at the middle. The maximum value of the shear stresses ( $S_{xz}$ ) is not at mid span because the contribution of the shear force is very low at that point (almost zero). At the transition between the hollow and the massive part the shear force is critical but the contribution of the torsional moment at that cross-section is not very high. This is the reason that the maximum value of the shear stress is found between these two areas for a uniformly distributed load.

For the right part of the viaduct the torsional moment increases the shear stress in the left web but for the left part of the viaduct the shear force has another sign, which means that the torsional moment and the shear force work in the same direction for the right web instead of the left web.

The values of the shear stress have a mirrored image. In the following figure the shear stresses over the span direction is presented for girder 1 (edge) and 6 (middle). The graphs left are both of the left web and the graphs at the right are of the right web. The bottom graphs are from girder 1 and the graph at the top are from the middle girder (#6).

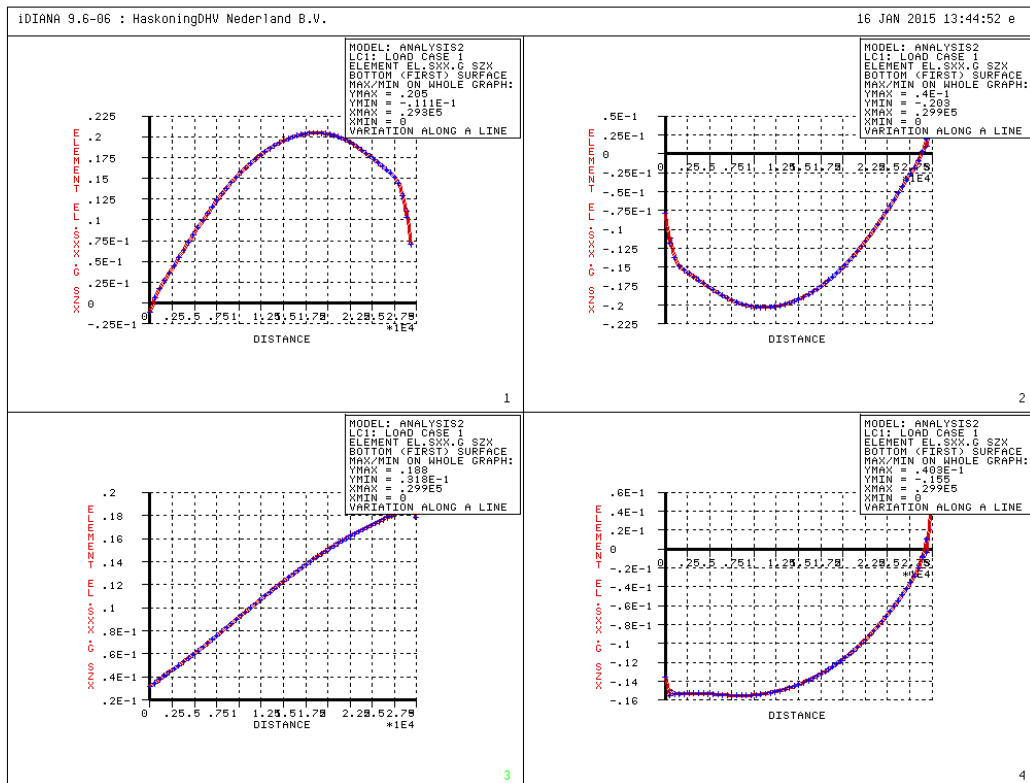


Figure 108, shear stress distribution in the webs for the first girder (bottom) and the sixth girder (top) [N/mm<sup>2</sup>]

The two cross-sections that have been considered in chapter 5.4.5. are considered here again. The cross-section at the transition point is the cross-section where the shear force is governing and the cross-section at mid span is the cross-section where the torsional moments are governing. For each cross-section both the right and the left web are presented. The results are compared in chapter 7.

### GOVERNING CONFIGURATION AND STRESSES

The following results show that for the 2,5D shell model the maximum shear stresses is almost equal for both configurations for a uniformly distributed load but found at a difference location (girder). The left web is still governing over the right web.

**CROSS-SECTION AT THE TRANSITION POINT**

Left web

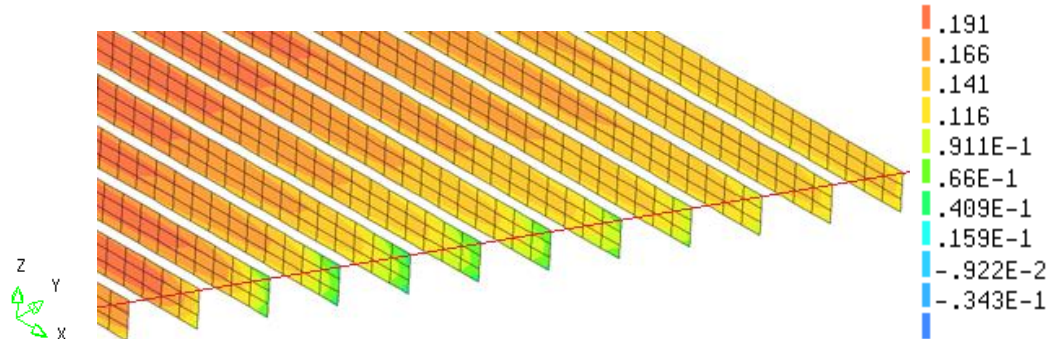


**Figure 109, contour plot of the shear stresses in the girders at the transition point [N/mm<sup>2</sup>]**

A graph is presented of these values. In this graph the values of the nodes of the elements through the line are presented. The average value is compared to the values found in the previous model in chapter 7.

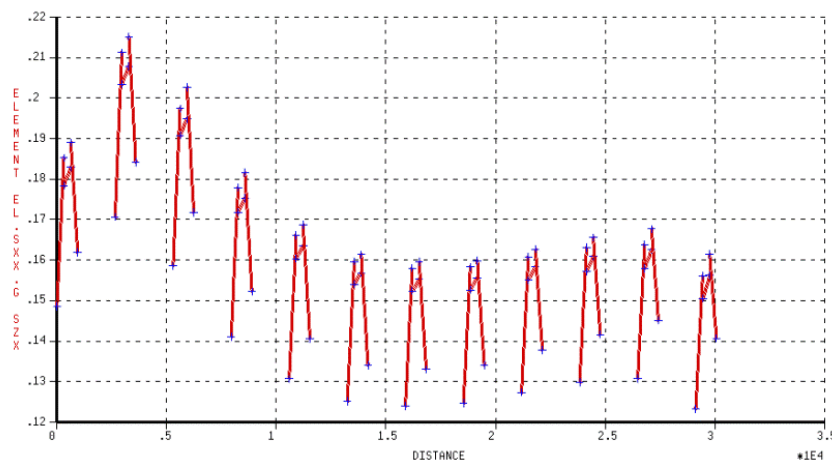


**Figure 110, shear stress values of the element (left web) [N/mm<sup>2</sup>]**

**Table 23, shear stresses per girder for the left web – transition point**

Girder	Shear stresses [N/mm <sup>2</sup> ]
1	0,17
2	0,20
3	0,19
4	0,17
5	0,16
6	0,15
7	0,16
8	0,15
9	0,15
10	0,16
11	0,16
12	0,15

Right web

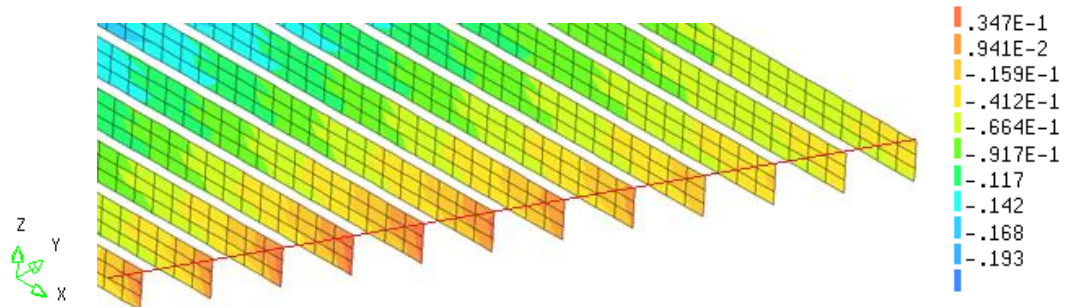


Figure 111, contour plot of the shear stresses in the girders at the transition point (right web) [N/mm<sup>2</sup>]

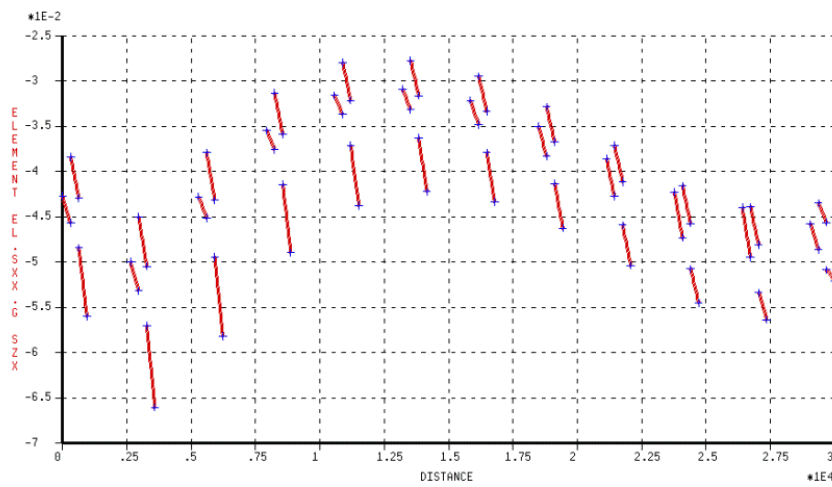


Figure 112, shear stresses at the right web – DIANA result [N/mm<sup>2</sup>]

Table 24, shear stresses per girder for the right web – transition point

Girder	Shear stresses [N/mm <sup>2</sup> ]
1	-0,05
2	-0,06
3	-0,05
4	-0,04
5	-0,04
6	-0,04
7	-0,04
8	-0,04
9	-0,05
10	-0,05
11	-0,05
12	-0,05

**CROSS-SECTION AT MID SPAN**

Left web

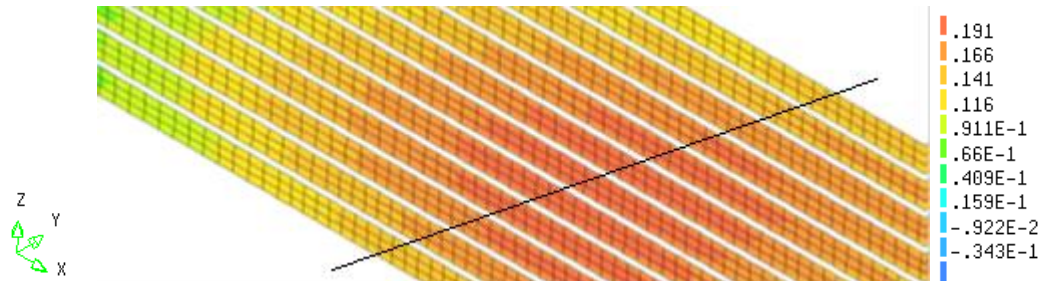


Figure 113, contour plot of the shear stresses in the girders at mid span (left web) [N/mm<sup>2</sup>]

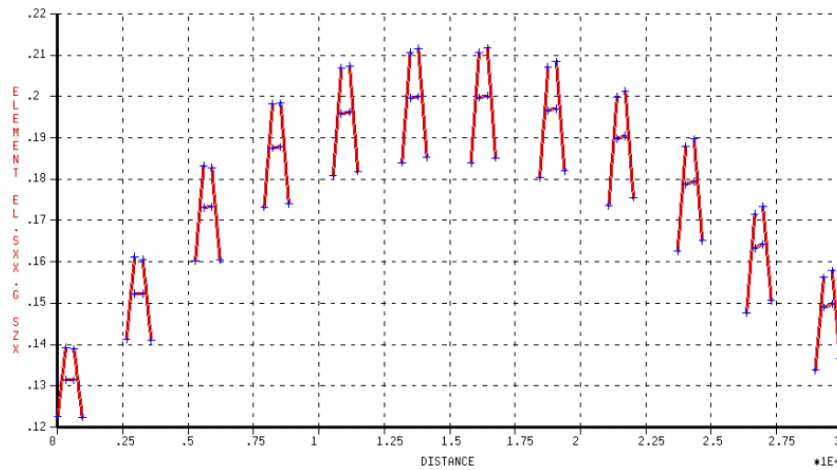


Figure 114, shear stresses at the right web mid span – DIANA result [N/mm<sup>2</sup>]

Table 25, shear stresses per girder for the left web – mid span

Girder	Shear stresses [N/mm <sup>2</sup> ]
1	0,13
2	0,15
3	0,18
4	0,19
5	0,20
6	0,20
7	0,20
8	0,19
9	0,19
10	0,18
11	0,16
12	0,15



*Right web*

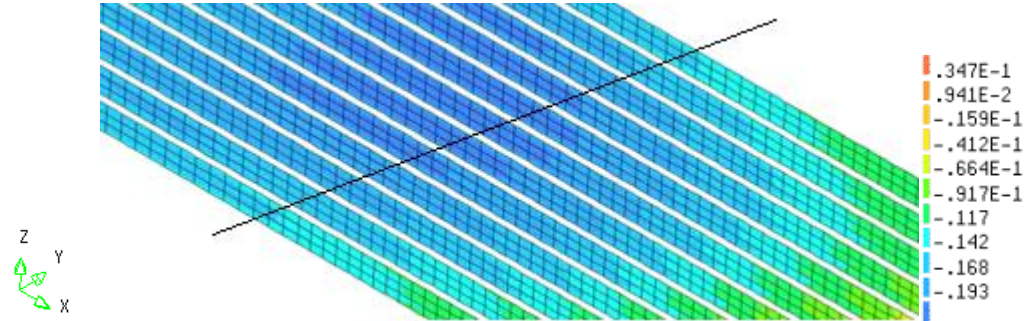


Figure 115, contour plot of the shear stresses in the girders at mid span (right web) [N/mm<sup>2</sup>]

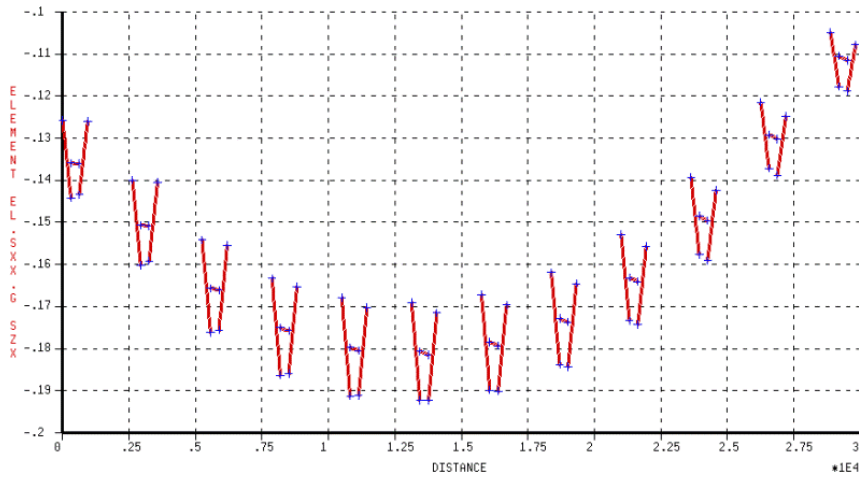


Figure 116, shear stresses at the left web mid span – DIANA result [N/mm<sup>2</sup>]

Table 26, shear stresses per girder for the right web – mid span

Girder	Shear stresses [N/mm <sup>2</sup> ]
1	-0,13
2	-0,15
3	-0,17
4	-0,18
5	-0,18
6	-0,18
7	-0,18
8	-0,17
9	-0,16
10	-0,15
11	-0,13
12	-0,11

### 6.4.3 Deformations due to torsion

For the translation of the forces from the plate to the girder the following schematization was used:

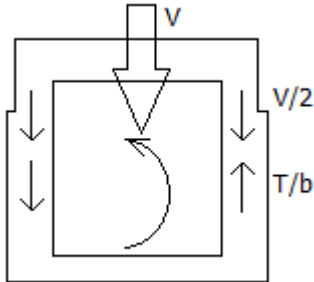


Figure 117, shear force and torsional moment working on the girder

The question remains what kind of influence this has on the deflection field and can this scheme of forces be explained when looking at the deflection of the webs or does the deflection field show something different. The plate has the same deformation pattern over the height (same cross-section). The real geometry of the girder is built of two webs and two flanges.

In the following figures the deflection of the plate (straight and skew) and the deflection of the webs (left and right) separately are presented. This is the deflection over the width at mid span ( $x=16$  m).

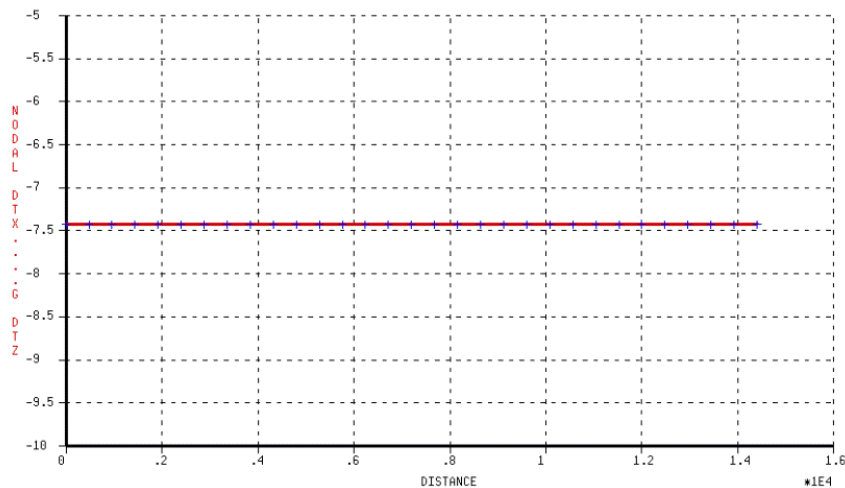


Figure 118, deflection at  $x=16$  m for a straight plate (uniformly distributed load) [mm]

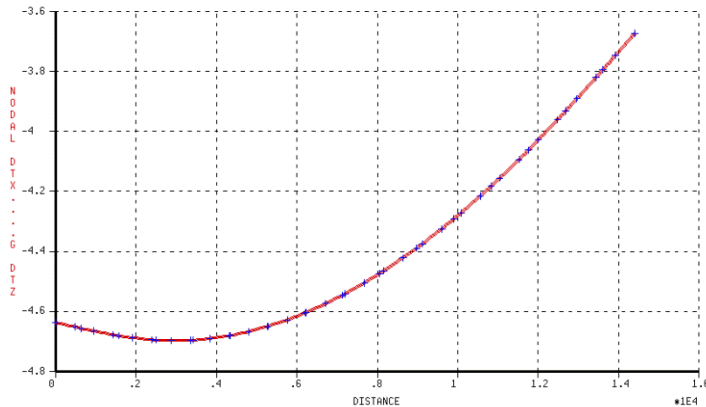


Figure 119, deflection at x=16 m for a skew plate (uniformly distributed load) [mm]

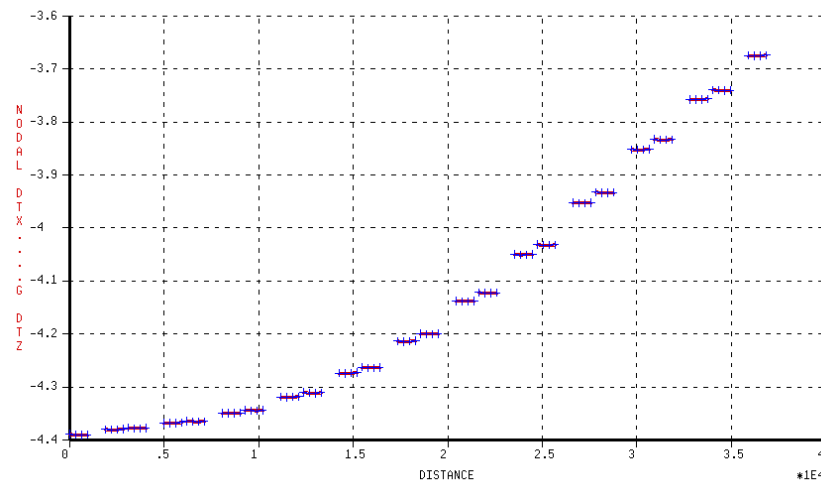


Figure 120, deflection of the webs (left and right) [mm]

A difference in deflection between a straight and skew viaduct is observed. For a straight plate the deflection at mid span is equal for the strip over the width. This is not the case of a skew viaduct. The deflection field shows that the deflection at one side is more than the deflection at the other side. This is dedicated to the torsion.

As is seen in figure 120, the torsion also has an effect on the deflection of the individual webs. This deflection is not the governing deformation and therefore very difficult to see.

## 6.5 Results Eurocode loading

In this paragraph the results are presented for the case study viaduct for the loads as described in paragraph 4.4.

For these results it is important to determine the governing cross-section and where the internal force should be checked. This is done for each internal force. The governing load combinations were presented in paragraph 4.5.

### 6.5.1 Tension and compression stresses $S_{xx}$

This paragraph includes the results of the internal forces due to the Eurocode traffic load. All the loads are inserted for this model as has been mentioned in paragraph 6.2.6. The load configurations have been determined with the skew orthotropic plate in appendix D.

In the contour plot of figures below the  $s_{xx}$  stresses are presented for both the bottom and the top flanges.

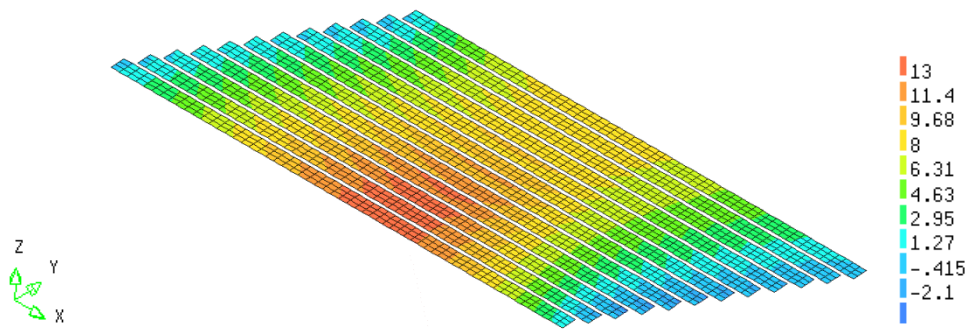


Figure 121,  $S_{xx}$  distribution of the 2,5D shell model for the bottom flange [N/mm<sup>2</sup>]

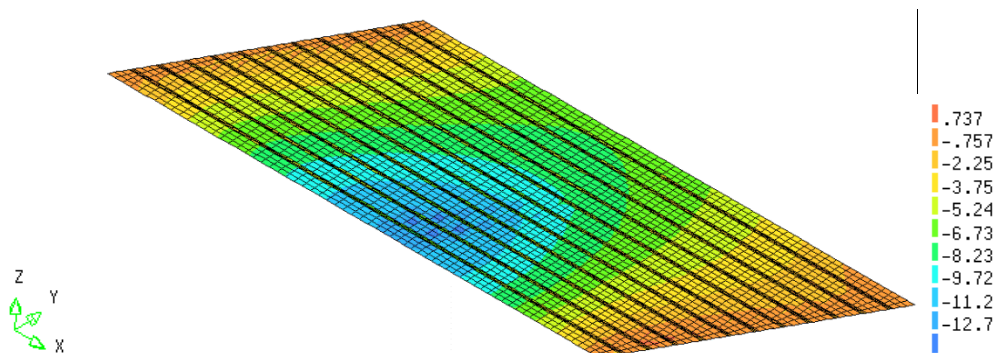


Figure 122,  $S_{xx}$  distribution of the 2,5D shell model for the top flange [N/mm<sup>2</sup>]

Maximum value is found in the second girder at the location of the wheel loads.

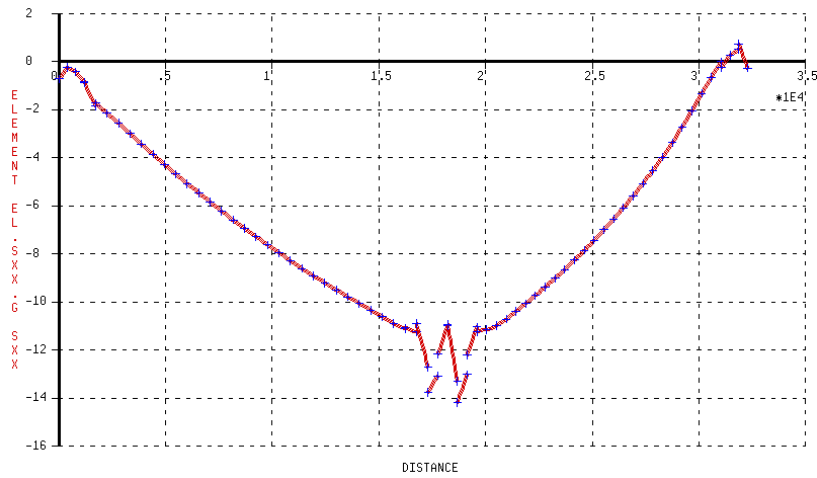


Figure 123, Sxx distribution in the top flange of the second girder over the span [N/mm<sup>2</sup>]

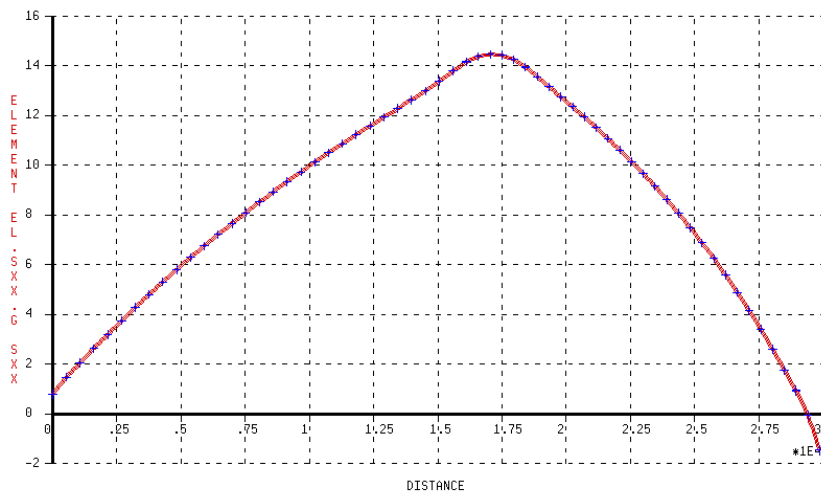


Figure 124, Sxx distribution in the bottom flange of the second girder over the span [N/mm<sup>2</sup>]

From the results of the skew orthotropic plate model it was found that the maximum moment for the strip along the edge is not exactly in the middle but more towards the obtuse corner. The same is found in the results above.

The maximum value for the 6<sup>th</sup> and 7<sup>th</sup> girder (middle of the viaduct) is at mid span:

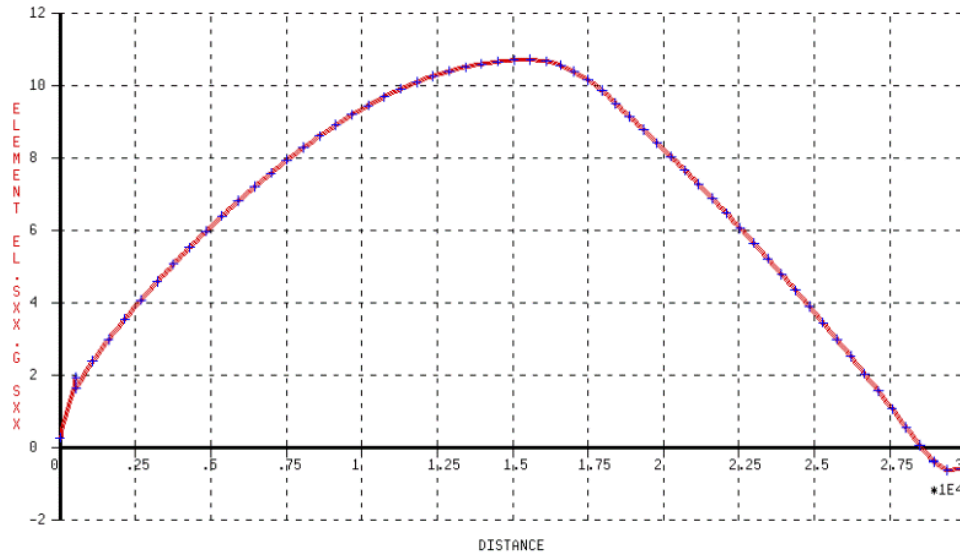


Figure 125, Sxx distribution in the bottom flange of the 7<sup>th</sup> girder [N/mm<sup>2</sup>]

The S<sub>xx</sub> stresses for the second girder are showed apart. The contour plot is very recognizable:

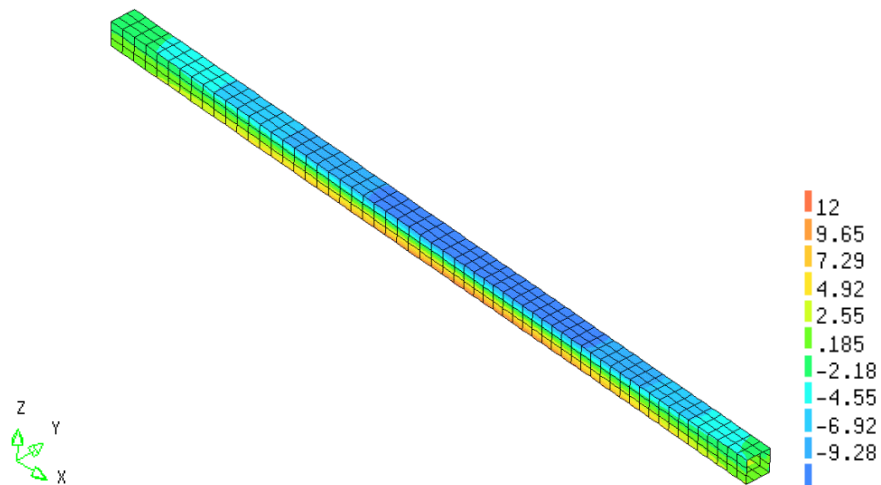


Figure 126, Sxx stresses for the second girder [N/mm<sup>2</sup>]

The same procedure is followed as has been shown in paragraph 6.4.1.

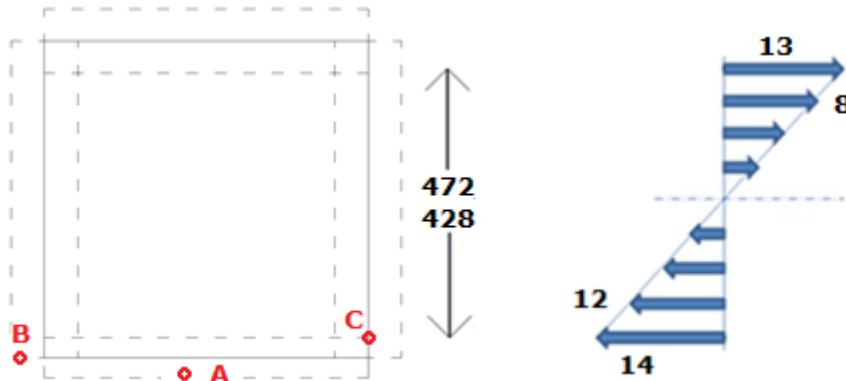


Figure 127, cross-section as shell elements and the stress distribution ( $S_{xx}$ ) [ $N/mm^2$ ]

Part one

$$14 * 528 * 0,5 = 3057 \text{ N}$$

$$13 * 472 * 0,5 = 2793 \text{ N}$$

$$M = 3057 * \left(\frac{2}{3}\right) * 528 + 2793 * \left(\frac{2}{3}\right) * 472 = 0,19 * 10^7 \text{ Nmm}$$

Part two

$$\left(\frac{13 + 8}{2}\right) * 90 = 860 \text{ N}$$

$$\left(\frac{14 + 12}{2}\right) * 60 = 798 \text{ N}$$

$$M = 990 * (528 - 90) + 780 * (472 - 60) = 0,71 * 10^6 \text{ Nmm}$$

Total moment of the cross-section:

$$\frac{0,19 * 10^7 * 240 + 0,71 * 10^6 * 940}{1088} = 0,112 * 10^7 \text{ Nmm}$$

The maximum value found for the longitudinal moment in the orthotropic plate model was  $0,119 * 10^7 \text{ Nmm}$ .

The overestimation of the orthotropic plate model is 6 percent.

## 6.5.2 Shear stresses $S_{xz}$

As stated before, the shear force and the torsional moments cannot be presented apart because both cause shear stresses. For the plate the maximum shear force was found at the obtuse corner and the maximum torsional moment was found with a different configuration at  $y=6 \text{ m}$  at end span. In this paragraph both configurations are examined to see which gives the highest shear stresses. Once again the webs of the girders are presented as these take up the shear forces ( $S_{xz}$ ).

**MAXIMUM SHEAR FORCE - LOAD COMBINATION 3 (PARAGRAPH 4.5)**

The maximum value for the shear stress (left web) is not at the same location as assumed from the plate model. In the plate model the maximum shear force was for the first girder at the edge. But the corresponding torsional moment (which also contributes to the shear stresses) does not have a maximum value at that location. The results from the 2,5D shell model shows that a combination of the shear force and the torsional moment at a different cross-section is governing for the shear stress.

Left web

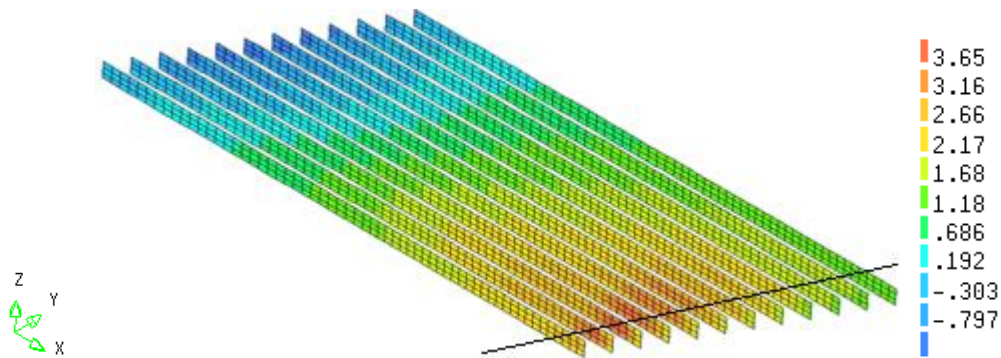


Figure 128, shear stress [N/mm<sup>2</sup>] in the left web - maximum shear force configuration

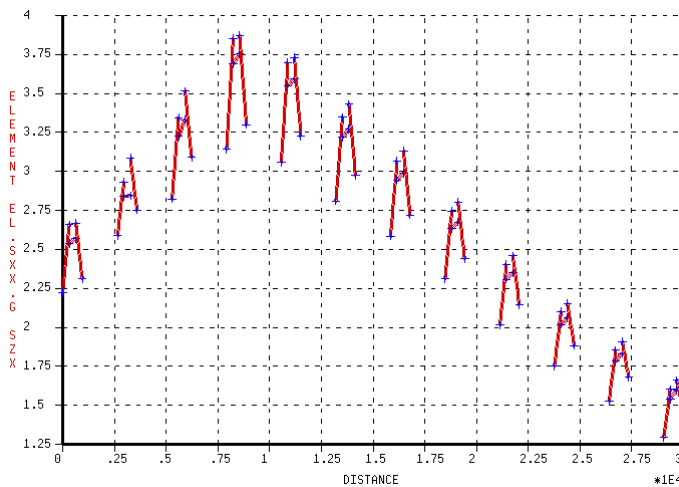


Figure 129, shear stress [N/mm<sup>2</sup>] in the left web - cross-section 1 - maximum shear force configuration

Table 27, shear stresses in left web - maximum shear force configuration

Girder	Shear stresses [N/mm <sup>2</sup> ]	Girder	Shear stresses [N/mm <sup>2</sup> ]
1	2,50	7	3,00
2	2,80	8	2,60
3	3,30	9	2,30
4	3,70	10	2,00
5	3,50	11	1,75
6	3,25	12	1,50



Right web

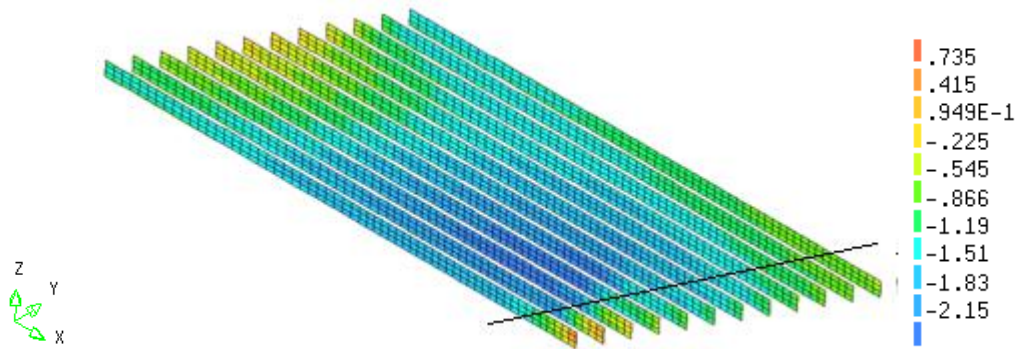


Figure 130, shear stress [N/mm<sup>2</sup>] in the right web - maximum shear force configuration

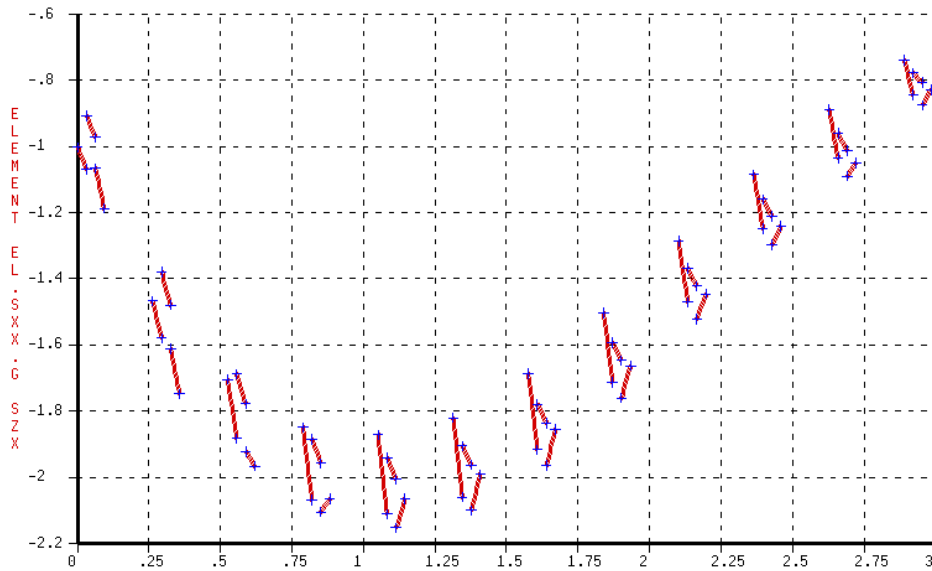


Figure 131, shear stress [N/mm<sup>2</sup>] in the right web – cross section 1 - maximum shear force configuration

Table 28, shear stresses in left web - maximum shear force configuration

Girder	Shear stresses [N/mm <sup>2</sup> ]	Girder	Shear stresses [N/mm <sup>2</sup> ]
1	-1,00	7	-1,80
2	-1,60	8	-1,70
3	-1,80	9	-1,40
4	-2,00	10	-1,20
5	-2,00	11	-1,00
6	-2,00	12	-0,80

**MAXIMUM TORSIONAL MOMENT - LOAD COMBINATION 4 (PARAGRAPH 4.5)**

The maximum value for the shear stress is found at approximately the same location as for the orthotropic plate for the same configuration. In the figures below the results are presented for the left web and for the right web.

Left web

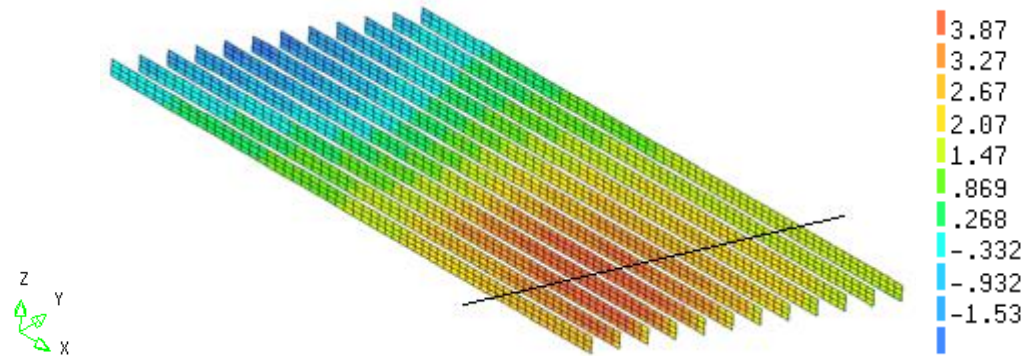


Figure 132, shear stress [N/mm<sup>2</sup>] in the left web - maximum torsional moment configuration

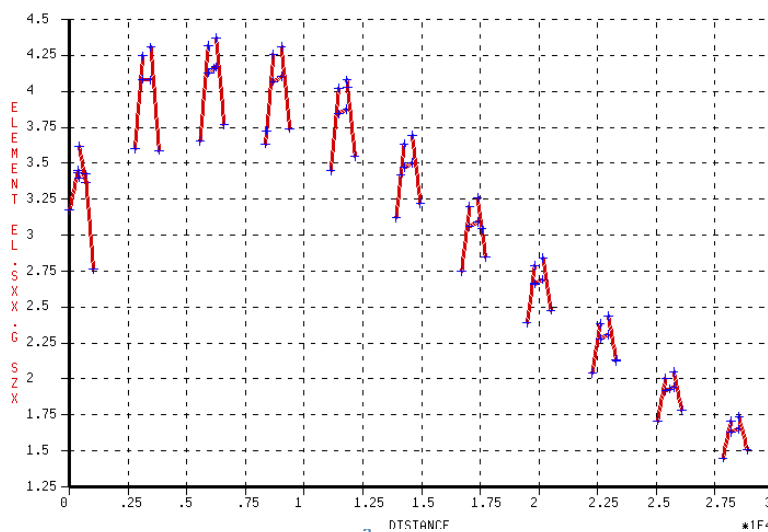


Figure 133, shear stress [N/mm<sup>2</sup>] in the left web over the width (cross-section 2) - maximum torsional moment configuration – 2,5D shell model

Table 29, shear stresses in left web - maximum torsional moment configuration

Girder	Shear stresses [N/mm <sup>2</sup> ]	Girder	Shear stresses [N/mm <sup>2</sup> ]
1	3,30	7	3,50
2	4,00	8	3,00
3	4,20	9	2,50
4	4,00	10	2,25
5	3,80	11	1,80
6	3,50	12	1,60

The shear stress over the length of the 6th girder is presented on the next page.

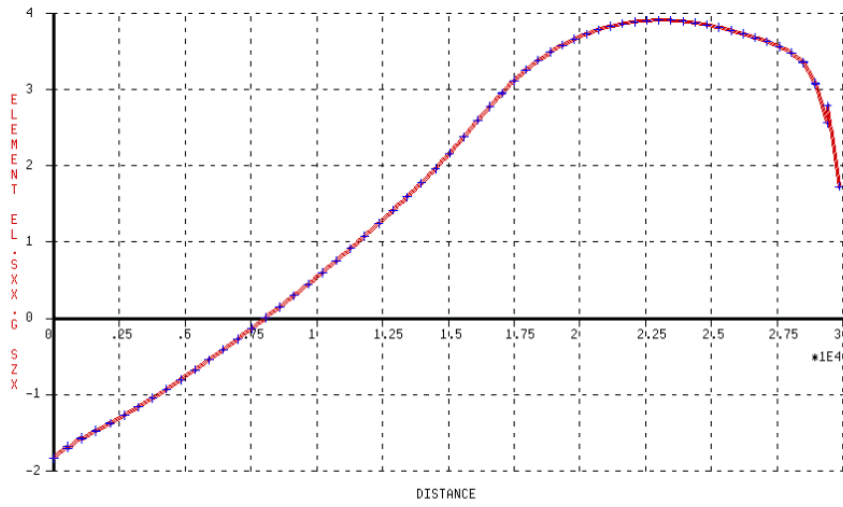


Figure 134, shear stress [N/mm<sup>2</sup>] in the left web of the sixth girder over the length of the girder - maximum torsional moment configuration – 2,5D shell model

Right web

The results for the right web are presented below:

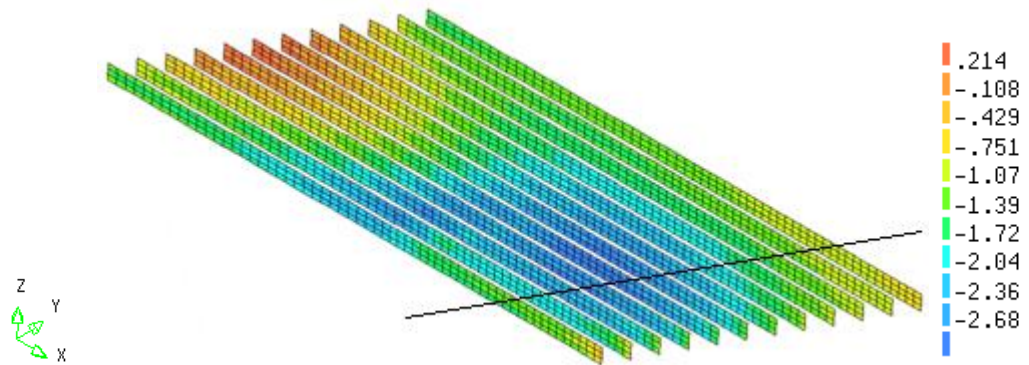


Figure 135, shear stress [N/mm<sup>2</sup>] in the right web - maximum torsional moment configuration

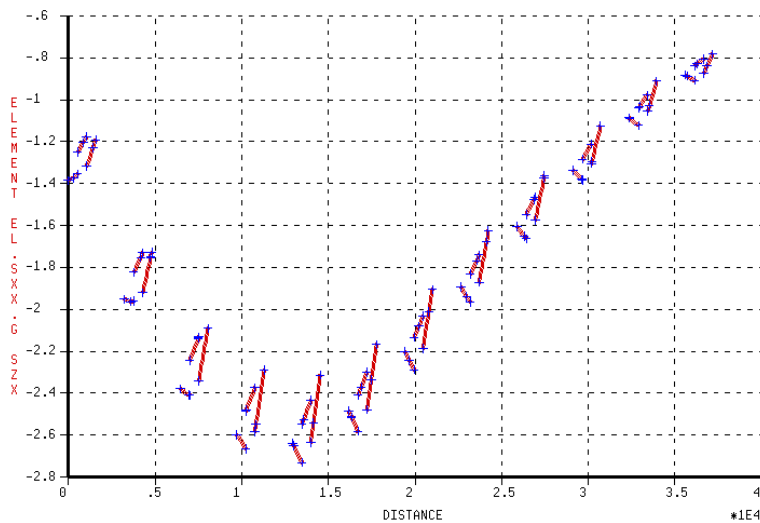


Figure 136, shear stress [N/mm<sup>2</sup>] in the right web over the width (cross-section 2) - maximum torsional moment configuration

Table 30, shear stresses in left web - maximum torsional moment configuration

Girder	Shear stresses [N/mm <sup>2</sup> ]	Girder	Shear stresses [N/mm <sup>2</sup> ]
1	-1,30	7	-2,10
2	-1,80	8	-1,80
3	-2,20	9	-1,50
4	-2,50	10	-1,20
5	-2,50	11	-1,00
6	-2,30	12	-0,80

The shear stress over the length of the 6th girder is presented below:

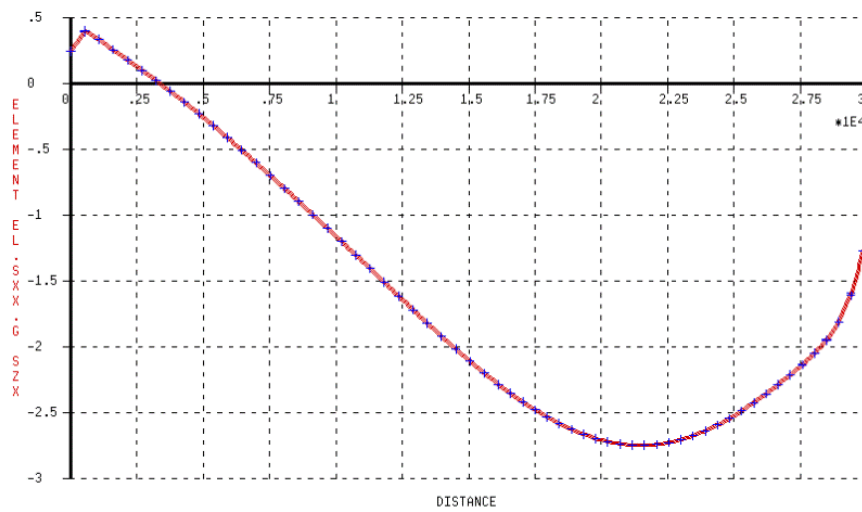


Figure 137, shear stress [N/mm<sup>2</sup>] in the right web of the sixth girder - maximum torsional moment configuration

## 6.6 Summary

In chapter 6 the results for the 2,5D shell model were presented. In this paragraph a short summary of the results and findings are given.

### 6.6.1 Modelling of the 2,5D shell model

If one has a lot of experience, it is not very difficult to insert an orthotropic plate model in DIANA. A 2,5D shell model takes longer because of the difficult geometry but less time is needed for the determination of the parameters. The mesh is more accurate. This will influence the calculation time. It is expected that for a very modern computer both models would result in limited calculation time but for an average computer the 2,5D shell model could take 10 or 20 times longer.

If one girder is inserted in DIANA then it is possible to copy this girder and apply it at a different location. This reduces the modelling time for the 2,5D shell model. To apply this one should determine the exact location of each part of the girder (x,y and z coordinates). But it is advised to do that in a few steps at once and to do intermediate checks.

It is also advised to create different sets for different part of the structure. This helps the interpreting the result in the post-processing. The output for this model is more difficult to interpret compared to the orthotropic plate model. The output is mainly stresses while in the orthotropic plate model these are forces and moments. Each shell has also three different layers; top, mid and bottom.

### 6.6.2 Results

The same aspects that have been modelled in the orthotropic plate model have been modelled in the 2,5D shell model.

The critical area for the longitudinal moment was found just over mid span towards the obtuse corner for the second girder, just as has been found for the orthotropic plate model.

In this model the total shear stresses were determined directly from the model.

The configuration for the maximum torsional moment with the accompanying shear force (load combination 4) was the governing configuration for the shear stresses in the orthotropic plate model. This was the case for the uniformly distributed load and the Eurocode loading.

The following results show that for the 2,5D shell model the maximum shear stresses is almost equal for both configurations for a uniformly distributed load but found at a difference location (girder). The left web is still governing over the right web. For the Eurocode loading the maximum torsional moment configuration was governing.

For the final values the shear stresses due to the self-weight and the prestressing are added up. This is done in chapter 7 for the final comparison between the two models.

## 7 COMPARISON

In this paragraph the results of the orthotropic plate model and the 2,5D shell model are compared. The results for the orthotropic plate model are found in paragraph 5.4 and 5.5. The results for the 2,5D shell model were presented in paragraph 6.4 and 6.5.

For the comparison two load situations are considered: a uniformly distributed load (7.1) and the Eurocode loading (7.2). The uniformly distributed load is used for the previous verification (paragraph 6.3) and is less interesting for the engineering practice. The results are still presented.

The focus is more on interesting load situation for the engineering practice, which is the load situation including the variable load from the Eurocode. For this comparison the internal forces due to the self-weight and prestressing are be added up with the results of the variable load from the Eurocode.

The left web was governing for both load situations concerning the shear stresses. Only this web is compared in this chapter.

### 7.1 Uniformly distributed load

In this paragraph the results for he distributed load are shortly presented.

#### 7.1.1 $S_{xx}$ stresses: longitudinal moment

#### ***2,5D SHELL MODEL***

When composed elements were used to integrate the stresses an average value for the moment at mid span was found of  $0,11 * 10^6$  Nmm.

The exact value, calculated by integrating the results for the  $s_{xx}$ , is  $0,980 * 10^5$  Nmm. This is a difference of 7% with the composed elements. The use of composed element does give a good first estimation but the exact value (detailed calculation) is more accurate.

**ORTHOTROPIC PLATE MODEL**

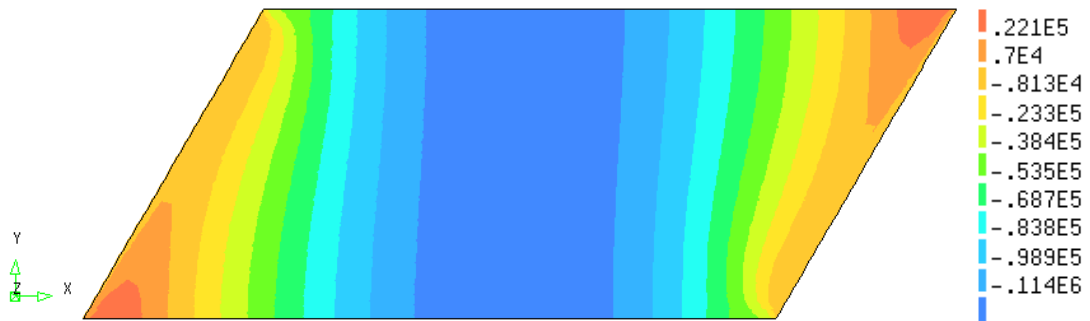


Figure 138,  $m_{xx}$  - skew plate – uniformly distributed load [Nmm/mm]

From a hand calculation a first estimation for the longitudinal moment is obtained. The plate is then schematized as a straight beam on simple supports:

$$M_{max} = \frac{1}{8} * q * l^2 = \frac{1}{8} * 0.001 * 14400 * 32250^2 = 1,75 * 10^9 \text{ Nmm for total girder}$$

$$\frac{1,75 * 10^9}{14400} = 0,13 * 10^6 \text{ Nmm/mm}$$

The contour plot shows a maximum moment of  $0,114 * 10^6$  Nmm/mm.

If shell elements are used for a plate model the  $S_{xx}$  stresses can also be integrated which gives more accurate results.

**COMPARISON**

The difference for the maximum value of the longitudinal moment is 12% if only the mobile loading of  $0,001 \text{ N/mm}^2$  is accounted for.

Table 31, difference between the two models for the longitudinal moment

Loading	Orthotropic plate model [Nmm/mm]	2,5D model [Nmm/mm]	shell	Overestimation [%]
Mobile load	$0,114 * 10^6$	$0,980 * 10^5$		12

The difference is less if the stresses are also integrated in the orthotropic plate model instead of using the  $m_{xx}$ . In practice there is always a load (self-weight and prestressing) which are calculated separately (without contribution to torsion) and has to be accounted for the total difference.

7.1.2  $S_{xz}$  stresses: shear stresses and torsional moments

The shear stresses are compared for two different cross-sections. One cross-section is at the transition point between hallow and massive (maximum shear force in a plate model) and one at mid span (maximum torsional moment in the plate model). Only the left web is compared because the governing values were found there.

**(1) CROSS-SECTION AT THE TRANSITION POINT (LEFT WEB)**

The shear stresses in the 2,5D shell model were directly determined from the model.

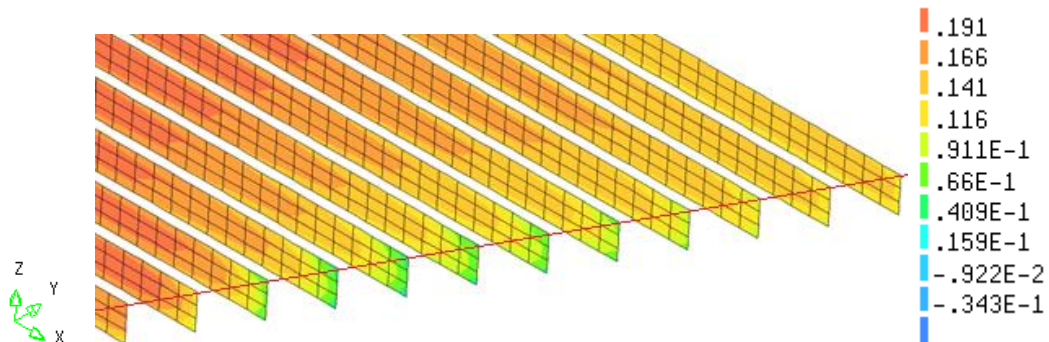


Figure 139, contour plot of the shear stresses in the girders at the transition point (left web) [N/mm<sup>2</sup>]

A graph is presented of these values. In this graph the values of the nodes of the elements through the line are presented. The average value is compared to the values calculated in the orthotropic plate model.

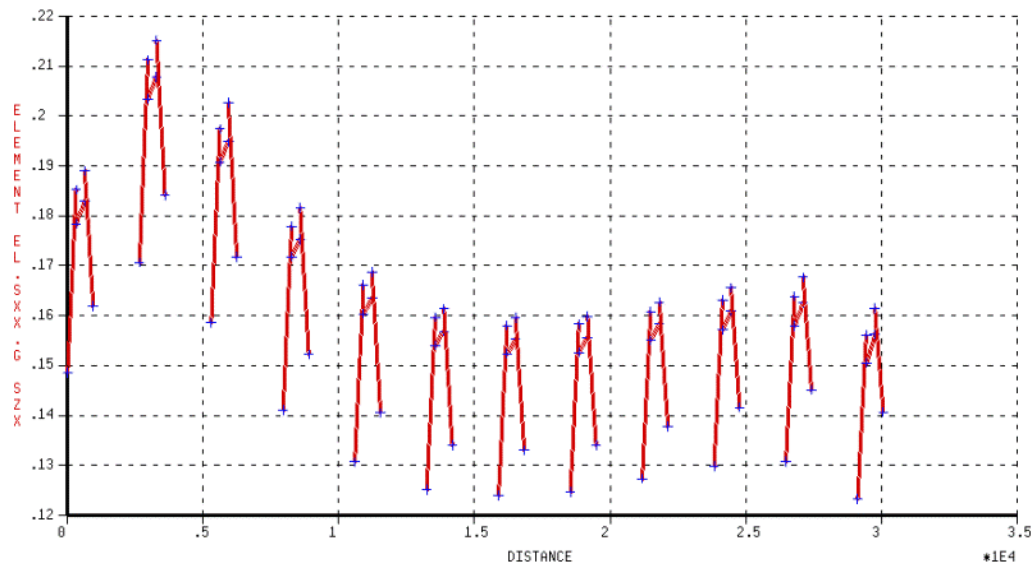


Figure 140, shear stress values of the element (left web) – 2,5D shell model [N/mm<sup>2</sup>]

In paragraph 5.4 the shear stresses in the orthotropic plate model were calculated for a uniformly distributed load. The following graph shows the values found for the left web of each girder.



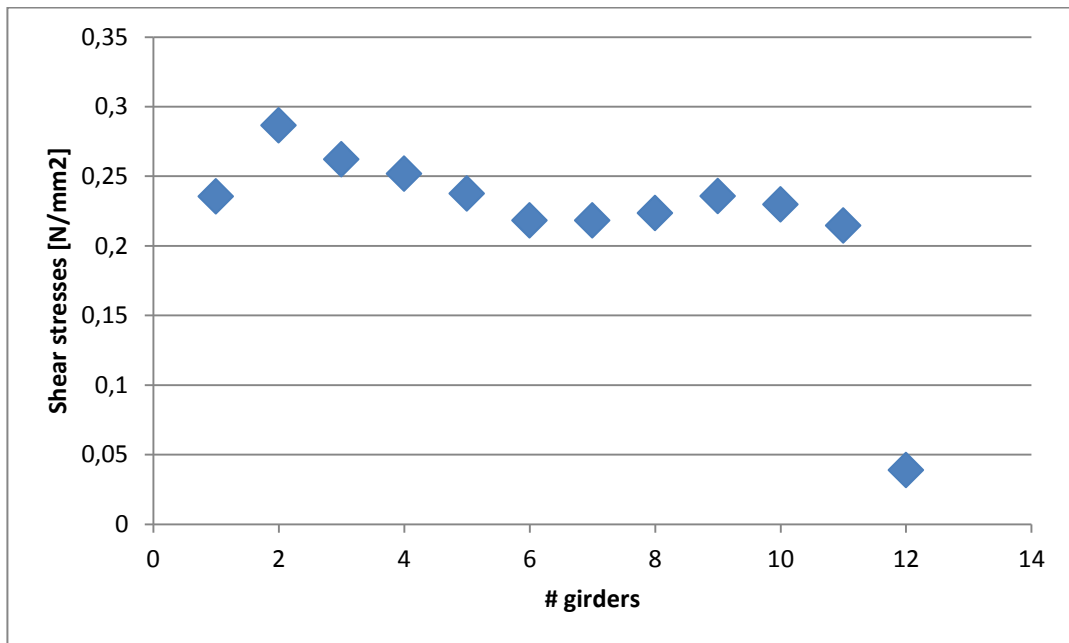


Figure 141, shear stress values of each girder (left web) near transition point (hollow – massive)

The comparison is presented in the following table:

Table 32, comparison for shear stress in left web [N/mm<sup>2</sup>] –cross-section at transition point - uniformly distributed load – maximum shear force configuration

# girder	Orthotropic plate model	2,5D shell model	Overestimation in %
1	0,24	0,17	38,5
2	0,29	0,20	45,3
3	0,26	0,19	38,0
4	0,25	0,17	48,2
5	0,24	0,16	48,5
6	0,22	0,15	45,5
7	0,22	0,16	40,8
8	0,22	0,15	48,9
9	0,24	0,15	57,2
10	0,23	0,16	43,6
11	0,21	0,16	34,1
12	0,04	0,15	-74,0

The maximum value is found at the same girder for both models. The orthotropic plate model gives an overestimation of approximately 45%.

**(2) CROSS-SECTION AT MID SPAN (LEFT WEB)**

The shear stresses in the 2,5D shell model were directly determined from the model.

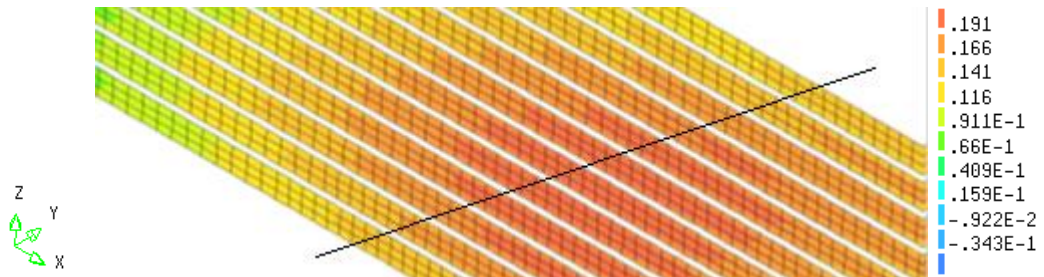


Figure 142, contour plot of the shear stresses in the girders at mid span (left web) [N/mm<sup>2</sup>/mm]

Again, a graph is presented of these values. In this graph the values of the nodes of the elements through the line are presented. The average value is compared to the values calculated in the orthotropic plate model.

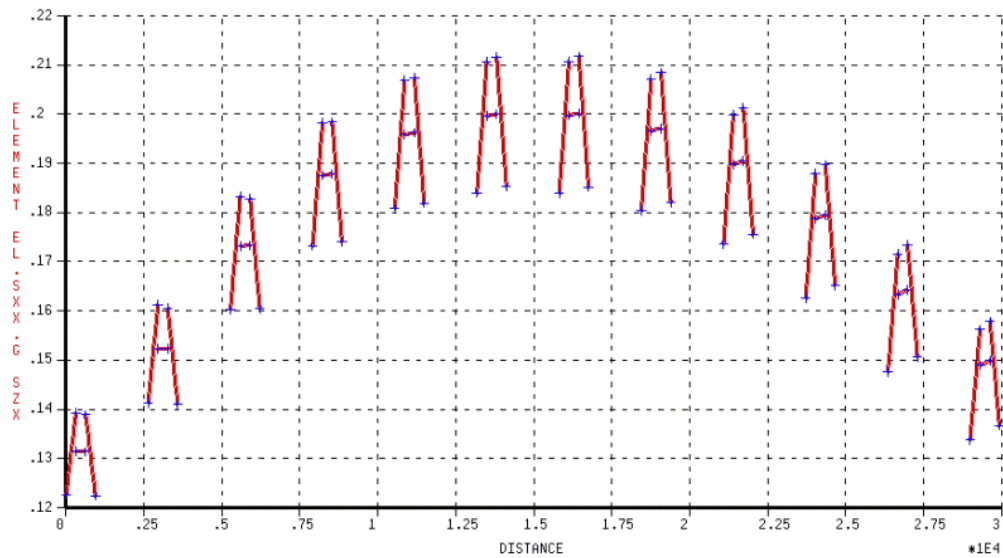


Figure 143, shear stresses at the right web mid span – DIANA result [N/mm<sup>2</sup>/mm]

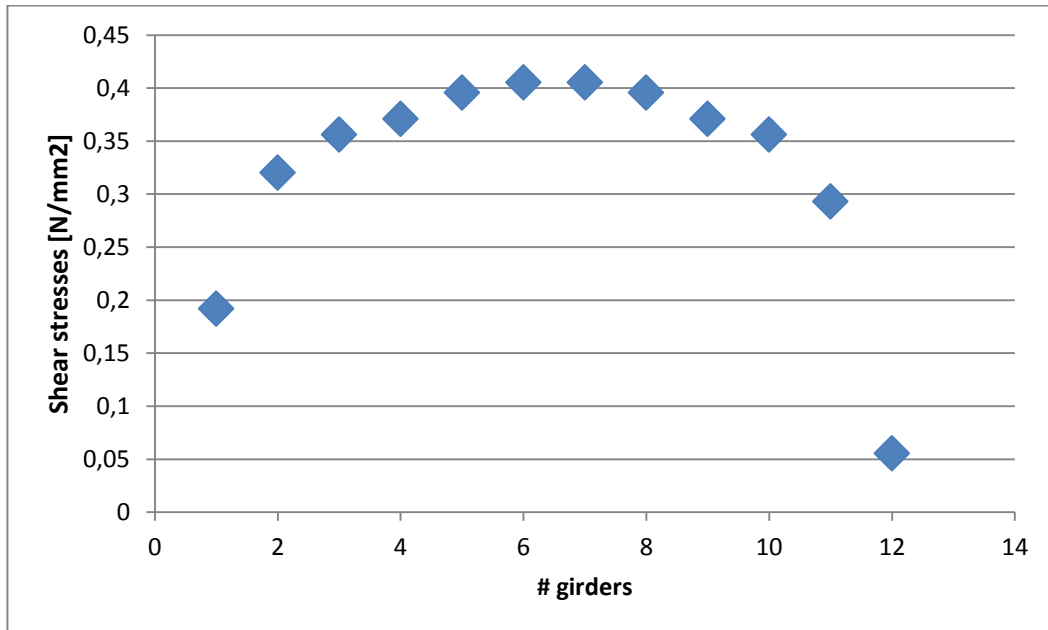


Figure 144, shear stress values of each girder (left web) at mid span

In the following table the results for both models are compared.

Table 33, comparison for shear stress [N/mm<sup>2</sup>] in left web – mid span - uniformly distributed load – maximum torsional configuration

# girder	Orthotropic plate model	2,5D shell model	Overestimation in %
1	0,19	0,13	47,5
2	0,32	0,15	113,5
3	0,36	0,18	97,8
4	0,37	0,19	95,2
5	0,40	0,20	97,8
6	0,41	0,20	102,7
7	0,41	0,20	102,7
8	0,40	0,19	108,2
9	0,37	0,19	95,2
10	0,36	0,18	97,8
11	0,29	0,16	83,1
12	0,06	0,15	-63,0

The maximum value for the shear stresses is found at the 6th and 7th girder for both models. A big difference is found for the results.

For mid span a maximum torsional moment was found in the plate model. But at that exact location the shear force has no contribution to the shear stresses. Schematization of forces is therefore not accurate if only torsional moments are present and the contribution of the shear force is negligible. This is the reason for the overestimation.

## 7.2 Eurocode loading

### 7.2.1 $S_{xx}$ stresses: longitudinal moment

#### **2,5D SHELL MODEL**

The maximum value found for the 2,5D shell model was approximately  $0,112 * 10^7$ . This value was also found at the same location as the orthotropic plate model: the second girder just over mid span towards the obtuse corner.

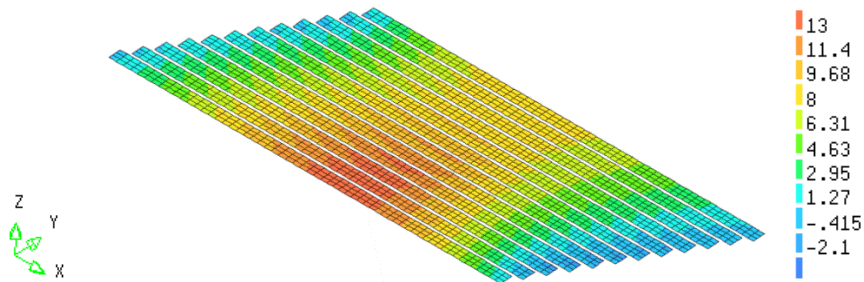


Figure 145,  $S_{xx}$  distribution of the 2,5D shell model for the bottom flange [ $N/mm^2$ ]

#### **ORTHOTROPIC PLATE MODEL**

The maximum value found for the longitudinal moment in the orthotropic plate model was  $0,119 * 10^7$  Nmm/mm. This was at the location of the second girder just over mid span towards the obtuse corner.

#### **COMPARISON**

In Excel a more detailed calculation has been done for every girder at the location of the maximum value for the longitudinal moment (just over mid span towards the obtuse corner). The results are found in the table below:

Table 34, difference in results for the longitudinal moment

# girder	Orthotropic plate model	2,5D shell model	Overestimation in %
1	1.189.999	1.012.377	17,3
2	1.190.000	1.123.366	6,5
3	1.185.000	1.119.047	5,3
4	1.170.000	1.011.666	14,2
5	1.090.000	969.079	10,2
6	1.050.000	936.837	11,1
7	1.030.000	879.574	16,9
8	990.000	780.160	25,6
9	975.000	728.967	33,3
10	950.000	698.809	35,5
11	930.000	677.245	37,1
12	920.000	644.044	42,6

In a plate model the stresses are well spread over the width of the girder. This is not the case for the 2,5D shell model where the high stresses are more local. If the peak stresses are spread they cause higher moments because they occur over more width and influence the total integration of stresses.

The longitudinal moment due to the self-weight and prestressing is not included for the 6,5% difference.

The maximum value found for the longitudinal moment due to the self-weight and the prestressing is  $0,62 * 10^6$  Nmm/mm. The calculation has been done in paragraph 4.6.

**Table 35, comparison of models for longitudinal moment Nmm / mm incl. self-weight and prestressing**

#2 girder	Orthotropic plate model	2,5D shell model	Overestimation in %
<b>Self-weight and prestressing</b>	618.333	618.333	0
<b>Mobile loads</b>	1.190.000	1.123.366	6,5
<b>Total</b>	1.800.833	1.741.452	3,5

The difference is now only 3,5%. It is an overestimation by the orthotropic plate model.

7.2.2  $S_{xz}$  stresses: shear force and torsional moment

The results for these stresses are presented per configuration for the left web only (governing for both configurations). The calculations have been made of the configuration for maximum shear force and the configuration for maximum torsional moment.

**(1) MAXIMUM SHEAR FORCE CONFIGURATION (LEFT WEB)**

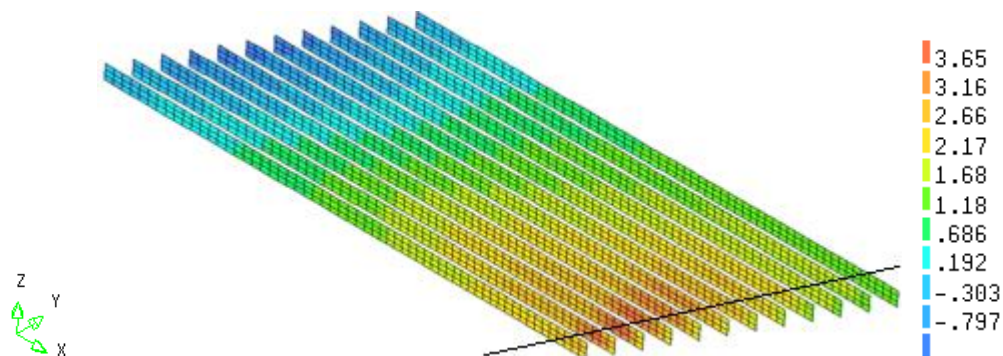


**Figure 146, shear stress [N/mm<sup>2</sup>] in the left web - maximum shear force configuration**

For this configuration the shear force induced shear stresses are governing over the shear stresses induced by the torsional moment. In the graphs on the next page the results from the previous paragraph are presented again after which a table is presented where the values are compared with each other.

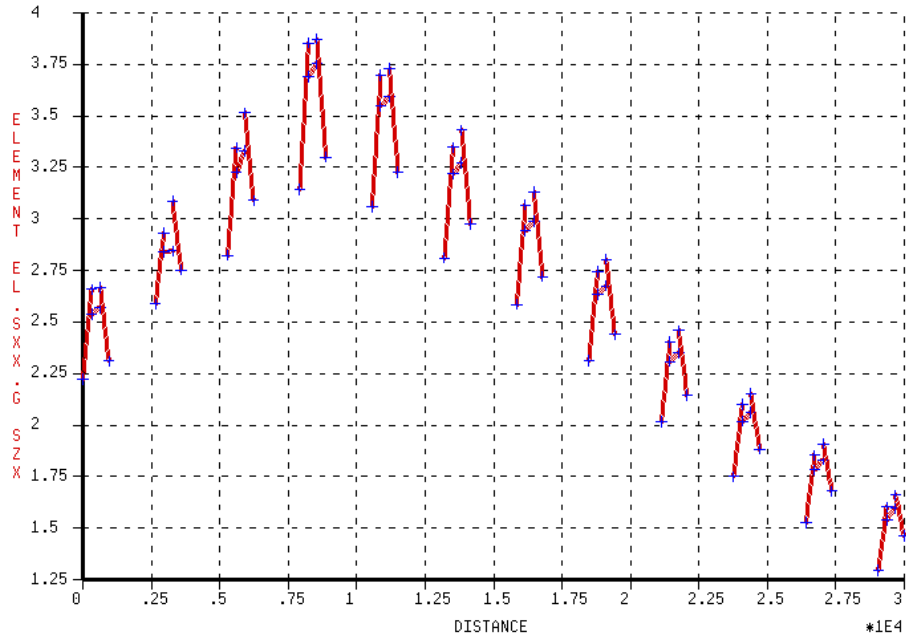


Figure 147, shear stresses [N/mm<sup>2</sup>] in the left web - maximum shear force configuration - 2,5D shell model

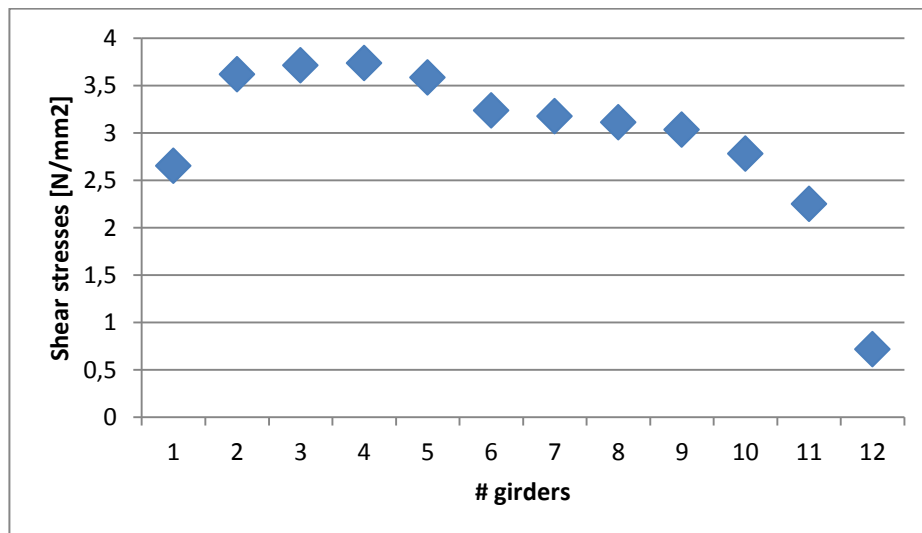


Figure 148, shear stresses in the left web - maximum shear force configuration - orthotropic plate model

The values for both models are compared at the next page.

Table 36, shear stresses [N/mm<sup>2</sup>] in the left web for the maximum shear force configuration

# girder	Orthotropic plate model	2,5D shell model	Overestimation in %
1	2,65	2,50	6,2
2	3,62	2,80	29,3
3	3,71	3,30	12,5
4	3,74	3,60	4,1
5	3,58	3,50	2,4
6	3,24	3,25	-0,4
7	3,17	3,00	5,8
8	3,11	2,60	19,7
9	3,03	2,30	31,9
10	2,78	2,00	39,1
11	2,25	1,75	28,6
12	0,72	1,50	-52,3

As can be seen from the results the shear stress is overestimated by the orthotropic plate model up to a maximum of 40 percent approximately (last result excluded). These are however not the governing results.

The governing value is found at girder number 4. The difference for the value at that girder is only 4,1%.

This is without the shear stresses due to the self-weight and the prestressing. The shear stresses due to these loads have been calculated in paragraph 4.6. Only the shear force has a contribution to the shear stresses since no torsional moments are present at the statically determined beam. Another important aspect is that the shear force distribution for a statically straight determined beam differs from the shear force distribution in a skew bridge. These two aspects cause a relatively low contribution of the shear stress to the self-weight and prestressing.

Table 37, governing shear stresses [N/mm<sup>2</sup>] for maximum shear force configuration

#4 girder	Orthotropic plate model	2,5D shell model	Overestimation in %
<b>Self-weight and prestressing</b>	0,52	0,52	0
<b>Mobile loads (EC)</b>	3,74	3,60	4,1
<b>Total</b>	4,26	4,12	3,3

The difference for the maximum value of the shear stresses is only 3,3%.

Before the amount of reinforcement is discussed the results of the configuration for maximum torsional moment are presented.

**(2) MAXIMUM TORSIONAL MOMENT CONFIGURATION (LEFT WEB)**

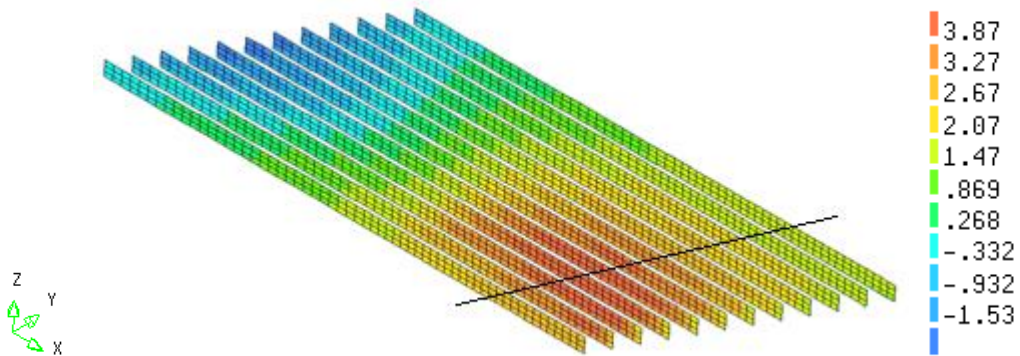


Figure 149, shear stress [N/mm<sup>2</sup>] in the left web - maximum torsional moment configuration

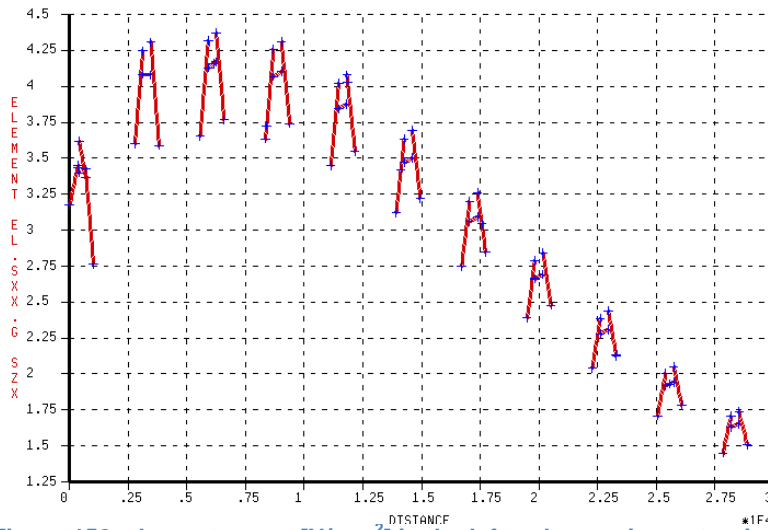


Figure 150, shear stresses [N/mm<sup>2</sup>] in the left web - maximum torsional moment configuration – 2,5D shell model

For the uniformly distributed load case it was observed that the configuration for maximum torsional moment gave the biggest inaccuracy for the results of the shear stresses. The following results are for the load situation including the Eurocode traffic load.



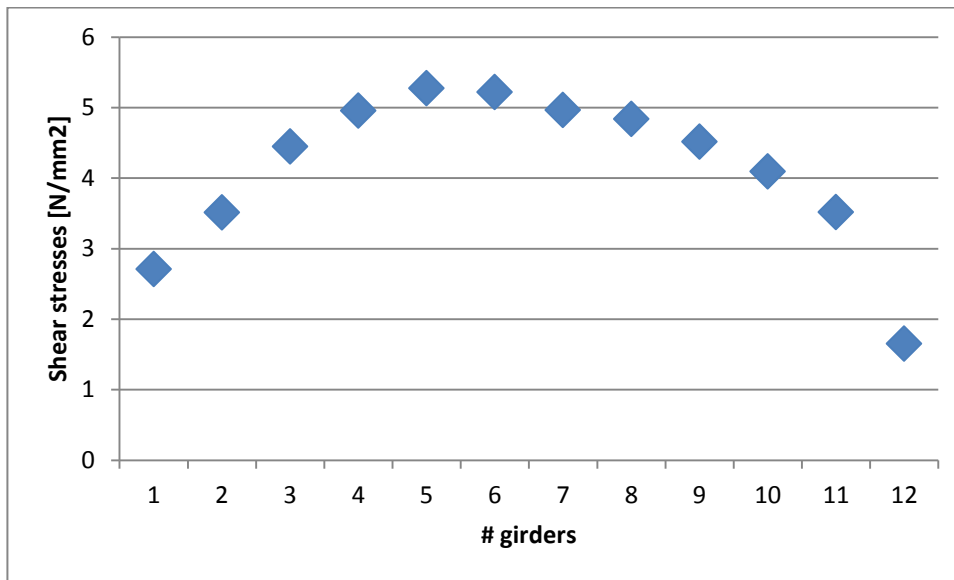


Figure 151, shear stresses in the left web - maximum torsional moment configuration – orthotropic plate model

In the following table the differences of both results are summarized and the overestimation is calculated.

Table 38, shear stresses in the left web for the maximum torsional moment configuration

# girder	Orthotropic plate model	2,5D shell model	Overestimation in %
1	2,71	3,30	-17,9
2	3,51	4,00	-12,2
3	4,45	4,20	5,9
4	4,96	4,00	24,0
5	5,27	3,80	38,7
6	5,22	3,50	49,1
7	4,97	3,50	41,9
8	4,84	3,00	61,3
9	4,51	2,50	80,6
10	4,09	2,25	81,9
11	3,52	1,80	95,3
12	1,65	1,60	3,2

As can be seen from the results, the shear stress is overestimated by the orthotropic plate model up to a maximum of 80 percent approximately (before last result excluded). These are however not the governing results.

The governing value is found at girder number 5. The difference for the value at that girder is only 38,7%. In the 2,5D shell model the maximum value is found at a different location and is 4,2 N/mm<sup>2</sup>. In this case the overestimation is 25%.

This is without the shear stresses due to the self-weight and the prestressing. The shear stresses due to these loads have been calculated in paragraph 4.6. Only the shear force has a contribution to the shear stresses since no torsional moments are present at the statically determined beam.

Table 39, governing shear stresses for maximum torsional moment configuration

#5 girder	Orthotropic plate model	2,5D shell model	Overestimation in %
Self-weight and prestressing	0,52	0,52	0
Mobile loads (EC)	5,27	4,20	25,2
<b>Total</b>	<b>5,79</b>	<b>4,72</b>	<b>18,4</b>

The difference for the maximum value of the shear stresses is 18,4% and these shear stresses are governing compared to the shear stresses calculated for the maximum shear force configuration.

The shear stress capacity for the web is calculated with the following formula from the Eurocode (6.2.2.). The last value is limited in the Eurocode to  $0,2 \cdot f_{cd}$  (governing).

$$\tau_{max} = C_{Rd} * k * (100 * \rho_l * f_{ck})^{\frac{1}{3}} + k_1 * \sigma_{cp}$$

The values are calculated and filled in:

$$\tau_{max,per\ web} = 0,12 * 1,45 * (100 * 0,018 * 40)^{\frac{1}{3}} + 0,15 * 5,3 = 1,3\ N/mm^2$$

With a minimum of:

$$\tau_{min} = 0,035 * k^{\frac{3}{2}} * f_{ck}^{\frac{1}{2}} = 0,5\ N/mm^2$$

This means that reinforcement is needed. Relatively, the amount of reinforcement is not changed for the two models when the shear stresses due to the self-weight and prestressing are added up. But this decreases the overestimation by the orthotropic plate model because the now the total values are taken in to account and the difference is originally only for the mobile loads.

$$\frac{A_{sw}}{s} = \frac{V_{Rd,s}}{z * f_{ywd} * \cot\theta}; (z = 0,9d, f_{ywd} = \frac{435N}{mm^2}, \theta = 21.8)$$

$$V_{Rd,s1} = 5,79 * 200 * 1100 = 1273800\ N\ (orthotropic\ plate\ model)$$

$$V_{Rd,s2} = 4,72 * 200 * 1100 = 1038400\ N\ (2,5D\ shell\ model)$$

$A_{sw1}/s = 1250\ mm^2 / m$  (incl. 10% execution aspects)  $\rightarrow 12\ \emptyset$  (n=2 per web, per 175 mm,  $\rightarrow 1293\ mm^2 / m$  (Orthotropic plate mode)

$A_{sw2}/s = 1010\ mm^2 / m$  (incl. 10% execution aspects)  $\rightarrow 10\ \emptyset$  (n=2 per web, per 150 mm,  $\rightarrow 1050\ mm^2 / m$  (2,5D shell model)

This means an increase of 23% for the shear reinforcement.

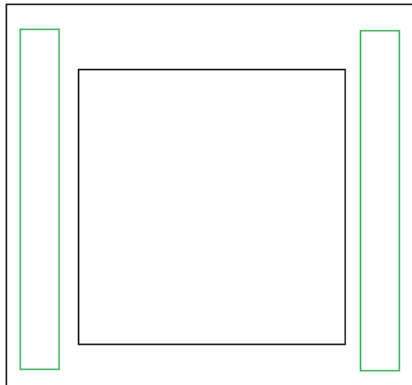


Figure 152, applied stirrups

It is assumed that the stirrups are designed according to the maximum value for the shear stresses as shown. It is also assumed that these stirrups are applied over the full length.

The cost can now be calculated. It is assumed that a kg of reinforcing steel costs 1,5 euro (incl. execution). The self-weight of steel is 7800 kg/m<sup>3</sup>.

Table 40, total costs for stirrups

	Orthotropic plate model		2,5D shell model	
<b>One bar area</b>	(Ø12) 113	mm <sup>2</sup>	(Ø10) 78,5	mm <sup>2</sup>
<b>Volume steel per web per m</b>	1.485.142	mm <sup>3</sup> /m	1.203.667	mm <sup>3</sup> /m
<b>Per girder (*2*32)</b>	95.049.142	mm <sup>3</sup>	77.029.714	mm <sup>3</sup>
<b>12 girders (*12)</b>	1.140.589.714	mm <sup>3</sup>	922.356.572	mm <sup>3</sup>
<b>12 girders in m<sup>3</sup></b>	1,14	m <sup>3</sup>	0,92	m <sup>3</sup>
<b>12 girders in kg steel</b>	8.892	kg	7.210	kg
<b>Price for 1 kg steel</b>	1,5	euro	1,5	euro
<b>Price</b>	13.338	euro	10.815	euro

Using the orthotropic plate model means 23% (approximately 2500 euros) more spend on stirrups. The volume of concrete of the total viaduct is 257 m<sup>3</sup> concrete. Per m<sup>3</sup> the price of the stirrups is only 52 euro for the orthotropic plate model. For the shell model this is 42 euro stirrups per m<sup>3</sup> concrete. The difference is 10 euro per m<sup>3</sup> concrete. This is 215 euro per girder.

First estimation of prices in the practice shows that a m<sup>3</sup> of a precast box girder costs 850 euro approximately in total. The stirrups are only about 5 percent of the costs of a box girder per m<sup>3</sup> concrete. The difference between the two models for the stirrups is 1,2% of the total costs.

Table 41, costs for stirrups in comparison with reinforcement and total for girder

Price in euros per m <sup>3</sup> girder	Orthotropic plate model	2,5D shell model
<b>Total for a box girder</b>	850	850
<b>Stirrups</b>	52	42
<b>Stirrups / total</b>	6,1%	4,9%

### 7.3 Summery

Different formulas and methods from literature have been used to translate the forces and moments from the orthotropic plate model into stresses in the box beam girder. These were then compared to the stresses found in the 2,5D shell model. The expectation was the results for the deflection and longitudinal moment would be approximately equal but that the results for the shear stresses would differ. This is exactly what has been found. In the comparison the focus was on the shear stresses and if these differences were relevant or not.

#### Comparison uniform distributed load

In the first analysis only a uniformly distributed load was inserted. The result showed that the displacement field and the longitudinal moment were very similar.

The values for the longitudinal moment are almost equal if the  $m_{xx}$  from the plate model is compared to the average moment calculated by the composed 'line' element. When the stresses are integrated in the 2,5D shell model the exact moment is found. This exact moment differs 12% from the  $m_{xx}$  in a plate (overestimation by the orthotropic plate).

The governing configuration for the orthotropic plate model was the maximum torsional moment configuration. The 2,5D shell model gave the same maximum shear stresses for both configurations. The maximum difference between the models was found for the torsional moment configuration. For mid span the shear stresses are mainly generated by torsional moment. The schematization of forces is therefore not accurate if only torsional moments are present and the contribution of the shear force is negligible.

The uniformly distributed load is used for the previous verification (paragraph 6.3) and is less interesting for the engineering practice. The results are still presented.

The focus is more on interesting load situation for the engineering practice, which is the load situation including the variable load from the Eurocode. For this comparison the internal forces due to the self-weight and prestressing are be added up with the results of the variable load from the Eurocode.

#### Comparison Eurocode loading

In the second analysis the Eurocode traffic load was included. For this load situation the results were presented in more details.

The maximum value for the longitudinal moment was found at the same location for both models. The difference was 6,5% approximately. This was found without the longitudinal moment of the self-weight and the prestressing included. The moment due to the self-weight and prestressing was approximately 35 percent compared to the moment due to the mobile loads. When this was included, the difference became only 3,5 percent. This is an overestimation by the orthotropic plate model.

The orthotropic plate model gave an overestimation of the shear stresses. Two configurations at two different cross-sections were again examined. The governing configuration was the maximum torsional moment configuration.

The governing value is found at girder number 5. The difference for the value at that girder is 38,7%. In the 2,5D shell model the maximum value is found at a different location and is 4,2 N/mm<sup>2</sup>. In this case the overestimation is 25%.

This is without the shear stresses due to the self-weight and the prestressing. When these are included the difference is 18,4%.

The stirrup reinforcement according to the orthotropic plate model is 1293 mm<sup>2</sup> / m.

The stirrup reinforcement according to the 2,5D shell model is 1050 mm<sup>2</sup> / m.

This means an increase of 23% for the shear reinforcement.

The cost can now be calculated. It is assumed that a kg of reinforcing steel costs 1,5 euro (incl. execution). The self-weight of steel is 7800 kg/m<sup>3</sup>.

Table 42, total costs for stirrups

	Orthotropic plate model		2,5D shell model	
<b>Price stirrup</b>	13.338	Euro	10.815	Euro
<b>Per girder</b>	1113	Euro	902	Euro
<b>Per m<sup>3</sup> concrete</b>	52	Euro	41	Euro
<b>Total costs box girder per m<sup>3</sup> concrete</b>	850	Euro	850	Euro
<b>% of total costs</b>	6,1	%	4,9	%

Using the orthotropic plate model means 23% (approximately 2500 euros) more spend on stirrups.

It is expected that the 2,5D shell model will take two weeks longer to analyze. This means that this will cost 7200 euro for engineering. It is therefore not worth to use the 2,5D shell model to save up money for the shear reinforcement (2500 euro).

It is assumed that the stirrups are designed according to the maximum value for the shear stresses as shown. It is also assumed that these stirrups are applied over the full length.

## 8 CONCLUSION

The objective of this research was to investigate the behavior of skew box beam viaduct, mainly concerning shear and torsion, and to find a good method approach for FEM. With reference of the sub questions, the conclusions are given.

The conclusions mentioned are valid for a skew box beam viaduct with a skew angle of 60 degree and for case study as mentioned in chapter 3.

The following aspects were important to take in to account:

- Correct calculation of the cross-sectional parameters as shown in appendix A & B
  - o An important parameter is the transverse bending stiffness
- Transverse prestressing
- Massive end beams
- Modelling of the bearing

The critical areas for the Eurocode loading were found with the orthotropic plate model:

- For the longitudinal moment, the maximum value was found at the second girder just over mid span towards the obtuse corner
- The maximum value for the shear force was found at the obtuse corner
- The maximum value for the torsional moment was found close to the support at the 6<sup>th</sup> girder (mid span of the width).

The forces and moments of the orthotropic plate model can be related to the stresses in the 2,5D shell model as follows:

- The local longitudinal moment of the orthotropic plate model can be related to the 2,5D shell model by integrating the  $s_{xx}$  stresses in the 2,5D shell model for one girder and dividing this value by the width to get the average longitudinal moment per mm.
- The shear force and the torsional moment in the orthotropic plate model can be translated in to shear stresses through the formulas and method approach as described in 5.4.5.

What model approach is the most accurate, efficient and gives the best results for this type of viaducts and what model approach is advised for the engineering practice?

**Accuracy:** the accuracy for the maximum value of the longitudinal moment seems to be around the 6% for the Eurocode loading. This is an overestimation by the orthotropic plate model. The accuracy becomes less at other location of the viaduct, but those locations are not governing because it is assumed that the design will be based on maximum values that are found.

The same aspect was found for the shear stresses. The schematization cannot represent the shear stresses values at every girder within 10%-20% accuracy. The overestimation by the orthotropic plate model for the shear stress was 25%.

**Self-weight and prestressing:** for the Eurocode loading it was found that the maximum value for the longitudinal moment was overestimated by 3,5 percent with the orthotropic plate model when the moment due to the self-weight and the prestressing was taken in to account.

The maximum value for the shear stresses was overestimated by the orthotropic plate model 18% when the shear stresses due to the self-weight and prestressing are taken in to account. This led to 23% more shear reinforcement.

**Costs:** it is expected that the 2,5D shell model will take two weeks longer to analyze. This means that this will cost 7200 euro for engineering. It is therefore not worth to use the 2,5D shell model to save up money for the shear reinforcement (2500 euro).

**Advice for the engineering practice:** it is advised that the orthotropic plate model can be used for the analysis of skew box beam viaducts with a skew angle of 60 degrees and as described in chapter 3 when the difference in costs for the two models are taken in to account. This is especially the case for new to be constructed viaducts.

The orthotropic plate model does not give accurate results at every location of the viaduct for the longitudinal moment and the shear stresses but the difference in maximum values does not lead to great increase in costs. It is assumed that the stirrups are designed according to the maximum value for the shear stresses as shown. It is also assumed that these stirrups are applied over the full length.

In case of a reassessment of an existing viaduct where the combination of shear force and torsional moment are governing, the difference of 18% for the shear stress could be decisive in whether the viaduct fulfills the current codes and requirements or not with the present shear reinforcement. If the viaduct does not fulfill the codes with the orthotropic plate model (overestimation of the shear stresses) the viaduct will not be approved and should be replaced. The 2,5D shell model gives more accurate results with better insight in the shear stresses. This can be decisive whether the viaduct should be reinforced (often not possible in practice) or that it should be replaced because it does not fulfill the current codes and requirements. In that case the 7200 euro more spent on the 2,5D shell model should be reconsidered because the limitation of traffic or replacement of the viaduct will cost much more time and money.

## 9 RECOMMENDATIONS

A few recommendations are given for further research concerning this topic;

### (1) Determination of the most critical load configuration for shear stresses

For this research it is assumed that the maximum shear stress in a girder is due to maximum shear force with accompanying torsional moment or due to maximum torsional moment with accompanying shear force. In a 2,5D or 3D model the shear stresses due to both can be presented. In this case there is a chance that a configuration might exist where a combination of values of shear force and torsional moment might give the extreme values instead of one of both being maximum.

### (2) Nonlinear analyses

For the calculation in this master thesis linear elastic material behavior is assumed. With a nonlinear analysis it would be possible to determine the crack pattern for these types of viaducts and gain information about the failure mechanisms. It could also be determined how the stiffness, of different directions, relates to each other after cracking.

### (3) Other skew angles and different width-span ratio

The skew angle considered for the case study viaduct is 60 degrees. It should be examined if the results would be the same if less skew angles are modelled.

In CUR rapport 53 it was mentioned that the width span ratio has an influence on the results found for the internal forces. The span was two times the width for this case study viaduct. Another ratio could be examined to be able to conclude about the validity and accuracy of using the orthotropic plate instead of the 2,5D shell model.

### (4) Make use of composed plate element

When analyzing the 2,5D shell model it was not directly possible to integrate the stresses in DIANA. With the latest version (9.6) it is possible to use composed elements. For shell elements only composed 'line' elements were available. This limits the possibilities. Composed 'plate' elements are currently only available for 3D elements. It would be an added value if composed 'plate' elements were available for shell elements also.

### (5) Comparison with more detail design of stirrups

For this thesis it is assumed that the stirrups are designed according to the maximum value for the shear stresses as shown. It is also assumed that these stirrups are applied over the full length. In practice it is sometimes possible to design the stirrups in more detail.

This means that stirrups needed for the maximum shear stress are not applied at the full length but only at the necessary area. This will make the 2,5D results more efficient. The area where minimum shear reinforcement must be applied will also have an influence on the efficiency of the 2,5D shell model. If the minimum reinforcement is applied for a large area then the difference between the two models will be reduced.



## 10 LITERATURE

- [1] **FIB - Task group 6.4** (2004), Precast concrete bridges
- [2] **Hans Binkhorst, Jan van den Hoonaard, Jan Manhoudt, Frans Remery e.a.** (2000), Bruggen in Nederland: Techniek in ontwikkeling 1950 – 2000.
- [3] **John J. Panak** (1977), Skewed multi-beam bridges with precast box girders
- [4] **Kassahun K. Minalu** (2010), Finite Element Modelling of Skew slab-girder bridges
- [5] **Eurocode 1: Actions on structures** – Part 2: Traffic loads on bridges
- [6] **Prof.dr.ir.Dr.-Ing.h.c. J.C. Walraven** (2011), Reader Structural Safety
- [7] **Prof.dr.ir. J.C. Walraven, dr.ir.drs. C.R. Braam** (2011), Reader Prestressed Concrete
- [8] **C. M. Frissen, M. A. N. Hendriks, N. Kaptijn, A. de Boer and H.Nosewicz** (2002), 3D FEA of multi-beam box girder bridges – assessment of cross-sectional forces in joints
- [9] **Jan G. Rots & Max A.N. Hendriks** (2012), Lectures Computational Modeling of Structures
- [10] **M.G.M. van den Hoogen** (2010), Beam or truss mechanism for shear in concrete
- [11] **DIANA online support manual** (2014), <https://support.tnodiana.com/manuals/d95/Diana.html>
- [12] **Rijkswaterstaat**, Richtlijnen Beoordeling Kunstwerken 1.1
- [13] **Ir. R.P.H. Vergoossen, Cement – 4** (2008), Het afschuifdraagvermogen volgens Nederlandse ontwerpnormen
- [14] **J. Blaauwendraad** (2010), Plates and FEM: Surprises and Pitfalls
- [15] **Angelo Simone** (2011), An Introduction to the Analysis of Slender Structures
- [16] **Evert van Vliet** (2012), Torsion in ZIP bridge system
- [17] **Khan, Waqar** (2010), "Load Distribution In Adjacent Precast "Deck Free" Concrete Box-Girder Bridges". Theses and dissertations. Paper 1504
- [18] **CUR Rapport 53** (1972), Scheve platen – gelijkmatig verdeelde belasting
- [19] **P.C.J. Hoogenboom** (2010), Aantekeningen over wringing

## 11 APPENDIX A: DETERMINING CROSS-SECTION PARAMETERS

### 11.1 Introduction

In the book of Blaauwendraad it is written that in the engineering practice a lot of problems occur when determining the cross-sectional parameters. When the results from different engineers were compared it was clear that the transverse bending stiffness and the torsional stiffness are the most unpredictable to determine.

In this appendix the stiffness parameters of the box beam cross-section are determined. Most parameters are calculated with a simple hand calculation but, DIANA will also be used to determine the transverse bending stiffness. The cross-section of the box girder is torsion stiff and will also transfer load in the transverse direction. These parameters are therefore very important.

The parameters are determined according the following literature: [14 – Part 4 Chapter 21 ]

### 11.2 Surface

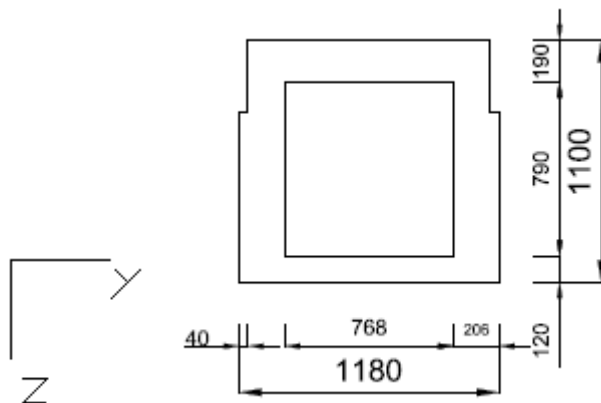


Figure 153, cross section

#### 11.2.1 X direction

$$\text{Total surface } [A_x] = (1180 * 1100) - (790 * 768) - (2 * 40 * 330) = 664880 \text{ mm}^2$$

Per mm width, the area is:

$$A_{x,per \text{ mm}} = \frac{664880}{1180} = 564 \text{ mm}^2 \text{ per mm}$$

#### 11.2.2 Y direction

$$\text{Surface } [A_{y,per \text{ mm}}] = 120 + 190 = 310 \text{ mm}^2 \text{ per mm}$$

#### 11.2.3 Z direction

$$\text{Surface } [A_{z,per \text{ mm}}] = 2 * 206 = 412 \text{ mm}^2 \text{ per mm}$$

### 11.3 Axial stiffness

The axial stiffness for the three directions is:

$$\frac{EA_x}{L} = 35000 * 564 = 1,80 * 10^7 \text{ N per mm}$$

$$\frac{EA_y}{L} = 35000 * 310 = 9,92 * 10^6 \text{ N per mm}$$

$$\frac{EA_z}{L} = 35000 * 412 = 1,32 * 10^7 \text{ N per mm}$$

### 11.4 Flexural stiffness

#### 11.4.1 X direction

The moment of inertia is calculated for one girder:

$$\begin{aligned} \text{Moment of inertia } [I_x] \\ &= \frac{1}{12} * b_{total} * h_{total}^3 - \frac{1}{12} * b_{inside} * h_{inside}^3 - \frac{2}{12} * b_{fill} * h^3 - 2 * A_{fill} \\ &\quad * a_{steiner}^2 = 9,46 * 10^{10} \text{ mm}^4 \end{aligned}$$

Per mm:

$$I_x = 9,46 * \frac{10^{10}}{1180} = 8,0 * 10^7 \text{ mm}^4 \text{ per mm}$$

$$EI_x = 35\ 000 * 8,0 * 10^7 = 2,81 * 10^{12} \text{ Nmm}^2 \text{ per mm}$$

#### 11.4.2 Y direction

For the stiffness in the transverse direction a few possibilities have been examined. This is written in more detail than other parameters because it was interesting to examine different models and examine the influence of boundary conditions.

For this stiffness parameter the ROBK (chapter 12.2.7) has also been used.

#### **HAND CALCULATION**

The same procedure, as has been done for the bending stiffness in the longitudinal direction, can be done for the transverse direction. Only upper flange, where the transverse prestressing is present, will contribute to the transverse stiffness according to this assumption. Where the transverse prestressing is present, the inner mould is different and the top flange is thicker. To take this in to account an average (with and without the red part) thickness is determined. The stiffness is calculated per millimeter.



Figure 154, front view of the girder and side view of the girders

The distance between the transverse prestressing is 1200 mm. The stiffness of that area in the transverse direction is calculated and it is transformed to stiffness per millimeter:

For the side view:

$$Z_{nc} = 117 \text{ mm}$$

The Steiner part is neglected.

$$I_{yy,red \text{ part}} = \frac{1}{12} * b * h_{total}^3 = \frac{1}{12} * 250 * 140^3 = 5,7 * 10^7 \text{ mm}^2 +$$

$$I_{yy,rest} = \frac{1}{12} * b * h_{total}^3 = \frac{1}{12} * 950 * 190^3 = 5,4 * 10^8 \text{ mm}^2 =$$

$$I_{yy,total} = I_{yy,red} + I_{yy,rest} = 6,0 * 10^8 \text{ mm}^4 \text{ per } 1200 \text{ mm}$$

$$I_{yy,total} = I_{yy,red} + I_{yy,rest} = 0,05 * 10^7 \text{ mm}^4 \text{ per mm}$$

$$EI_{yy,total} = 35000 * 6,0 * \frac{10^8}{1200} = 17,5 * 10^9 \text{ Nmm}^2 \text{ per mm}$$

### **DIANA MODEL**

The flexural rigidity in this direction ( $D_{yy}$ ) can be determined by subjecting one box beam to a bending moment and calculate the rotation  $\varphi$  at each end. The relation is:

$$C = \frac{m_{yy}}{2\varphi}$$

Because of  $m_{yy} = D_{yy} * \kappa_{yy}$  the final stiffness can be found by

$$EI_{yy} = D_{yy} = \frac{C}{b}$$

**\*subscripts mentioned are in the global xyz direction**

**2D Plane strain model/condition**

**Type: Structural 2D**

**Millimeter, Newton, Kg**

**Element: Infinite shell, CL9PE (three-node numerically integrated)**

**Degrees of Freedom:  $U_x, U_y, \varphi_z$**

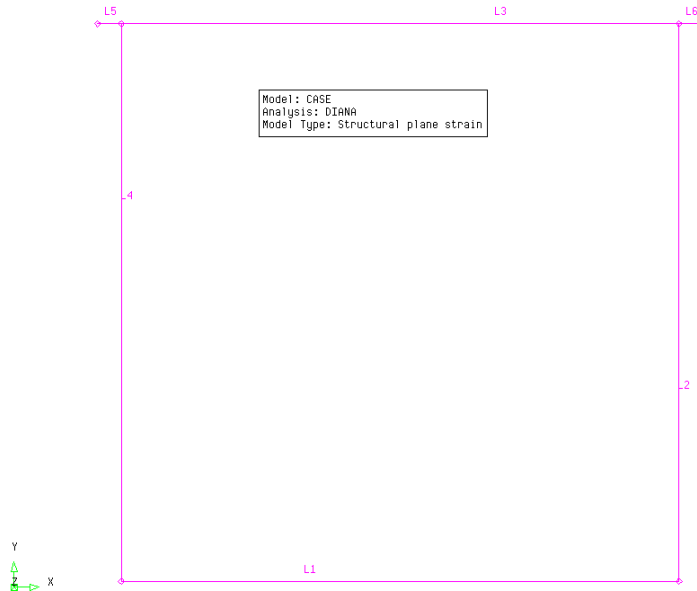


Figure 155, geometry of the cross-section in DIANA

Table 43, material and physical input

Material	E-modules [N/mm <sup>2</sup> ]	Poisson [-]	Physical	Thickness [mm]
1	35000	0.2	1	120
2	30000	0.2	2	206
			3	190*

Table 44, element information

Line #	Length [mm]	Width [mm]	Elements #	Elements #	Element [mm]	Material	Physical
1	1180	1	10	10	118	1	1
2	1100	1	10	10	110	1	2
3	1180	1	10	10	118	1	3
4	1100	1	10	10	110	1	2
5	50	1	2	2	25	2	3
6	50	1	2	2	25	2	3

\*weakest cross-section without the filling for the prestressing

### LOADING & BOUNDARY CONDITION

The cross-section is loaded with a moment of  $1 \times 10^6$  Nmm at the end of line 5 and 6. The rotation is around the z-axis. The box girder has supports at each ends in x and y direction.

### RESULTS

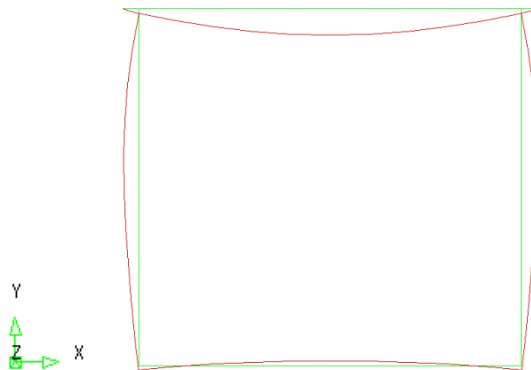


Figure 156, rotation of the cross-section

The rotation at the point where the moment is applied can be found, the stiffness can be calculated according to the following relation:

$$EI_{yy} = \frac{m_{yy} * W_{beam}}{2\varphi}$$

$$m_{yy} = 1\,000\,000 \text{ Nmm}$$

$$W_{beam} = 1180 \text{ mm}$$

The rotation found at the point of application of the moment is:  $1,24 \times 10^{-2}$  rad.

$$EI_{yy} = \frac{1e6 * 1180}{2 * 1,24 * 10^{-2}} = 46 * 10^9 \text{ Nmm}^2 \text{ per mm}$$

$$I_{yy} = 46 * \frac{10^9}{35000} = 0,13 * 10^7 \text{ mm}^4 \text{ per mm}$$

### MODEL CHECK

The output of the model should satisfy the following conditions:

1. The displacement in the z direction should be 0
2. Rotation only in z direction
3. The final result should be more than the hand calculation because in this model the influence of the webs and bottom flange is taken in to account.
4. Only moments are applied (in equilibrium)
5. When applying one moment, the supports should make equilibrium.

### Alternative method

As an alternative it is possible to model the girders, for example 3, next to each other and apply the following:

$$EI_{yy} = \frac{F * W^3_{beam}}{48 * w}$$

### **LOADING & BOUNDARY CONDITION**

The cross-section is loaded with a distributed load of 1000 N/mm over 100 mm in the middle. The box girder has supports at each ends in x and y direction.

### **RESULTS**

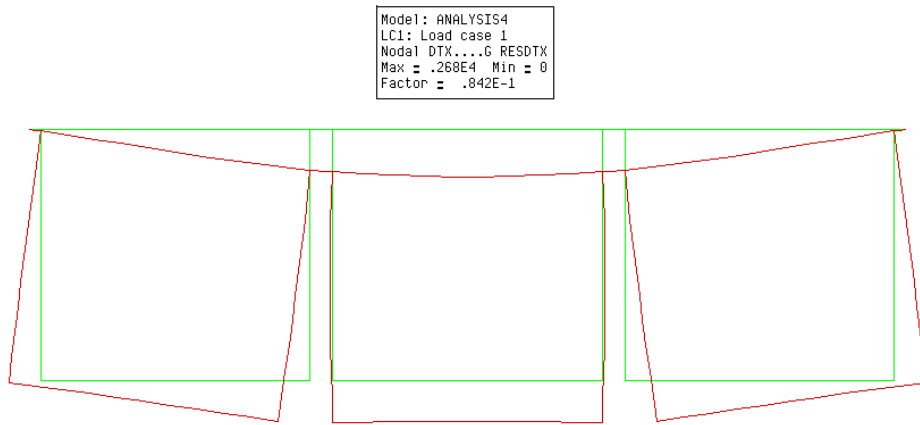


**Figure 157, geometry and deflection due to point load (schematized as distributed load)**

The rotation at the point where the moment is applied can be found, the stiffness can be calculated according to the following relation:

$$EI_y = \frac{F * W^3_{beam}}{48 * w}$$

$$F = 100 * 1000 = 100\ 000\ \text{N}$$

$$W_{beam} = 1180\ \text{mm}$$

The deflection found is:  $0.27 * 10^4\ \text{mm}$

$$D_{yy} = EI_{yy} = \frac{100 * 1000 * ((1180 + 100) * 3)^3_{beam}}{48 * 0,27 * 10^4} = 48 * 10^9\ \text{Nmm}^2\ \text{per mm}$$

### **MODEL CHECK**

The output of the model should satisfy the same conditions as specified before. In this case vertical force equilibrium can be checked:

$$F_{external} = 100 * 1000 = 100\ 000\ \text{N}$$

$$F_{internal} = 2 * 0,5 * 10^5\ \text{N}$$

**CONCLUSIONS FOR DETERMINING THE TRANSVERSE STIFFNESS OF A BOX BEAM**

It is best to apply two moments at each ends for one box beam girder. Because the moments are in equilibrium, the boundary conditions do not affect the result. If this is not done (only one moment for example), the exact stiffness should be determined of the joints between the girders.

A hand calculation, as presented, is a safe assumption but the exact stiffness is much higher and should be determined by a FEM.

It is also possible to apply a few girders next to each other and to apply the following relation:

$$EI_{yy} = \frac{F * w_{beam}}{48 * w}$$

Where 'w' is the deflection. This solution has less accuracy because of the boundary conditions. These are modelled with fixed support while in the real situation a translation spring would be a better model.

11.4.3 Coupling/Off-diagonal term

This term,  $D_v$ , is related to the top plane stiffness only:

$$D_v = v * D_{yy, top\ flange}$$

In in this case only the top flange has to be considered. This means that the stiffness of that plane in the transverse direction has to be found first. The steps are as followed:

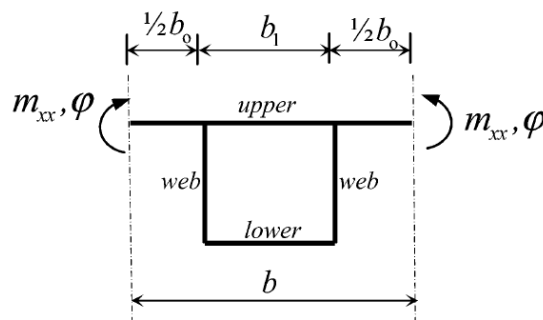


Figure 158, model for determining the stiffness - fig 21.8 [14]

The x direction in the figure is the y direction in the case study:

$$D_{yy, top\ flange} = \frac{b_0 * m_{yy} + b_1 * m_{yy, 1}}{b * m_{yy}} * D_{yy}$$

$$D_{yy, top\ flange} = \frac{100 * 1e6 + 1180 * 3e5}{1280 * 1e6} * 46 * 10^9 = 16 * 10^9\ Nmm^2\ per\ mm$$

$$I_{yy, top\ flange} = 16 * \frac{10^9}{35000} = 4,5 * 10^5\ mm^4$$

$$I_v = 0,2 * 4,5 * 10^5\ mm^4 = 0,9 * 10^4\ Nmm^2$$



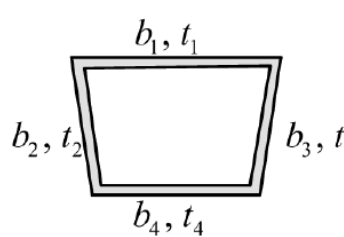
## 11.5 Torsional stiffness

The constitutive law for torsion is:

$$M_t = G * I_t * \theta$$

With G as the shear modulus and  $I_t$  as the polar moment of inertia. For isotropic plates the stiffness properties are the equal in both directions. This is not the case for box girder beams. For these types of beams orthotropic parameters has to be determined.

Some formulas are available for the case of thin walls (t) compared to the width (b) where the contribution of the walls are neglected, see figure 159.



$$I_i = \frac{4A^2}{\sum \frac{b_i}{t_i}} \quad i = 1, 2, 3, 4$$

$$I_i = \frac{4A^2 t}{B} \quad \text{for constant } t$$

Figure 159, formulas for twisting bars - part of fig 21.2 [14]

A is the area enclosed by the center lines of the four composing walls.

The walls of the concrete box are not that thin, as the case is for steel for example, their contribution must be taken in to account for the torsional rigidity. For orthotropic plates the torsional deformation is still the same ( $\rho_{xy}$ ) but the twisting moments are not equal. For a quick calculation an average value can be used for orthotropic plates:

$$D_{av} = G * \frac{i_{av}}{2}$$

$$i_{av} = \frac{1}{2} * (i_{xy} + i_{yx})$$

### CALCULATION OF THE STIFFNESS

In case of thin walls it was assumed that the inner walls had negligible contribution to the total torsional stiffness of the cross-section. For this cross-section and its dimensions the contribution of the walls has to be added to the total rigidity.

### 11.5.1 X direction

For the longitudinal direction the contribution of the whole cross-section has to be taken in to account, according to figure 159:

$$i_{xy} * b = I_t + t_{top}^3 * \frac{b}{6} + t_{bottom}^3 * \frac{b_{bottom}}{3} + 2 * (t_{web}^3 * \frac{b_{web}}{3})$$

$$I_t = 4 * A^2 * \frac{t_{gem}}{B_{total}} = 4 * (1180 * 1100)^2 * \frac{170}{1180 * 2 + 1100 * 2} = 1,53 * 10^{11} \text{ mm}^4$$

$$i_{xy} * b = 2,53 * 10^{11} + 190^3 * \frac{850}{6} + 120^3 * \frac{850}{3} + 2 * (185^3 * \frac{790}{3}) =$$

$$i_{xy} = \frac{(2,53 * 10^{11} + 0,01 * 10^{11} + 0,005 * 10^{11} + 2 * 0,02 * 10^{11})}{1180}$$

$$= 1,60 * 10^8 \text{ mm}^4 \text{ per mm}$$

### 11.5.2 Y direction

For the transverse direction the contribution of the top flange is taken in to account:

$$i_{yx} = \frac{1}{6} * t_{top}^3$$

$$i_{yx} = \frac{1}{6} * 190^3 = 1,1 * 10^6 \text{ mm}^4 \text{ per mm}$$

## 11.6 Shear stiffness

For the box beam cross-section the shear rigidity is in between the case where it is negligible and totally dominant.

### 11.6.1 X direction

The real area must be considered that transfers the shear force. In this case the webs. The shear rigidity:

$$D_{sx} = G * \frac{A_{sx}}{b}$$

$$G = \frac{E}{2(1 + \nu)} = \frac{35000}{2(1 + 0,2)} = 14580 \text{ N/mm}^2$$

$$A_{sx} = 2 * 1100 * 206 = 4,5 * 10^5 \text{ mm}^2$$

$$D_{sx} = 14580 * \frac{4,5 * 10^5}{1180} = 5,5 * 10^6 \text{ N per mm}$$

11.6.2 Y direction

To get the exact solution for the stiffness in the transverse direction a FEM analysis must be performed. This can be done in the same procedure as has been done with the  $D_{xx}$ . The difference is that when applying a constant shear force a linear moment distribution will be present. A case with only constant shear is not possible. This means that the shear distortion will interact with flexural deflection. To determine the  $D_{sx}$ , the  $D_{yy}$  must also be known. This is obtained from the previous analyses.

$$\delta = v_y * \frac{b^3}{12 * D_{yy}} + v_y * \frac{b}{D_{sy}}$$

$$D_{yy} = 46 * 10^9 \text{ Nmm}^2 \text{ per mm}$$

$$b = 1180 \text{ mm}$$

$$\delta = 500 \text{ mm}$$

The  $D_{sy}$  is the only unknown.

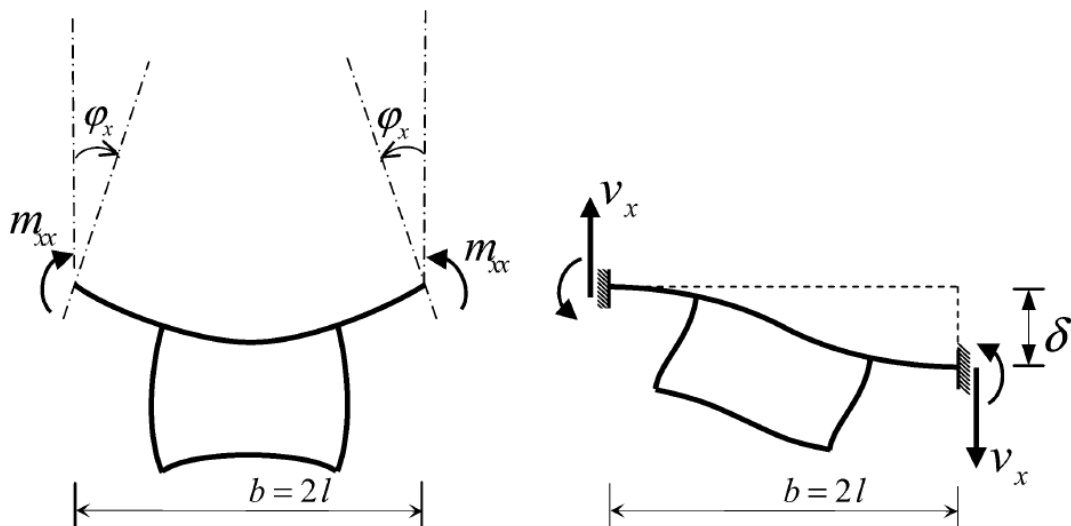


Figure 160, model for determining the shear stiffness - fig 21.10 [14]

**HAND CALCULATION**

It is safe to assume that only the top flange have shear stiffness in the transverse direction.

$$A_{sy} = 190 = 190 \text{ mm}^2 \text{ per mm}$$

$$D_{sy} = 14580 * 190 = 2,7 * 10^6 \text{ Nmm}^2 \text{ per mm}$$

**DIANA**

The value of  $2,7 * 10^6$  Nmm<sup>2</sup> per mm can be compared to the finite element analysis:

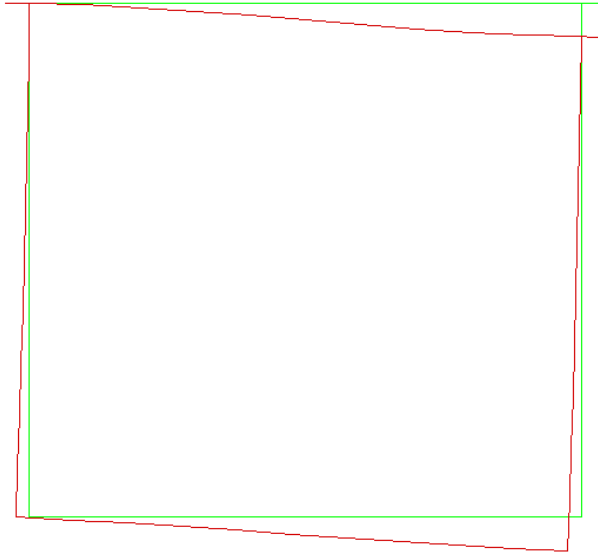


**Figure 161, shear deformation of the cross-section**

$$b = 1180 \text{ mm}$$

$$\delta = 500 \text{ mm}$$

Obtained from the analysis:  $v_y = 5,83 * 10^4$  N

$$\delta = \frac{v_y}{K_{sx}}$$

$$K_{sx} = \frac{v_y}{\delta} = 5,83 * \frac{10^4}{500} = 116 \text{ N per mm}$$

$$\delta = \frac{v_y}{K_{sx}} = v_y * \frac{b^3}{12 * D_{yy}} + v_y * \frac{b}{D_{sy}}$$

$$D_{yy} = 46 * 10^9 \text{ Nmm}^2 \text{ per mm}$$

$$116 = \frac{1180^3}{12 * 46 * 10^9} + \frac{1180}{D_{sy}}$$

$$D_{sy} = 0,21 * 10^6 \text{ Nmm}^2 \text{ per mm}$$

$$A_{sy} = 0,18 * \frac{10^6}{14580} = 12,5 \text{ mm}^2 \text{ per mm}$$

Unfortunately this result is not the expected result. This analysis is very sensitive. Therefore the hand calculation is taken in to account and not the analysis. It is also expected that this value will not have a big impact on the results.

## 11.7 Summary of the parameters

A summary can be found in the table below.

Table 45, summary of the orthotropic parameters for the cross-section

Parameter	Symbol	Value	Unit
<b>Young's Modules</b>	E	$3,50 * 10^4$	N/mm <sup>2</sup>
<b>Poisson's Ratio</b>	$\nu$	$2,00 * 10^{-1}$	[-]
<b>Shear Modules</b>	G	$1,50 * 10^4$	N/mm <sup>2</sup>
<b>Flexural Stiffness (x)</b>	$i_x$	$8,00 * 10^7$	mm <sup>4</sup> per mm
<b>Flexural Stiffness (y)</b>	$i_y$	$0,13 * 10^7$	mm <sup>4</sup> per mm
<b>Diagonal Term</b>	$i_v$	$0,90 * 10^4$	mm <sup>4</sup> per mm
<b>Surface</b>	$A_x$	564	mm <sup>2</sup> per mm
<b>Surface</b>	$A_y$	310	mm <sup>2</sup> per mm
<b>Torsional Stiffness (xy)</b>	$i_{xy}$	$1,6 * 10^8$	mm <sup>4</sup> per mm
<b>Torsional Stiffness (yx)</b>	$i_{yx}$	$1,1 * 10^6$	mm <sup>4</sup> per mm
<b>Shear Area (x)</b>	$A_{sx}$	$4,5 * 10^2$	mm <sup>2</sup> per mm
<b>Shear Area (y)</b>	$A_{sy}$	$1,9 * 10^2$	mm <sup>2</sup> per mm

## 12 APPENDIX B: GEOMETRY ORTHOTROPY AND MATERIAL ORTHOTROPY

For the orthotropic plate model several types of elements can be used to cope with the orthotropy. The orthotropy can be coped with using a plate bending orthotropy element. With this type of element orthotropic parameters can be inserted as geometry orthotropy.

The disadvantage of these types of elements is that it can only be loaded within its plane.

Because the influence of the prestressing could also be modelled, it is better to use, flat or curved, shell elements. These are a combination of plate bending element and a plane stress element. Flat shell element can cope with geometry orthotropy. This can be inserted in DIANA as input for the elements. Curved shell elements are the best type of element to model a skew box beam viaducts. These types of elements are numerically integrated.

The only disadvantage is that it cannot cope with geometry orthotropy, only with material orthotropy. This means that the geometrical properties of the viaduct have to be transformed in material geometry.

This chapter will examine the differences between the types of elements for an uniformly distributed load. The results for a straight plate are shown. The same procedure has been done for other load configurations. These results are not included.

### 12.1 Defining the material orthotropy

In appendix A the geometrical orthotropic parameters of the cross section were determined.

Table 46, geometrical orthotropic parameters as determined in appendix A

Parameter	Symbol	Value	Unit
<b>Young's Modules</b>	E	$3,50 * 10^4$	N/mm <sup>2</sup>
<b>Poisson's Ratio</b>	$\nu$	$2,00 * 10^{-1}$	[-]
<b>Shear Modules</b>	G	$1,50 * 10^4$	N/mm <sup>2</sup>
<b>Flexural Stiffness (x)</b>	$i_x$	$8,00 * 10^7$	mm <sup>4</sup> per mm
<b>Flexural Stiffness (y)</b>	$i_y$	$0,13 * 10^7$	mm <sup>4</sup> per mm
<b>Diagonal Term</b>	$i_v$	$0,90 * 10^4$	mm <sup>4</sup> per mm
<b>Surface</b>	$A_x$	564	mm <sup>2</sup> per mm
<b>Surface</b>	$A_y$	310	mm <sup>2</sup> per mm
<b>Torsional Stiffness (xy)</b>	$i_{xy}$	$1,6 * 10^8$	mm <sup>4</sup> per mm
<b>Torsional Stiffness (yx)</b>	$i_{yx}$	$1,1 * 10^6$	mm <sup>4</sup> per mm
<b>Shear Area (x)</b>	$A_{sx}$	$4,5 * 10^2$	mm <sup>2</sup> per mm
<b>Shear Area (y)</b>	$A_{sy}$	$1,9 * 10^2$	mm <sup>2</sup> per mm

Element: CQ40S (8-node quadrilateral shell element)

The orthotropic plate parameters (sub script xx and yy) has to be converted to material orthotropy parameters (sub script 1 and 2). The width (b) is left out of the calculation because the results are per millimeter. The ratio of the stiffness  $EI_{xx}$  and  $EI_1$  must be the equal. This is also valid for the axial stiffness. The equations are:

$$EI_{xx} = E_1 * I_1 = E_1 * \frac{1}{12} * h_{plate-1}^3 \quad (1)$$

$$EI_{yy} = E_2 * I_2 = E_2 * \frac{1}{12} * h_{plate-2}^3 \quad (2)$$

$$EA_x = E_1 * h_{plate-1} \quad (3)$$

$$EA_y = E_2 * h_{plate-2} \quad (4)$$

In these four equations, there are 4 unknowns but the equations are not coupled. Only one of the bottom two equations can be used. The following must also hold:

$$h_{plate-1} = h_{plate-2}$$

To solve these equations, the axial stiffness in one of the direction has to be left out. The axial stiffness in the transverse direction is the one left out of the equation. This means that the strains in the transversal direction are not valid.

From equation (3):

$$E_1 = \frac{EA_x}{h} = 1,97 * \frac{10^7}{h}$$

The 'h' of the plate can now be calculated using equation (1):

$$EI_{xx} = 35000 * 8,0 * 10^7 = 2,8 * 10^{12} = E_1 * \frac{1}{12} * h^3 = 1,97 * \frac{10^7}{h} * \frac{1}{12} * h^3$$

$$h = 1306 \text{ mm}$$

The  $E_{1,2}$  can be determined:

$$E_1 = 15135 \frac{N}{mm^2}$$

$$E_2 = 250 \frac{N}{mm^2}$$

The stiffness can also be derived when the height is known:

$$I_1 = \frac{1}{12} * h_{plate}^3 = 1,85 * 10^8 \text{ mm}^4$$

$$I_2 = \frac{1}{12} * h_{plate}^3 = 1,85 * 10^8 \text{ mm}^4$$

In the same procedure as for the flexural stiffness, the shear stiffness should be calculated to gain the fictional shear modules  $G_1$  and  $G_2$ .

$$G * A_{sx} = G_1 * h$$

$$G = \frac{E}{2(1 + \nu)} = \frac{35000}{2(1 + 0,2)} = 14583$$

$$G_1 = \frac{14583 * 4,5 * 10^2}{1306} = 5000 \frac{N}{mm}$$

$$G * A_{sy} = G_2 * h$$

$$G_2 = \frac{14583 * 1,9 * 10^2}{1306} = 2000 \frac{N}{mm}$$

Table 47, overview of the parameters

Parameter	Symbol	Values real structure	Material orthotropy	Unit
<b>Young's Modules</b>	E	$3,50 * 10^4$	$E_1 = 15135$	$N/mm^2$
			$E_2 = 250$	$N/mm^2$
<b>Poisson's Ratio</b>	$\nu$	$2,00 * 10^{-1}$	$2,00 * 10^{-1}$	[-]
<b>Shear Modules</b>	G	$1,50 * 10^4$	$G_1 = 5000$	$N/mm$
			$G_2 = 2000$	
<b>Flexural Stiffness (x)</b>	$i_x$	$8,00 * 10^7$	$1,85 * 10^8$	$mm^4 \text{ per mm}$
<b>Flexural Stiffness (y)</b>	$i_y$	$0,13 * 10^7$	$1,85 * 10^8$	$mm^4 \text{ per mm}$
<b>Diagonal Term</b>	$i_v$	$0,90 * 10^4$	[ * ]	$mm^4 \text{ per mm}$
<b>Surface</b>	$A_x$	564	1306	$mm^2 \text{ per mm}$
<b>Surface</b>	$A_y$	310	1306	$mm^2 \text{ per mm}$
<b>Torsional Stiffness (xy)</b>	$i_{xy}$	$1,6 * 10^8$	[ * ]	$mm^4 \text{ per mm}$
<b>Torsional Stiffness (yx)</b>	$i_{yx}$	$1,1 * 10^6$	[ * ]	$mm^4 \text{ per mm}$
<b>Shear Area (x)</b>	$A_{sx}$	$4,5 * 10^2$	1306	$mm^2 \text{ per mm}$
<b>Shear Area (y)</b>	$A_{sy}$	$1,9 * 10^2$	1306	$mm^2 \text{ per mm}$

[ \* ] = this is no input for the material input.



## 12.2 Hand calculation

### 12.2.1 Deflection

$$w_{max} = \frac{5}{384} * \frac{ql^4}{E * I_x}$$

When the values are filled in:

$$w_{max} = \frac{5}{384} * \frac{0.001 * 14400 * 32250^4}{35000 * 8,0 * 10^7 * 14400} = 5 \text{ mm}$$

### 12.2.2 Moment in longitudinal direction

$$M_{max} = \frac{1}{8} * q * l^2 = \frac{1}{8} * 0.001 * 14400 * 32250^2 = 1,85 * 10^9 \text{ Nmm}$$

$$\frac{1,85 * 10^9}{14400} = 1,3e5 \text{ Nmm}$$

Per mm width this is:  $1,3 \times 10^5$  Nmm

### 12.2.3 Support reactions

From hand calculation the total force applied on the plate can be calculated:

$$1 \left[ \frac{N}{mm^2} \right] * 14400 [mm] * 32250 [mm] = 464400000 \text{ N}$$

For each side this is:  $232200000 \text{ N} = 2,322 \times 10^8 \text{ N}$

## 12.3 Comparing FEM elements

Before the skew plate is modelled, a (normal) straight plate is modelled with the same dimensions with the different elements.

The following is equal for all the models:

*Type: Structural 3D*  
*Millimeter, Newton, Kg*

*Span: 32250 mm*  
*Width: 14400 mm*

*Amount of elements: 1800*  
*Elements size: 560 x 480 mm*

The boundary conditions are simple supports and only vertically restrained in z direction.

The plate is loaded with different kind of loads to examine the difference. In this paragraph only the results for a uniformly distributed load are presented.

### 12.3.1 Plate bending elements CQ24P

Shape must be in plane (xy). Force F must be out of plane. The moment M must be in plane.

In the Mindlin-Reissner plate theory the transverse displacements and rotations of the mid surface normals are independent and obtained by employing an isoparametric interpolation respectively from the translations and rotations in the nodes. This technique includes transverse shear deformation. Elements implemented according to this theory are simply called 'Mindlin plate elements'.

Type: eight-node quadrilateral isoparametric

Degrees of freedom:  $U_z, \varphi_y, \varphi_x$

Linear in x direction and quadratic in y direction:  $k_{xx}, m_{xx}, q_{xz}$ ,

Linear in y direction and quadratic in x direction:  $k_{yy}, m_{yy}, q_{yz}$ ,

Can take up forces: only out of plane

Geometry orthotropy possible: yes

Numerical integration

### 12.3.2 Flat shell elements CQ40F

Shape must be in plane (xy). Force F can be in plane and out of plane. The moment M must be in plane.

There is no coupling between the plate bending and membrane behavior.

Degrees of freedom:  $U_x, U_y, U_z, \varphi_y, \varphi_x$

Linear in x direction and quadratic in y direction:  $\epsilon_{xx}, n_{xx}, k_{xx}, m_{xx}, q_{xz}$ ,

Linear in y direction and quadratic in x direction:  $\epsilon_{yy}, n_{yy}, k_{yy}, m_{yy}, q_{yz}$ ,

Geometry orthotropy possible: yes

### 12.3.3 Curved shell elements CQ40S

The curved shell elements in DIANA are based on isoparametric degenerated-solid approach by introducing two shell hypotheses:

Straight-normals: assumes that normals remain straight, but not necessarily normal to the reference surface. Transverse shear deformation is included according to the Mindlin-Reissner theory.

Zero-normal-stress: assumes that the normal stress component in the normal direction of a lamina basis is forced to zero.

A big difference is that geometry orthotropy cannot be inserted with these types of elements. Therefore geometrical orthotropy is transformed to material orthotropy. The advantage is that Cauchy stresses can be calculated and presented for this model.

The rest is the equal to the flat shell element.

## 12.4 Results distributed load

The results of the models are presented in this paragraph.

### 12.4.1 Deflection

As calculated in the previous paragraph the deflection should be 5 mm. In DIANA the deflected shape of the structure can be presented.

This looks similar for all elements as expected. The maximum deflection can be found in table 48.

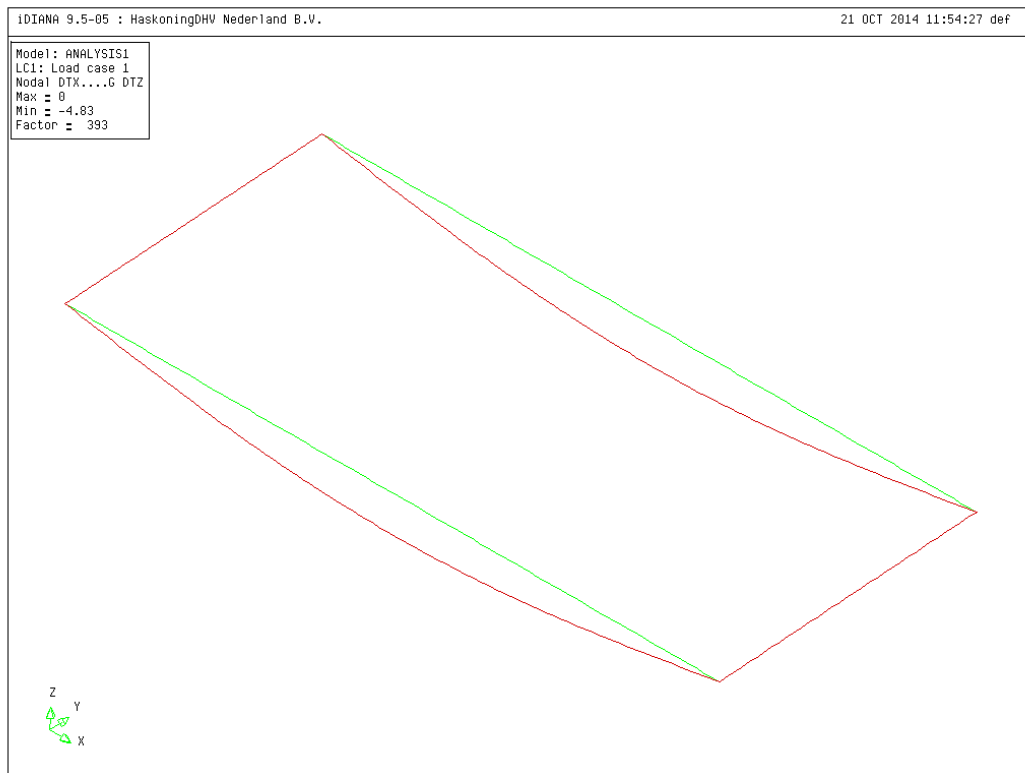


Figure 162, deflection shape

The plate bending elements and the flat shell elements give the same results. The curved shell element is the most accurate.

Table 48, maximum deflection results

Element Type	Result DIANA [mm]	Hand calculation [mm]
<b>Plate bending</b>	4,85	5
<b>Flat shell</b>	4,85	5
<b>Curved shell – EA<sub>1</sub> used</b>	5,05	5

12.4.2 Longitudinal moment

The longitudinal moment in DIANA can be presented in a graph or in contour levels. The longitudinal moment over the span is presented in figure 163 (Nmm/mm) using plate bending elements. The form is similar for the other elements. The maximum values can be found in table 49.

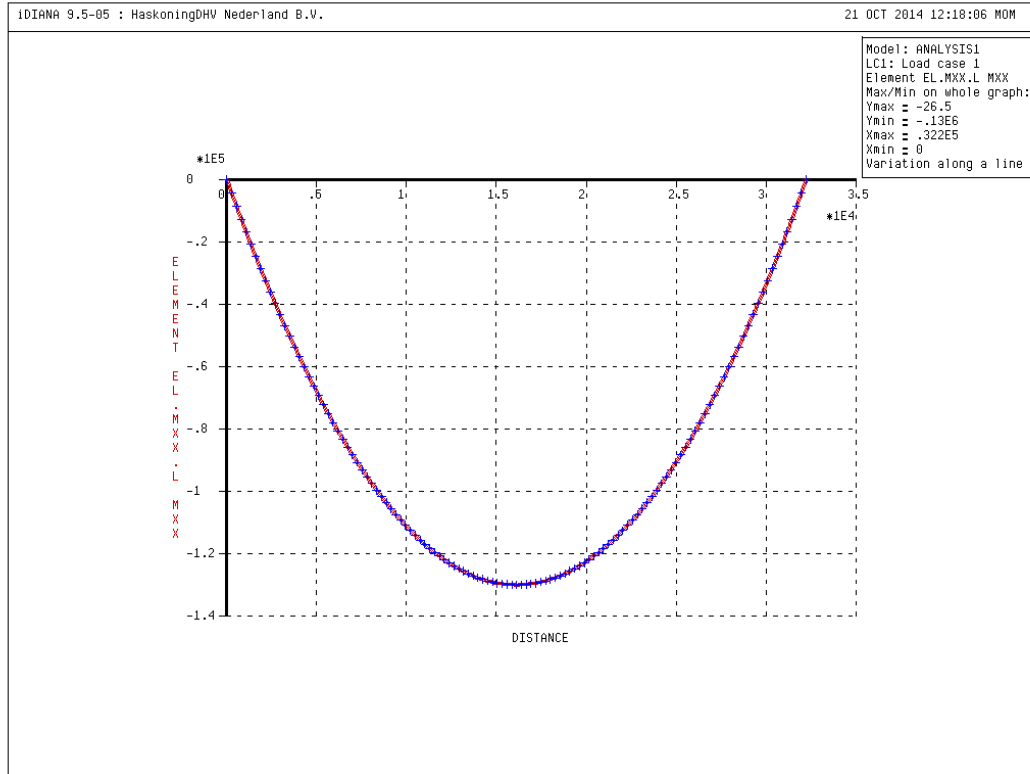


Figure 163, moment distribution over the span

The maximum value is as expected in the middle of the plate. The values do not differ a lot when compared to each other.

Table 49, maximum moment results for different elements

Element Type	Result DIANA [Nmm]	Hand calculation [Nmm]
Plate bending	$1,30 \times 10^5$	$1,3 \times 10^5$
Flat shell	$1,30 \times 10^5$	$1,3 \times 10^5$
Curved shell	$1,30 \times 10^5$	$1,3 \times 10^5$

### 12.4.3 Support reactions

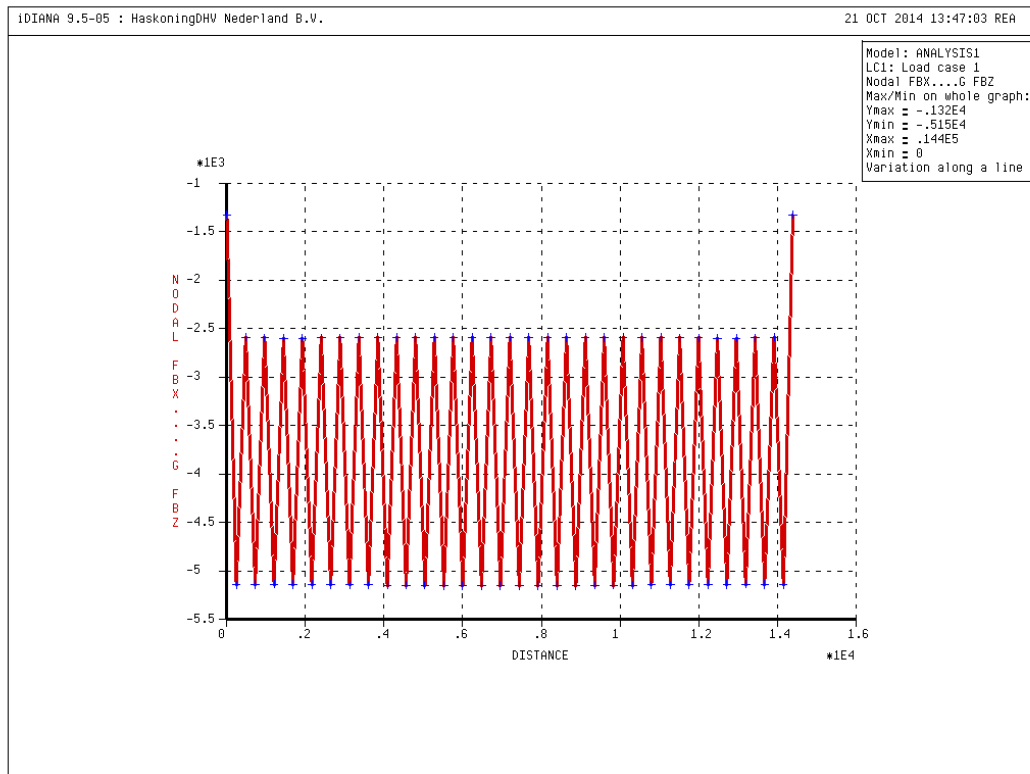


Figure 164, support reactions in nodes along width

As can be seen in figure 164, the average nodal support reaction is  $3,75 \times 10^6$  N.

In the width 60 nodes are present. The total force is:

$$60 * 3,75 * 10^6 = 2,25 * 10^8 \text{ N}$$

Table 50, Result of the support reactions per type of element

Element Type	Result support [N]	Support reaction [N]
Plate bending	$2,25 * 10^8$	$2,322 * 10^8$
Flat shell	$2,25 * 10^8$	$2,322 * 10^8$
Curved shell	$2,25 * 10^8$	$2,322 * 10^8$

## 12.5 Conclusion

In conclusion the curved shell elements are the most applicable. They can take up membrane forces and with material orthotropy an orthotropic plate can be modelled.

When calculating the results for deflection, these types of elements give more accurate results as a result of the numerical integration.

## 13 APPENDIX C: STIFFNESS OF THE BEARINGS

### 13.1 Introduction

In CUR Rapport 53 [18] it is advised to model the stiffness of the supports and not schematize them as hinged supports. This will give better results without local peaks and numerical imperfections. Each beam has one bearing at each side.

In practice the supports are modelled as springs with a stiffness that causes a 0,5 mm deflection as a result of own weight of the girders.

Great differences compared to hinged supports will only occur if the distance between the bearings is assumed as relatively big. For this case the supports are modelled with an interface element over the full width.

### 13.2 Stiffness

For this viaduct a stiffness of  $536 \cdot 10^3$  N per millimeter is inserted. This can be derived as followed:

$$A_{girder} = 664880 \text{ mm}^2$$

$$Selfweight = 25 \frac{kN}{m^3} = 25 \cdot 10^{-6} \frac{N}{mm^3}$$

$$Force \text{ per bearing} = 25 \cdot 10^{-6} * \frac{32250 * 664880}{2} = 268 \text{ kN}$$

$$For \ 1 \text{ mm the stiffness is: } 268 * 2 = 536 * 10^3 \text{ N per mm.}$$

In DIANA an interface element is used. The thickness of the bearing is 38 mm, the width of the bearing is 500 mm approximately.

### 13.3 Finite element modelling

#### 13.3.1 Load; self-weight

A straight plate is modelled, with plate bending elements, with the same stiffness, length and width as the viaduct. The self-weight is modelled as an external surface load:

$$G = S * \frac{A}{W} = 25 \cdot 10^{-6} \frac{N}{mm^3} * \frac{664880}{1200} = 0.014 \text{ N/mm}^2$$

#### 13.3.2 Interface element

At the boundary of the plate an interface element is inserted: CL24I - line, 3+3 nodes.

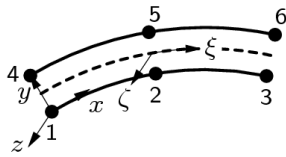


Figure 165, CL24I element

The bottom line is supported with hinges (pinned). The interface element has one element over the height and the division in the transverse direction is the same as for the plate.

In the property manager the thickness (line) is inserted as 500 mm. The stiffness is inserted in the material properties (interface) with a stiffness of:

$$k = \frac{K}{d * 1200} = 536 * \frac{10^3}{500 * 1200} = 0.9 \frac{N}{mm^3} \text{ per mm}$$

d = the thickness of the interface element (bearing)  
1200 = is because the stiffness should be per mm

## 13.4 Results

### 13.4.1 Deflection

The total deflection can now be obtained:

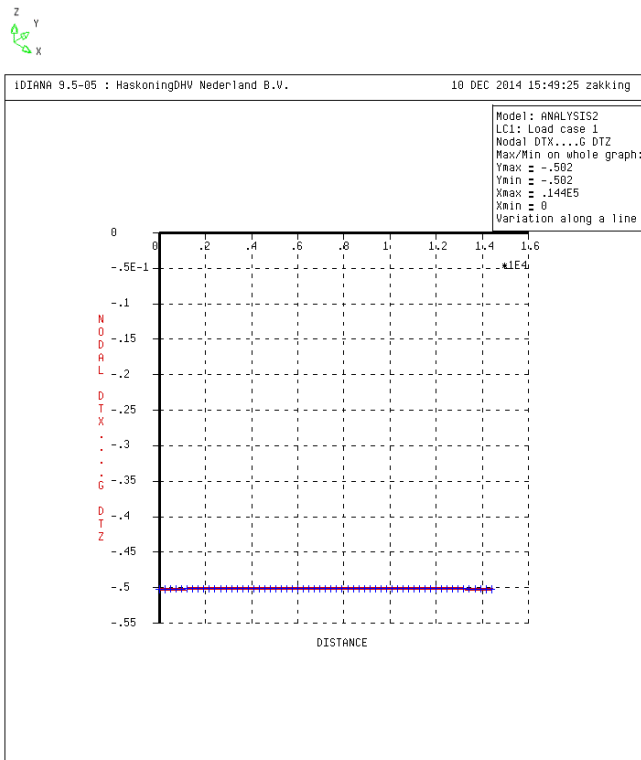
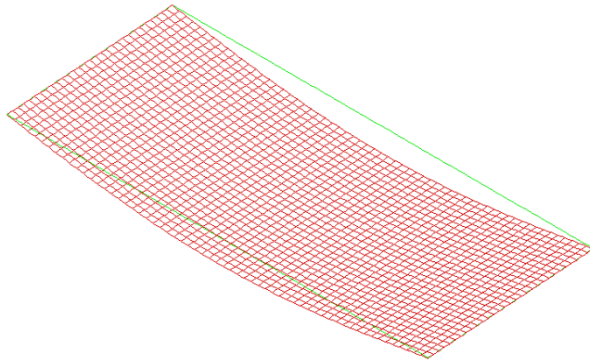


Figure 166, total deflection of the plate

The deflection of the support can also be requested:

As expected the deflection is 0,5 mm over the width.



#### 13.4.2 Support reactions

The total load inserted is:

$$G = S * \frac{A}{W} = 25 * 10^{-6} \frac{N}{mm^3} * \frac{664880}{1200} = 0.014 N/mm^2$$

$$Total\ load: 0.014 \frac{N}{mm^2} * 14400 * 32250 = 6501\ 600\ N$$

The total load per side is: 3250800 N.

In the OUTPUT file the total load is presented: TR Z -0.6502E+07

In EXCEL the output can also be checked. This has been done using the 'utility print' option.

The values are exactly the same.

#### 13.5 Conclusions

- It is important to use a SET for the plate (element mesh). In the post-processing the set must be selected first before the results for the deflections are requested. If this is not the case the results will include the deflections of the pinned base of the interface element.
- The height of the one interface element must not be chosen to big, else other effects will interfere and deflection in the z-direction will not be the governing mechanism.
- The support reactions can be checked using the graph option in DIANA but can also be done through the OUTPUT file and in EXCEL.
- It is important to add the following code in the DATA file or to specify it in DIANA:  
XAXIS 1 0 0 > the x-axis of the element in which the thickness is specified  
PERIME 0 > perimeter of the reinforcement

## 14 APPENDIX D: THE MOST CRITICAL CONFIGURATION

### 14.1 Introduction

In this chapter the most critical configurations for the internal forces are determined. It is important to reason what the starting point is when searching for these internal forces. This can be determined from theory and practice.

For this short study the viaduct is modelled with shell elements using material orthotropy to cope with the geometrical orthotropy as discussed in appendix B. The ends of the beams are modelled as massive parts. See chapter 4.

From Minalu (4): End diaphragm beams decreases the bending and twisting moments in the girders and the deck. However, this reduction was insignificant as compared to the torsional moments occurring in the diaphragm beams.

The distribution of the internal forces is determined according to the difference in stiffness of the elements and the boundary condition. In appendix C the stiffness of the bearing had been determined.

In the final assessment a distinction has to be made between the massive part and the hollow part. The massive part of the girder is much stiffer and therefore “attracts” more force. The capacity is also bigger. This means that in the final assessment both (capacity and acting forces) has to be taken in to account comparing to the hollow part. For most internal forces it is expected that this will not play a role.

### 14.2 Finite element modelling; load masks

To insert the load in DIANA two main options are available:

- 1) **Surfaces: apply surfaces and append the load to this surfaces**
- 2) **Load masks:** by applying a load mask in DIANA, specific areas can be excluded or appended to a uniformly distributed load. With this option the distributed load can be applied over the full viaduct and only specific areas can be made effective.

The second option is the best way to model the loads in DIANA because surfaces can be used to model differences in geometrical or material properties.

#### Distributed loads

For the distributed loads four load masks are needed at least:

Table 51, y-axis boundaries for the load masks, applied over full x-axis.

Location	Begin [mm]	End [mm]	Begin [-]	End [-]	Load Mask
<b>Between rails</b>	01 000	13 400	0.069	0.931	1
<b>Edge area*</b>	00 000	01 000	0.000	0.069	2
<b>Lane 1 at edge</b>	01 000	04 000	0.069	0.277	3
<b>Lane 1 at mid</b>	05 700	08 700	0.396	0.604	4

\*The edge area at the other side is also included in this load mask

Each load mask needs four boundaries. Two boundaries for each axis (x and y). Load mask 1 - 4 are determined for the distributed loads which are applied over the full span of the viaduct. So only the y-axis boundaries are presented.

### Wheel loads

To determine the most critical configuration due to the wheel loads, a model with only the wheel loads as external loading is used.

To each wheel load per lane a load mask is applied. In Excel, a sheet is developed with different coordinates and boundaries for each wheel loads. This is done for each tandem axle for each lane. A bath file (file with commands) is created and this is inserted in DIANA.

An example is given for the position of mid of the span:

**Table 52, magnitude and positions of the wheel loads**

From x=0,5L	From y=0	Lane 1	Position 1	Mid of Lane			
<b>Wheel</b>	Dimensions	Force	Q [N/mm <sup>2</sup> ]	Boundaries			
				x_begin	x_end	y_begin	y_end
<b>1</b>	400 x 400	150000	0,9375	0	400	1300	1700
<b>2</b>	400 x 400	150000	0,9375	1200	1600	1300	1700
<b>3</b>	400 x 400	150000	0,9375	0	400	3300	3700
<b>4</b>	400 x 400	150000	0,9375	1200	1600	3300	3700

From this the batch file for DIANA can be created:

<b>Cons</b>	<b>Lmask</b>	<b>lm1</b>	<b>sur</b>	<b>0</b>	<b>0,0124031</b>	<b>0,09027778</b>	<b>0,11805556</b>
<b>prop</b>	att	lo1	lm1				
<b>Cons</b>	Lmask	lm2	sur	0,037209	0,0496124	0,09027778	0,11805556
<b>prop</b>	att	lo2	lm2				
<b>Cons</b>	Lmask	lm3	sur	0	0,0124031	0,22916667	0,25694444
<b>prop</b>	att	lo3	lm3				
<b>Cons</b>	Lmask	lm4	sur	0,037209	0,0496124	0,22916667	0,25694444
<b>prop</b>	att	lo4	lm4				

### 14.3 Load cases

#### 14.3.1 Distributed loads

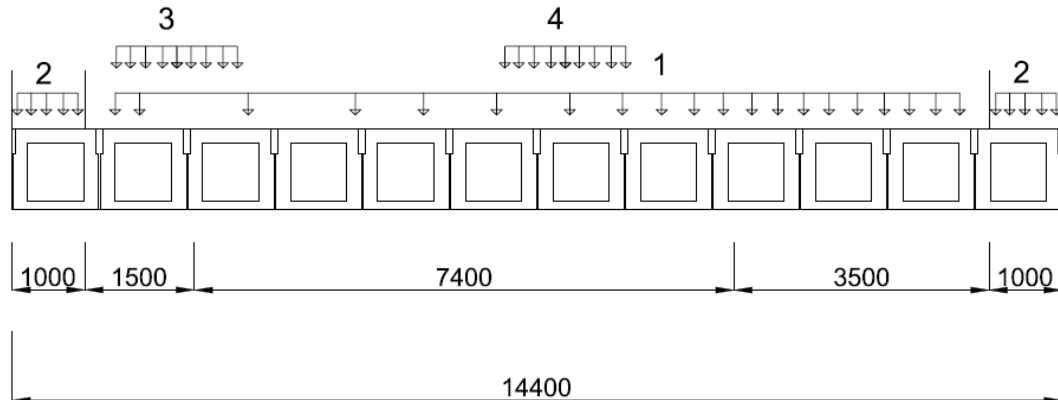


Figure 167, load masks for the distributed loads

Table 53, distributed loads

Load case				Load mask
1	Self-weight	0.014	N/mm <sup>2</sup>	All deck
2	Asphalt	0.0028	N/mm <sup>2</sup>	1
3	Edge line	4.8300	N/mm	Line
4	Edge surface	0.0045	N/mm <sup>2</sup>	2
5	Distributed traffic load	0.0025	N/mm <sup>2</sup>	1
6	Lane 1 extra load (side)	0.0065	N/mm <sup>2</sup>	3
7	Lane 1 extra load (mid)	0.0065	N/mm <sup>2</sup>	4

Making use of the load masks does not give exact results because of the distribution of the load over the element. In the output files the total support reaction is checked. The results are more accurate if surface in the geometry are created but this option is difficult to use if the division in surfaces is also needed to append geometrical or material differences. Therefore the output is checked in DIANA and a correction factor is applied.

Table 54, correction factor for the distributed loads

Load case		Area	Hand calculation	DIANA	Correction factor	
1	Self-weight	0.014	32250 * 14400	6501600	6502000	-
2	Asphalt	0.0028	32250 * 12400	1119720	1112000	1.06
3	Edge line	4.8300	32250 * 2	311535	311500	-
4	Edge surface	0.0045	32250 * 2000	290250	322500	0.90
5	Distributed traffic load	0.0025	32250 * 12400	999750	993300	-
6	Lane 1 extra load (side)	0.0065	32250 * 3000	628875	603700	1.04
7	Lane 1 extra load (mid)	0.0065	32250 * 3000	628875	603700	1.04

### 14.3.2 Wheel loads

Besides the distributed loads, three tandem axles are present with the following dimensions:

Table 55, wheel loads

Tandem axle	Load case	Weight per wheel [N]	Area per wheel [mm <sup>2</sup> ]	Distributed load [N/mm <sup>2</sup> ]	Correction factor
1	12	150 000	400 x 400	0.9375	0.80
2	13	100 000	400 x 400	0.6250	0.81
3	14	050 000	400 x 400	0.3125	0.84

A correction factor other than 1 means that the chosen mesh should be taken finer.

NOTE: the self-weight and the prestressing are presented here along the load cases but will not be inserted in the plate model because these forces work on the beams before they are coupled with the transverse prestressing.

## 14.4 Longitudinal moments

### 14.4.1 Distributed loads

The starting point is to find the maximum longitudinal moment due to the permanent distributed loads.

The variable UDL for the heavy lane is placed at the edge. At that location the load can spread less and the moment per mm is more than when this UDL is placed in the middle of the viaduct for example. This same conclusion can be found in the CUR 53 Rapport [18].

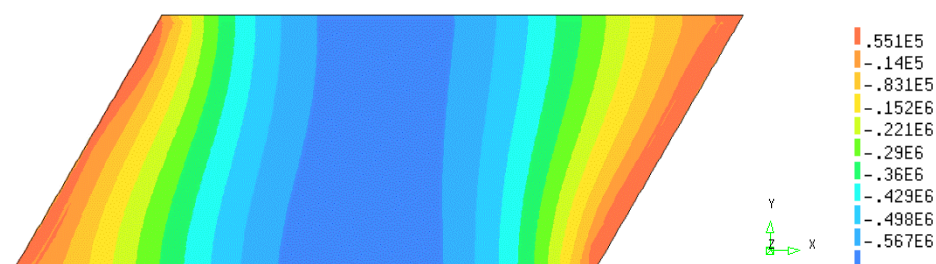


Figure 168, longitudinal moment due to distributed loads

As can be seen from the contour plot (figure 168) and in graphs of figure 169 and 170 there is not a big difference between the bending stiffness of the hollow and the massive part. The reason for this is that the most part of the stiffness comes from the rule of Steiner for these types of cross-section. This part does not change a lot when the cross-section changes from hollow to massive for the small part in the middle of the cross-section.

For a straight plate the maximum moment is always in the middle for every strip. This can also be observed in the skew plate when the longitudinal moment over the mid cross-section of the plate is determined (figure 169).

When the longitudinal cross-section at the edge is chosen, the maximum moment is not exactly in the middle but just right of it towards the obtuse corner (figure 170).

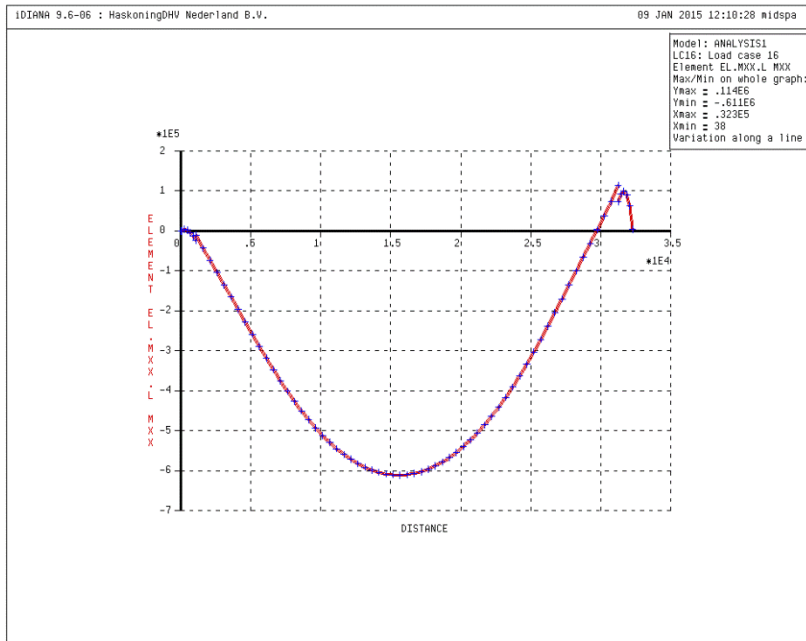


Figure 169, longitudinal moment at  $y=7,2$  m (mid)

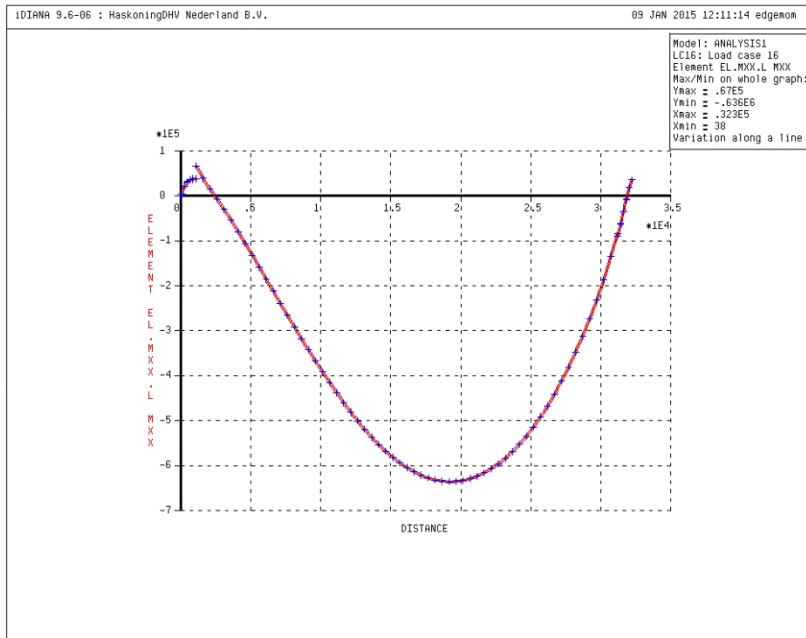


Figure 170, longitudinal moment at first girder ( $y=0,5$  m)

Another aspect that can be observed in figure 169 & 170 is the moment at the supports. These supports (skew viaduct) can be schematized as a rotational spring because of their boundary condition. Also numerical imperfections are present because of change in geometry and edge effects. The load path is not perpendicular. This means that the moments at those points are not 0 as for a simply supported plate but also not maximum as they would be with a fully rigid support. At the end an interface element is present and at that point the moment should be zero. Because of the width of the bearing (500 m) and the massive part of the girder a very small negative moment is present. This is not relevant for the check because the governing cross-section is not at that point.

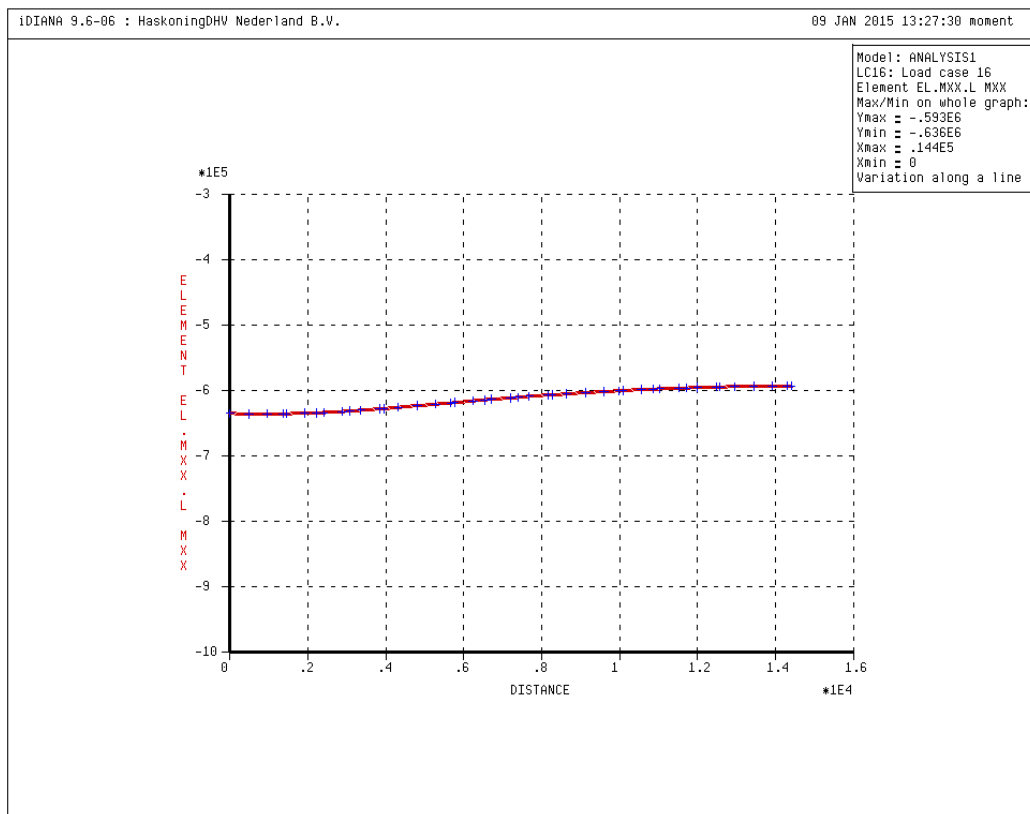


Figure 171, longitudinal moment over the transverse direction at x=19,5 meter

From the graph above (figure 171) the position of the maximum longitudinal moment in the transverse direction can be found. The maximum longitudinal moment can be found at the middle of the first girder at y=0,5 meter.

14.4.2 Wheel loads

Introduction

After the governing cross-section for the distributed loads is determined, the critical configuration for that cross-section due to the wheel loads has to be determined.

As explained before the wheel loads are inserted as distributed loads and only the wheel area is made effective.

It is known that for a straight plate (90 degree angle) the maximum moment occurs at half the span. This is also the governing position for the tandem axles. This is the reason that this will also be the first position to examine. From that position on, the tandem axle is placed 1 'd' (for this case d is taken as 1500 mm) further towards the obtuse corner.

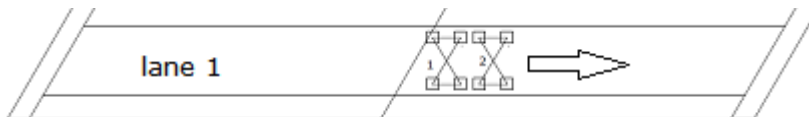


Figure 172, positions of the wheel loads

Tandem axle 1: lane 1

This tandem axle consists of 4 wheel loads of 150 kN.

If the wheel loads are placed 1 d towards the obtuse corner from mid span the moment is maximum at the same location as for the distributed loads.

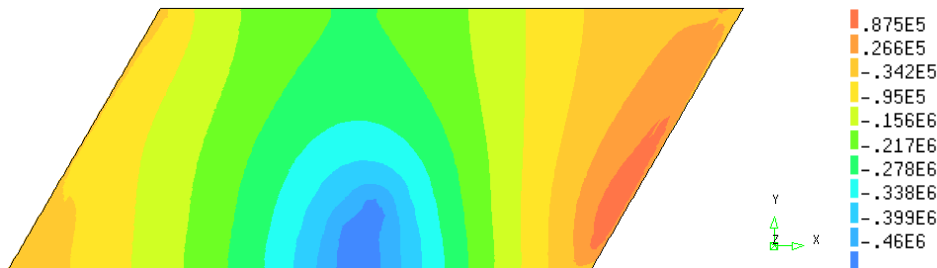


Figure 173, longitudinal moment contour due to tandem axle 1 in lane 1



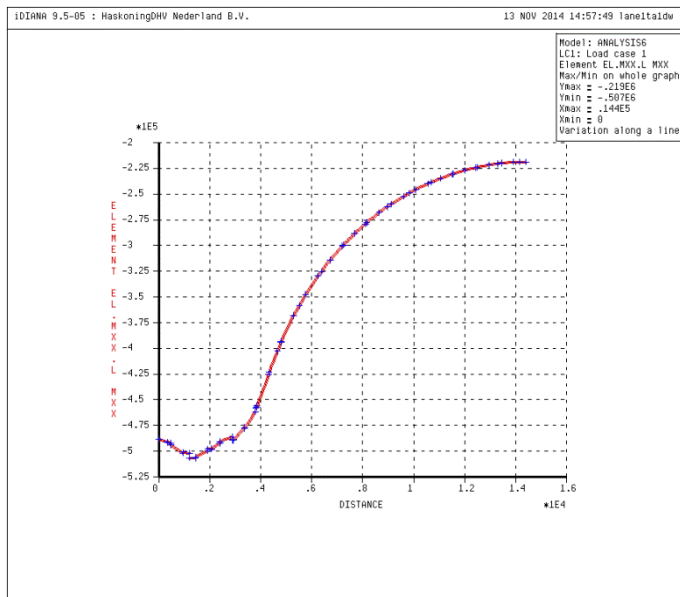


Figure 174, longitudinal moment over the transverse direction at  $x=19,5$  m

For the distributed load the maximum was at  $y = 0,5$  m. From this result it can be seen that the maximum value due to the wheel loads in the transverse direction is at 1 meter approximately. The difference between the values is not that big. This means that the value at  $y= 0,5$  meter will still be governing when the values of the distributed load is also considered.

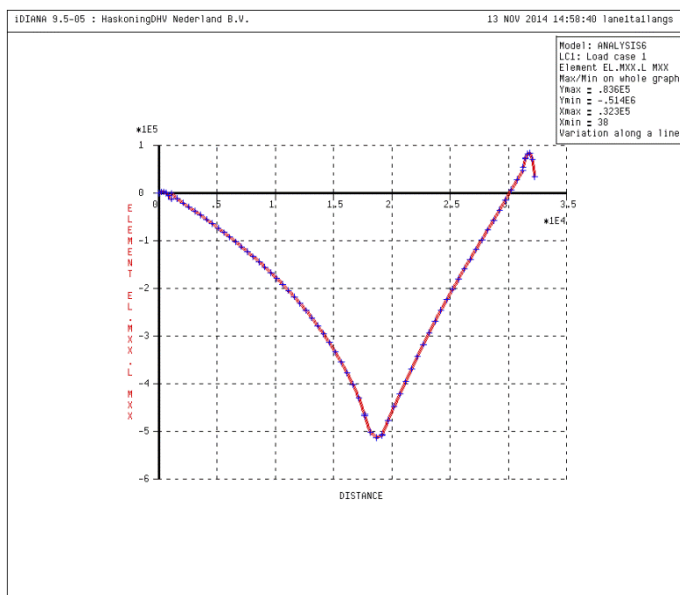


Figure 175, longitudinal moment over the span direction,  $y = 0,5$  m

The maximum is at  $x= 19,5$  m. At the obtuse corner a negative bending moment is present and at the sharp corner this moment is almost zero. These effects are because of geometrical discontinuities (massive end beams) and boundary conditions. These locations are not important for the critical areas.

Tandem axle 2: lane 2 & Tandem axle 3: lane 3

For these two tandem axles (100 kN per wheel and 50 kN per wheel) the same has been done as described for the first tandem axle.

In the Excel sheet once again the positions have been calculated and inserted in DIANA. First position for the loads was at mid span and it is moved 1 d (1500 mm) towards the obtuse corner.

In the figures below the contour plots are given for the longitudinal moment due to tandem axle 2 and tandem axle 3.

Tandem axle 2 caused the biggest moment when it was placed 2 d (3000 mm) right of the span.

The influence of the exact position tandem axle 3 is less than other to axles because of its magnitude and position on the viaduct. The maximum value was found when the tandem axle was placed 1 d from half span.

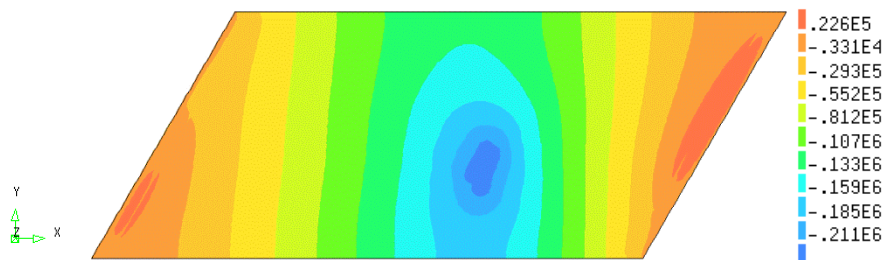


Figure 176, longitudinal moment contour plot due to tandem axle 2 at position 2d (3000 mm) from half of the span

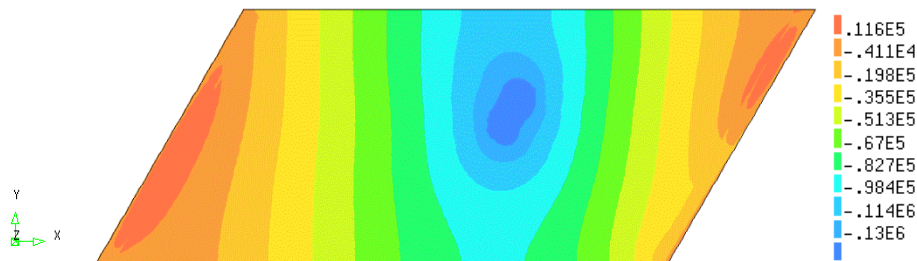


Figure 177, longitudinal moment contour plot due to tandem axle 3 at position 1d (1500 mm) from half of the span

## 14.5 Transverse moments

To find the most critical configuration for the transverse moment another placement of the heavy traffic lane has to be considered. To get the most spreading in the transverse direction the heavy lane should be placed in the middle of the deck. This is schematized as load mask 4 (load case 7) in figure 167.

### 14.5.1 Distributed loads

If the contour plots are plotted in the same manner as has been done for the longitudinal moment than the result would not be very useful. This is because of the big difference in stiffness between the hollow and the massive part of the girder as can be seen in the figure below.

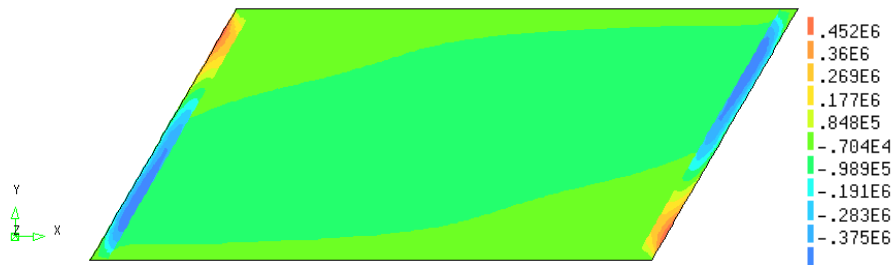


Figure 178, transverse moment due to distributed loads (full mesh)

This can be solved by creating a set “GIRDERS” without the end massive beams. In the post processing only this set has to be selected first. After which the results will give better insight:

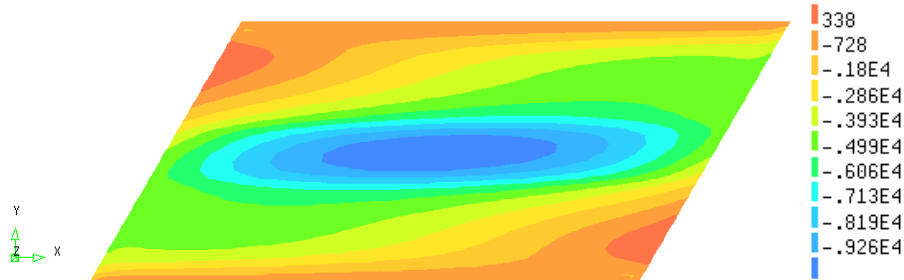


Figure 179, transverse moment due to distributed loads (without end massive beams mesh)

The maximum value can be found in the middle of the plate. At the edges the girders will not (negligible) transfer forces by transverse moments due to the distributed loads but more due to other internal forces like longitudinal moments, shear and torsion.

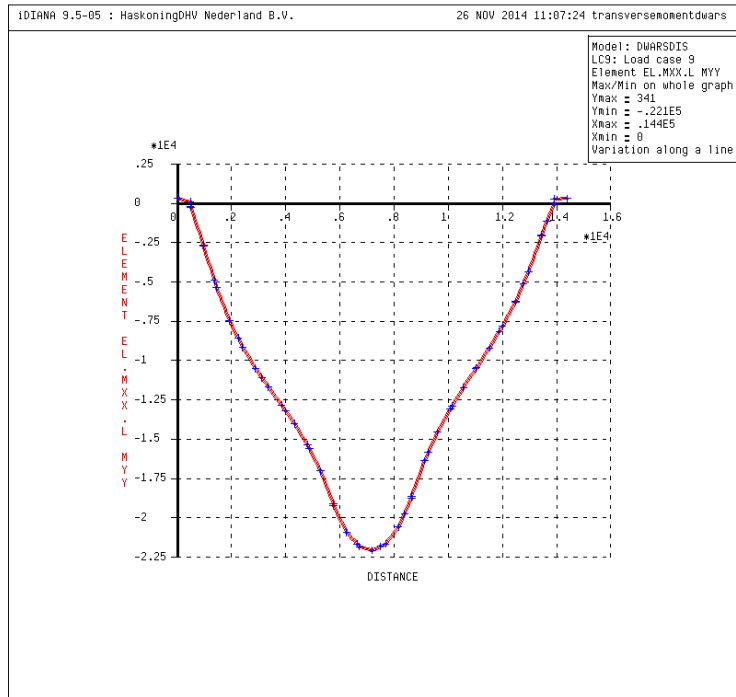


Figure 180, the distribution of the transverse moment over the width of the viaduct at  $x = 20$  m (mid span for the middle strip)

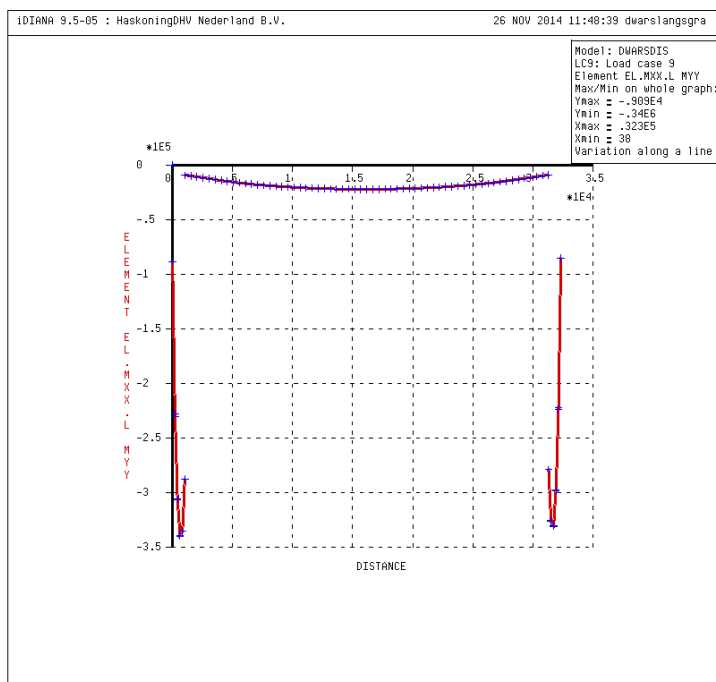


Figure 181, transverse moment at  $y = 7,2$  m

The big difference in value between the massive part and the hollow part can be observed very well in figure 181. For the assessment both cross-sections should be checked. The last part of the line goes very steep. This has to do with the modelling of the interface element which has a thickness of 500 mm. In that last 500 mm this effect appears. For the hollow part the maximum value is indeed at the middle of the span.

14.5.2 Wheel loads

The analysis for this internal force is done in the same way as done before. The heavy lane was placed in the middle to find the maximum transverse moment. The tandem axle of 150 kN per wheel is also placed in the middle of the deck first after which it is placed 1 d further for every step.

Tandem axle 1: lane 1

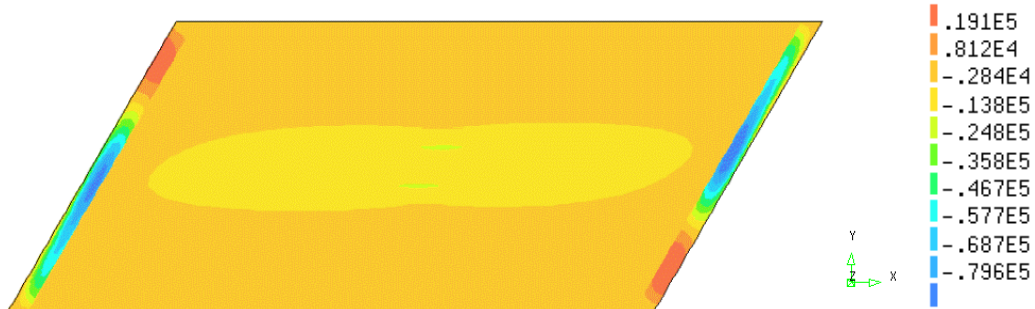


Figure 182, transverse moment contour plot due to wheel loads

At the location of the wheel loads a peak can be seen. This becomes clearer when the graph over the width is plotted.

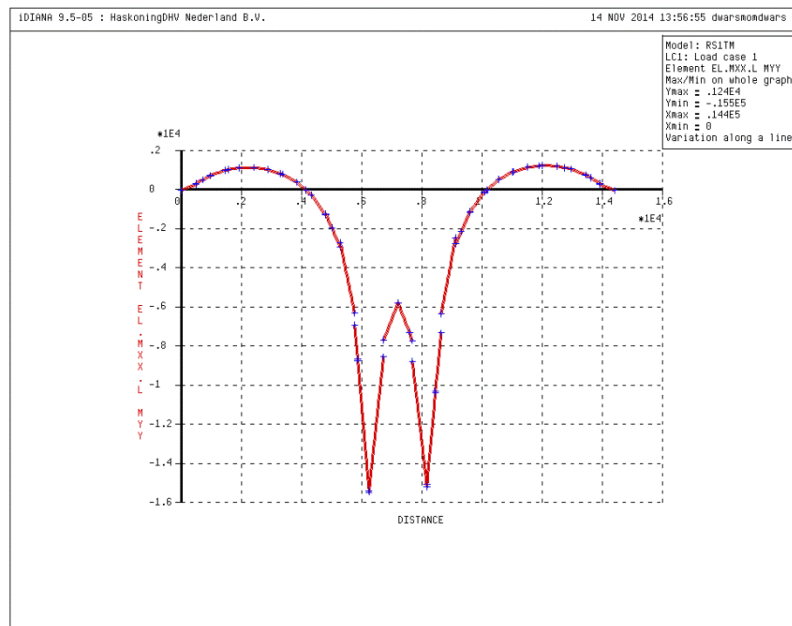


Figure 183, transverse moment over the width at x = 20 m

This peak can be explained by considering the relatively low transverse stiffness of the girder. The force is very local because the spreading is not a lot. In another model, where the stiffness has been made 10 times larger, this effect is reduced. This is shown in figure 183.

For the same reason the first 5 meters of the width of the deck at mid span will get a positive curvature.

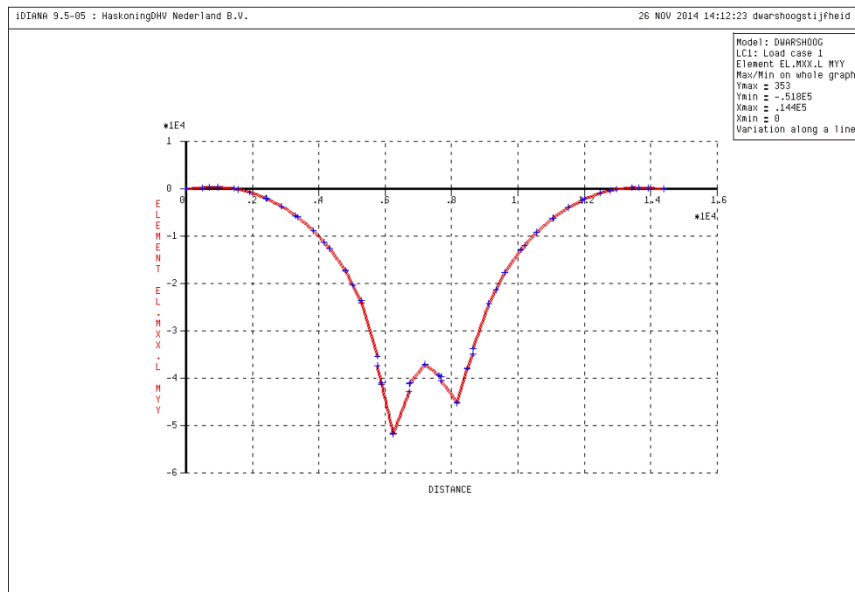


Figure 184, transverse moment over the width at x=20 m

Lane 2 and 3:

The same has been done for tandem axle 2 and 3. The result can be found in the Excel file and the final configuration can be found in paragraph 4.5.

**14.6 Shear force**

14.6.1 Distributed load

From previous studies and from the first calculations it is known that at the support the shear force is higher at the obtuse corner. For that reason the same configuration for the shear force is used as for the longitudinal moment. This means that the heavy lane is placed at the edge of the viaduct from  $y=1$  m till  $y=4$  m.

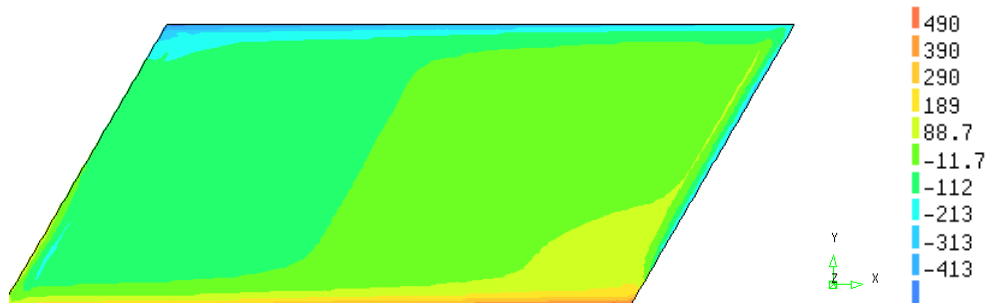


Figure 185, shear force contour plot - lane 1 loaded with heavy traffic load

The shear force distribution is as expected in the middle of the span ( $y=7,2$  m). At that strip the force is divided almost equally over the support.

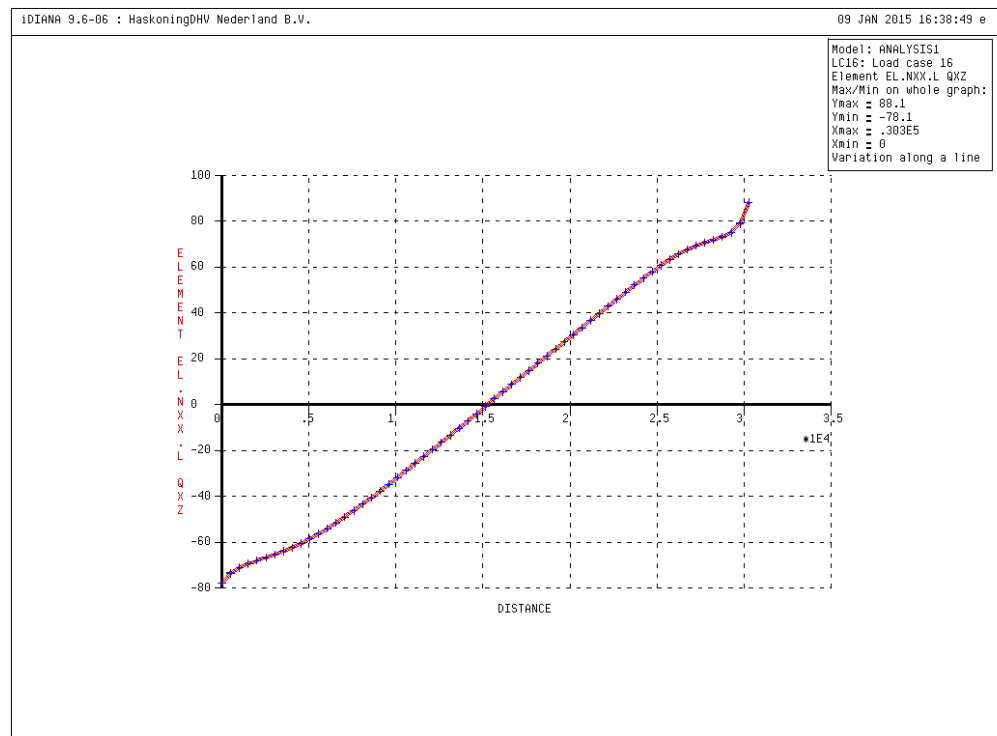


Figure 186, shear force distribution over the span ( $y=7,2$  m)

When looking at the edge the distribution is different because of the obtuse and sharp corner. The force is transferred to the obtuse corner; the shear force is very high at that location. This distribution can be found in figure 186.

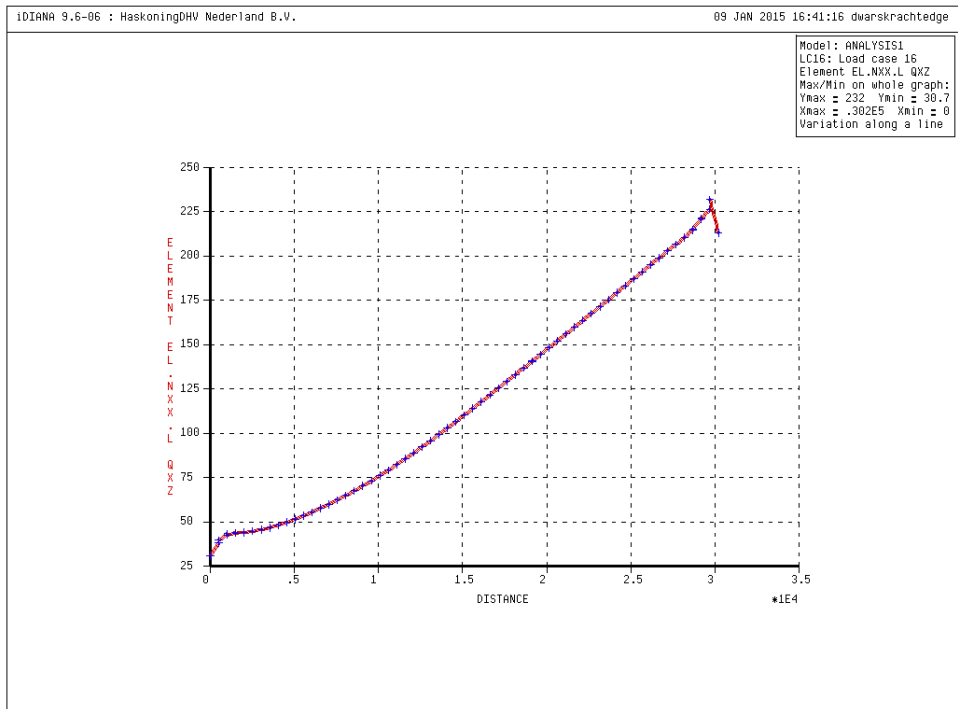


Figure 187, shear force distribution at the edge (y=0,5 m)

#### 14.6.2 Wheel loads

The wheel loads are placed at the corner first so the maximum value of the shear force can be found. From that position on the second position is 1 d further to the left. The same analysis is carried out for the other tandem axles. The results are found in paragraph 4.5.



Figure 188, first two locations of the wheel loads for maximum shear force



Figure 189, shear force contour due to the wheel loads on lane 1



## 14.7 Torsional moments

The configuration for the governing torsional moments is more difficult to determine than other internal forces, because there is not a lot of information available for it concerning skew box beam viaducts. Minalu [4] did a study about this internal force and determined two configurations, one for maximum and one for minimum torsional moment at the obtuse corner, besides the ones that were available from practice. That study is used as starting point.

The plate modelled by Minalu had a different width span ratio and different stiffness ratio than this viaduct. In his viaduct ZIP girders were used instead of box beam girders. So the results from that study are compared with the Finite Element modelling for this type of viaduct. First only the permanent distributed loads are included in the analysis. This is because there is not a lot of background information available about the position of the heavy UDL from the EC1.

The torsion calculated is in accordance with the theory of Mindler Reissner. The deformation by shear force is taken in to account but the shear stress is assumed as constant while in fact this is parabolic. The torsional moments are 0 at the edge of the plate.

### 14.7.1 Distributed loads (without traffic heavy lane)

The first step is to analyze where the maximum torsional moment is due to the permanent distributed load.

The results are shown in figure 190.

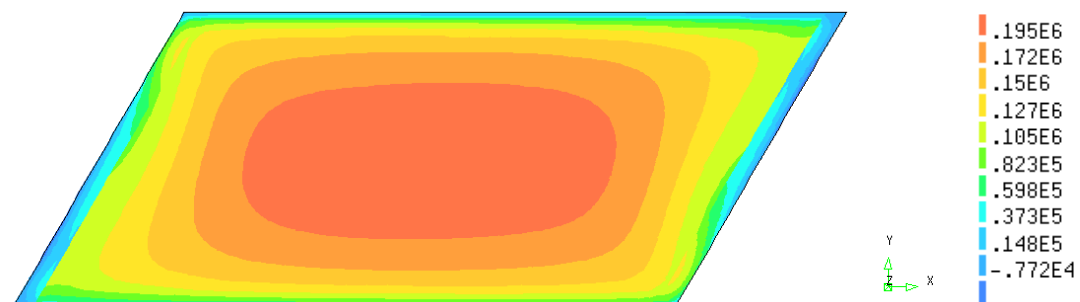


Figure 190, Torsional moments without heavy traffic load lane 1, self-weight and prestressing

The maximum value can be found in the middle of the plate ( $0.2E6$  Nmm) but at the obtuse corner, in the massive part of the girder, some torsional moments are also present ( $0.18E6$ ).

### 14.7.2 UDL traffic loads

The position of the distributed load is fixed. Only the position of heavy lane (lane 1) is changed. Several positions over the width are tested. The heavy lane ( $9 \text{ kN/m}^2$ ) is placed at notional lane 1, 2, 2+ and 3 (which is already over the mid of the viaduct). The 2+ location is exactly in the middle as has been done for the transverse moment configuration.

In the report of Minalu it is mentioned that the sign of the torsional moment changes and that the maximum value of the torsional moment is found at the obtuse corner. In that case the width was two times the span and the skew angle was 45 degrees.

The same analyses have been done (with less variation of position) for this viaduct in DIANA:

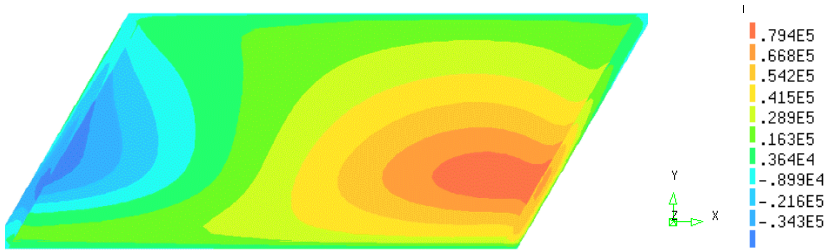


Figure 191, lane 1 loaded - maximum value (red)  $8E4$  Nmm

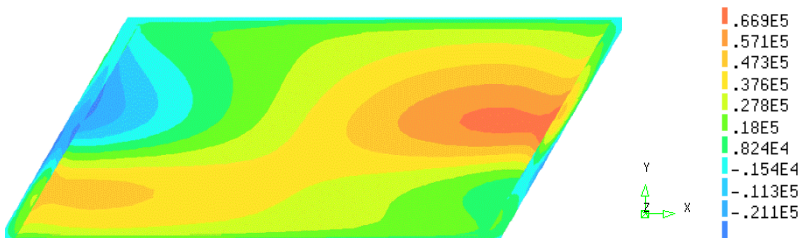


Figure 192, lane 2 loaded - Value at maximum location of figure 190 is  $2,5E4$  Nmm.

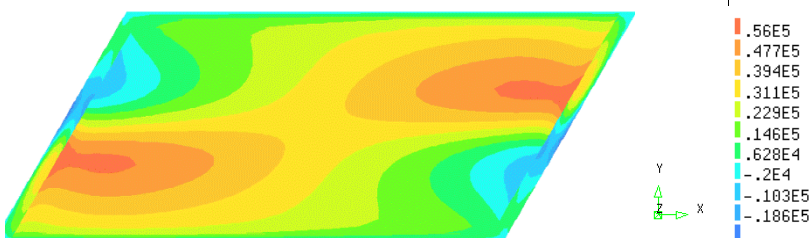


Figure 193, lane 2+ loaded - Value at maximum location of figure 190 is  $-1E4$  Nmm.

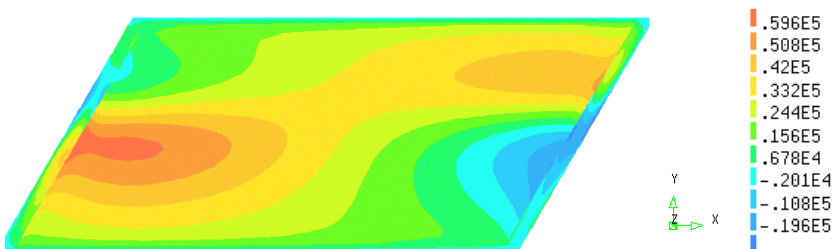


Figure 194, lane 3 loaded - Value at maximum location of figure 190 is  $-2E4$  Nmm.

A few observations compared to the conclusions from Minalu:

- The position for the maximum torsion is not exactly at the obtuse corner but at  $y = 4,2$  meter. This is due to the less skew angle of this viaduct and the ratio of the stiffness (bending and torsion). It is expected that if this viaduct would have a skew angle of 45 degree than the location of the torsional moment would be find more in the obtuse corner.
- The sign of the maximum value of the torsional moment indeed does change when the UDL is moved in the transverse direction. When lane 2 (between  $y = 4000$  mm and  $7000$  mm) is loaded the value at the location of maximum torsion from configuration one is still positive. When the UDL is moved a little in the transverse direction to the middle of the viaduct (location 2+) the sign changes.

This means the maximum positive value is obtained when only lane 1 and 2 are loaded and the maximum negative value is obtained when lane 3,4 and the rest area are loaded.

### 14.7.3 Tandem axles

The position of the tandem axles must be chosen so that these will give maximum torsional moments where the distributed loads also give the maximum torsional moments.

For the previous analysis several DIANA BATCH files (to append the load masks) were already written to define the wheel loads. This means no new batch files have to be written. In the Excel files a reference is made into the earlier used batch files.

For every lane at least four different positions are investigated. If needed, more positions should be investigated.

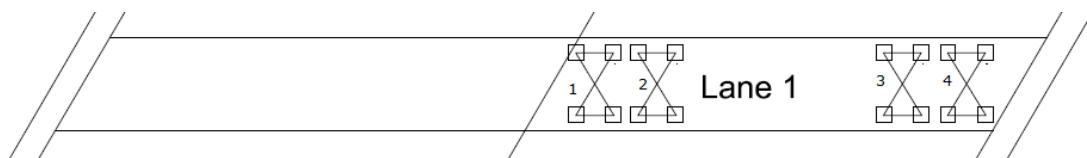


**Figure 195, location of the tandem axle in the first lane**

Position 1 & 2 were defined in the analysis of the longitudinal moment. Position 3 & 4 is from the analysis of the shear.

Torsional moment, lane 1

It is found that for the first lane, position 1 will give the highest positive torsional moment for the position near obtuse corner (position  $y=1,7$  m). As the axle moves towards the obtuse corner the value at that location becomes less.

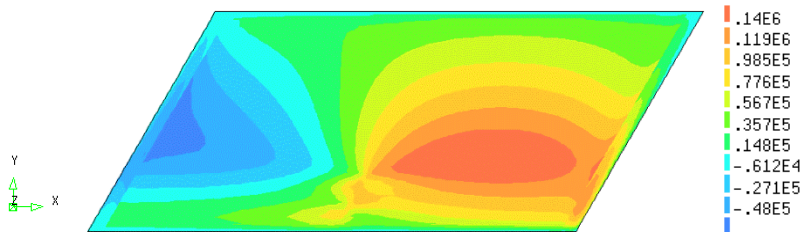


Figure 196, lane 1 position 1 - torsional moment

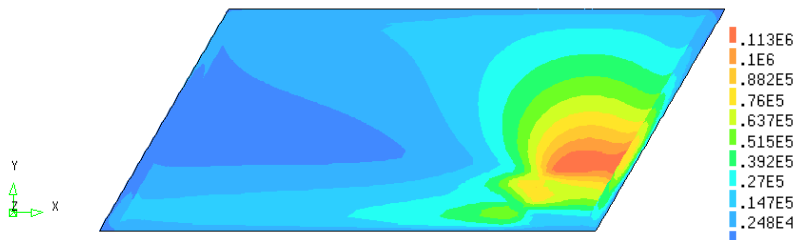


Figure 197, lane 1 position 4 - torsional moment

Torsional moment, lane 2

The same analysis has been done for the second lane and it can be observed that for position 1 still a (very low) positive torsional moment is present but as the axle moves to the right the massive part gets a more negative torque and the hollow part gets a lower positive torque.

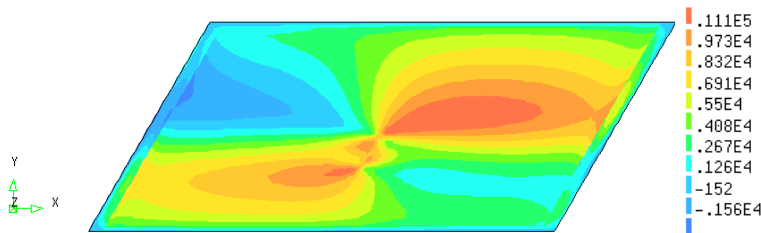


Figure 198, lane 2 position 1 - torsional moment

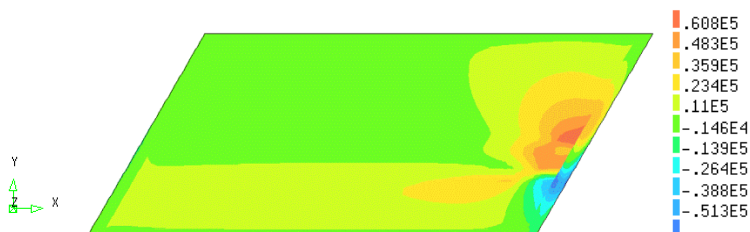


Figure 199, lane 2 position 4 - torsional moment

Torsional moment, lane 3

Only position 1 has still a low positive contribution to the torsional moment. From the second position on the value of the moment becomes negative.

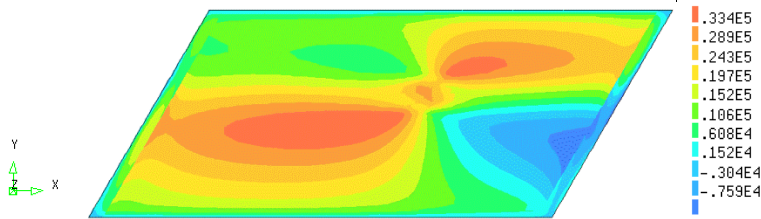


Figure 200, lane 3 position 1 - torsional moment

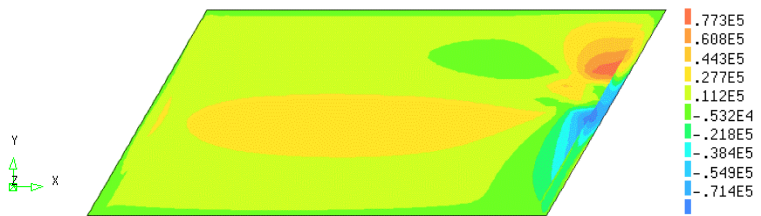


Figure 201, lane 3 position 4 - torsional moment

From this analysis it can be concluded that for transversal and torsional moments the value can differ a lot between the massive and the hollow section of the girder. This should be considered in the check. Not only has the value of the torsional moments changed, but also its sign when the UDL and the tandem axle according to the EC change position.

## 15 EXCEL SHEETS

### 15.1 Load mask

	A	B	C	D	E	F	G	H	I	J	K	L	M	N	O
1	Viaduct														
2	Span	32250													
3	Width	14400													
4															
5	From x=0,5L	Lane 1	Position 0	Mid of Lane											
6	From y=0														
7															
8	Wheel	Dimensions	Force	Q		Boundaries						In Ratio			
9						x_begin	x_end		y_begin	y_end		x_begin	x_end	y_begin	y_end
10		1 400 x 400	150000	0,9375		0	400		1300	1700		0	0,024806	0,090278	0,118056
11		2 400 x 400	150000	0,9375		0	400		1300	1700		0	0,024806	0,090278	0,118056
12		3 400 x 400	150000	0,9375		0	400		3300	3700		0	0,024806	0,229167	0,256944
13		4 400 x 400	150000	0,9375		0	400		3300	3700		0	0,024806	0,229167	0,256944
14															
15	Batchfile rs1m														
16															
17	Cons	Lmask	lm1	sur	0	0,0248062	0,09027778	0,11805556							
18	prop	att	lo1	lm1											
19	Cons	Lmask	lm2	sur	0	0,0248062	0,09027778	0,11805556							
20	prop	att	lo2	lm2											
21	Cons	Lmask	lm3	sur	0	0,0248062	0,22916667	0,25694444							
22	prop	att	lo3	lm3											
23	Cons	Lmask	lm4	sur	0	0,0248062	0,22916667	0,25694444							
24	prop	att	lo4	lm4											
25															
26	Resultaten														
27															
28	MXX		3,40E+05												

Figure 202, example for the making of BATCH files for the location of the wheel loads

### 15.2 Orthotropic plate model – calculation of shear stresses

Maximum shear force configurations															
Shear															
gemid															
*1200															
per web															
stress															
1	47	7	15	1	56400	7	18000	1	28200	7	9000	1	0,128182	7	0,040909
2	20	8	14	2	24000	8	16800	2	12000	8	8400	2	0,054545	8	0,038182
3	19	9	14	3	22800	9	16800	3	11400	9	8400	3	0,051818	9	0,038182
4	17	10	11,66667	4	20400	10	14000	4	10200	10	7000	4	0,046364	10	0,031818
5	16	11	9,166667	5	19200	11	11000	5	9600	11	5500	5	0,043636	11	0,025
6	15	12	-10	6	18000	12	-12000	6	9000	12	-6000	6	0,040909	12	-0,02727
Torsion															
gemid															
*1200*10000															
stress															
total															
shear															
torsion															
left															
right															
1	2,333333	7	3,583333	1	28	7	43	1	0,115374	7	0,177182	0,12	0,115374	0,235374	0,004626
2	4,583333	8	3,75	2	55	8	45	2	0,226628	8	0,185423	0,06	0,226628	0,286628	-0,16662
3	4,25	9	4	3	51	9	48	3	0,210146	9	0,197785	0,052	0,210146	0,262146	-0,15815
4	4,083333	10	4	4	49	10	48	4	0,201905	10	0,197785	0,05	0,201905	0,251905	-0,15191
5	3,916667	11	3,833333	5	47	11	46	5	0,193664	11	0,189544	0,044	0,193664	0,237664	-0,14966
6	3,583333	12	1,333333	6	43	12	16	6	0,177182	12	0,065928	0,041	0,177182	0,218182	-0,13618
												0,038	0,185423	0,223423	-0,14742
												0,038	0,197785	0,235785	-0,15978
												0,032	0,197785	0,229785	-0,16578
												0,025	0,189544	0,214544	-0,16454
												-0,027	0,065928	0,038928	-0,09293

Figure 203, example from the calculation of the shear stresses for the maximum shear force configuration due to uniformly distributed load

## 16 DIANA FILES

### 16.1 Introduction

After the model is built in DIANA the program can write a DATA file. In this DATA file all the information about the model is presented. The MeshEditor can open this DATA file and do the analysis.

The output of the analysis is several files. One of them is the .out file which contains the summary of the analysis: calculation time, iteration and the summation of the forces and moments.

In the following paragraph a few parts of these files are given:

### 16.2 DATA files

: Diana Datafile written for Diana 9.5

FEMGEN MODEL : SKEW

ANALYSIS TYPE : Structural 3D

'UNITS'

LENGTH MM

TIME SEC

TEMPER KELVIN

FORCE N

'COORDINATES'

1	8.400000E+03	1.440000E+04	-3.800000E+01
2	8.120000E+03	1.392000E+04	-3.800000E+01
3	7.840000E+03	1.344000E+04	-3.800000E+01
4	7.560000E+03	1.296000E+04	-3.800000E+01
5	7.280000E+03	1.248000E+04	-3.800000E+01
6	7.000000E+03	1.200000E+04	-3.800000E+01
7	6.720000E+03	1.152000E+04	-3.800000E+01
8	6.440000E+03	1.104000E+04	-3.800000E+01
9	6.160000E+03	1.056000E+04	-3.800000E+01
10	5.880000E+03	1.008000E+04	-3.800000E+01

----- etc. -----

6620	3.786775E+04	1.440000E+04	0.000000E+00
6621	3.837125E+04	1.440000E+04	0.000000E+00
6622	3.887475E+04	1.440000E+04	0.000000E+00
6623	3.937825E+04	1.440000E+04	0.000000E+00

'ELEMENTS'

CONNECTIVITY

1	CL24I	1	63	2	32	93	33
2	CL24I	2	64	3	33	94	34
3	CL24I	3	65	4	34	95	35
4	CL24I	4	66	5	35	96	36
5	CL24I	5	67	6	36	97	37
6	CL24I	6	68	7	37	98	38
7	CL24I	7	69	8	38	99	39

8 CL24I 8 70 9 39 100 40  
 9 CL24I 9 71 10 40 101 41  
 10 CL24I 10 72 11 41 102 42  
 11 CL24I 11 73 12 42 103 43  
 12 CL24I 12 74 13 43 104 44

----- etc. -----

58 CL24I 150 212 151 181 242 182  
 59 CL24I 151 213 152 182 243 183  
 60 CL24I 152 214 153 183 244 184  
 61 CQ40S 62 400 245 405 250 410 61 122  
 62 CQ40S 245 401 246 406 251 411 250 405  
 63 CQ40S 246 402 247 407 252 412 251 406  
 64 CQ40S 247 403 248 408 253 413 252 407  
 65 CQ40S 248 404 249 409 254 414 253 408  
 66 CQ40S 61 410 250 415 255 420 60 121  
 67 CQ40S 250 411 251 416 256 421 255 415  
 68 CQ40S 251 412 252 417 257 422 256 416  
 69 CQ40S 252 413 253 418 258 423 257 417  
 70 CQ40S 253 414 254 419 259 424 258 418  
 71 CQ40S 60 420 255 425 260 430 59 120  
 72 CQ40S 255 421 256 426 261 431 260 425

MATERIALS

/ 1-60 / 2  
 / 211-1110 1261-2160 / 3  
 / 61-210 1111-1260 / 4

GEOMETRY

/ 1-60 / 2  
 / 211-1110 1261-2160 / 3  
 / 61-210 1111-1260 / 4

'MATERIALS'

2 NAME MA2  
 DSTIF 9.00000E-01 9.00000E-01 9.00000E-01  
 3 NAME MA1  
 YOUNG 1.51350E+04 2.50000E+02 2.50000E+02  
 POISON 2.00000E-01 2.00000E-01 2.00000E-01  
 SHRMOD 5.00000E+03 2.00000E+03 5.00000E+03  
 4 NAME MA3  
 YOUNG 3.50000E+04 3.50000E+04 3.50000E+04  
 POISON 2.00000E-01 2.00000E-01 2.00000E-01  
 SHRMOD 1.45830E+04 1.45830E+04 1.45830E+04

'GEOMETRY'

2 NAME PH2  
 THICK 5.00000E+02  
 xAXIS 1 0 0  
 PERIME 0



```

3 NAME    PH1
  THICK   1.30600E+03
4 NAME    PH3
  THICK   1.10000E+03

----- etc. -----

'SUPPORTS'
NAME SET_1
/ 1-31 63-92 123-153 185-214 / TR  1
/ 1-31 63-92 123-153 185-214 / TR  2
/ 1-31 63-92 123-153 185-214 / TR  3
'LOADS'
CASE 1
ELEMEN
/ 61-210 /
  FACE
  FORCE    -0.140000E-01
  DIRECT  3
/ 211-1110 /
  FACE
  FORCE    -0.140000E-01
  DIRECT  3
/ 1111-1260 /
  FACE
  FORCE    -0.140000E-01
  DIRECT  3
/ 1261-2160 /
  FACE
  FORCE    -0.140000E-01
  DIRECT  3

----- etc. -----

'DIRECTIONS'
  1  1.000000E+00  0.000000E+00  0.000000E+00
  2  0.000000E+00  1.000000E+00  0.000000E+00
  3  0.000000E+00  0.000000E+00  1.000000E+00
'END'

```

### 16.3 OUTPUT files

```

/DIANA/AP/LS41 19:05:36 0.02-CPU 0.14-IO 13-FA BEGIN
ELEM. STIFFNESS STORED.
RHS-VECTORS INITIALIZED: ML= 2 ND= 16987 SF.RHSIDE
EXTER. LOAD INITIALIZED: ML= 2 ND= 16987 SF.EXTLOD
CONST.DISP. INITIALIZED: ML= 2 ND= 16987 SF.DISCON
ELEMENTLOAD TO RHS-VECT: NV= 2 SF.RHSIDE
ELEMENTLOAD TO EXT.LOAD: NV= 2 SF.EXTLOD

SUM OF EXT.LOAD TO CALC: ML= 2 ND= 16987 SF.EXTLOD

```

SUM OF EXTERNAL LOADS:

```
=====
LOADSET POSITION TR X   TR Y   TR Z   RO X   RO Y   RO Z
  1      0.0000E+00 0.0000E+00 -0.1288E+06 -0.1838E+09 0.2091E+10
0.0000E+00
  2      0.0000E+00 0.0000E+00 -0.6502E+06 -0.4681E+10 0.1048E+11
0.0000E+00
SPARSE: DIM=16621 NNZ(MAT)=388698 NNZ(LU)=1864628
DECOMPOSITION EXECUTED: DIM=16621 SD=7.77e+01 HD=1.40e+06
SOLVE: REDUCTION RES=0.57E-07 (INIT. RES=0.66E+04) NI= 1
SOLVE: REDUCTION RES=0.12E-06 (INIT. RES=0.15E+05) NI= 1
FEMVIEW file RECHT_ISO.V72 opened
/DIANA/AP/LS41 19:05:39 2.40-CPU 0.61-IO 2438-FA LINSTA
/DIANA/DC/END 19:05:39 2.40-CPU 0.61-IO 2438-FA STOP
```